


2009-01-01

# Computational Modeling Studies of the Structures and Properties of Organotin(IV) and Stannyl-Thioether Systems with Comparisons to X-ray Crystallography

Michelle R. Stem Joseph

University of Texas at El Paso, [mrstem@utep.edu](mailto:mrstem@utep.edu)

Follow this and additional works at: [https://digitalcommons.utep.edu/open\\_etd](https://digitalcommons.utep.edu/open_etd)

 Part of the [Atomic, Molecular and Optical Physics Commons](#), [Inorganic Chemistry Commons](#), [Materials Science and Engineering Commons](#), and the [Mechanics of Materials Commons](#)

---

## Recommended Citation

Stem Joseph, Michelle R., "Computational Modeling Studies of the Structures and Properties of Organotin(IV) and Stannyl-Thioether Systems with Comparisons to X-ray Crystallography" (2009). *Open Access Theses & Dissertations*. 363.  
[https://digitalcommons.utep.edu/open\\_etd/363](https://digitalcommons.utep.edu/open_etd/363)

This is brought to you for free and open access by DigitalCommons@UTEP. It has been accepted for inclusion in Open Access Theses & Dissertations by an authorized administrator of DigitalCommons@UTEP. For more information, please contact [lweber@utep.edu](mailto:lweber@utep.edu).

COMPUTATIONAL MODELING STUDIES OF THE STRUCTURES AND  
PROPERTIES OF ORGANOTIN(IV) AND STANNYL-THIOETHER SYSTEMS  
WITH COMPARISONS TO X-RAY CRYSTALLOGRAPHY

MICHELLE R. STEM JOSEPH

Materials Science and Engineering

APPROVED:

---

M. Lawrence Ellzey, Ph.D., Chair

---

Rosa Fitzgerald, Ph.D.

---

Luis Trueba, Ph.D.

---

Santiago Ibarreche, Ph.D.

---

Patricia D. Witherspoon, Ph.D.  
Dean of the Graduate School

Copyright ©

by

Michelle R. Stem Joseph

2009

## **Dedication**

To my beloved husband, Jimmie - I am a success because you love me.

The peace and purpose of one, the purified power of the other

Also~

To the Stem family, Viking and Highland Scot, we succeed today

To my marital family, the Josephs – I am proud to be part of such an honorable family



COMPUTATIONAL MODELING STUDIES OF THE STRUCTURES AND  
PROPERTIES OF ORGANOTIN(IV) AND STANNYL-THIOETHER SYSTEMS  
WITH COMPARISONS TO X-RAY CRYSTALLOGRAPHY

By

MICHELLE R. STEM JOSEPH, MBA, B.S.

DISSERTATION

Presented to the Faculty of the Graduate School of

The University of Texas at El Paso

in partial fulfillment

of the requirements

for the degree of

Doctor of Philosophy

Materials Science and Engineering

THE UNIVERSITY OF TEXAS AT EL PASO

May 2009

## **Acknowledgements**

My successful navigation through earning the Ph.D. in Materials Science and Engineering would have been far more difficult without the wise assistance of many people at The University of Texas at El Paso (e.g. professors, administrators, secretaries, janitors, etc.). The following people have made particularly significant contributions:

1. Dr. M. Lawrence Ellzey: a magnificent mentor of academics and wisdom, from whom I have been privileged to learn how to be a proper academician
2. Dr. Keith Pannell: invested effort on behalf of my research project and kindly provided me with a nice office
3. Dr. Winston Lloyd: his door was always open to me
4. Dr. William Herndon: made sure that I understood the fine details
5. Drs. Anny Morrobel-Sosa and Richard Schoephoerster: for following through
6. Dr. Cyril Parkanyi: my undergraduate advisor and long-time mentor, a gentleman whose quiet class and scientific enthusiasm have inspired me
7. Dr. Joel Liebman: my longtime colleague and friend, with great insight and honesty

## Abstract

Controlling the toxic effects of organotin(IV) compounds involves engineering the structure of the molecules to optimize their properties. Molecular engineering, coupled with improved capabilities to generate reliable computational optimization models (COMs), will enable researchers to have greater success at harnessing the highly specific cytotoxicity of organotins. For example, as the thio<sub>n</sub> ligand phenyl groups were replaced with Cl atoms, the S-Sn intramolecularity was strengthened, the bond distance decreased, and the stannyl tetrahedral structure was deformed from its triphenyl conformation. With each substitution, conformation deformations lowered the damaging bioactivity levels of thio<sub>n</sub>. Bonding various ligands to organotin(IV) compounds to control structure and electron density, is a significant method of using steric or chemical effects to control the properties of these compounds.

Numerous computational optimization treatments (COTs) were applied to *o*-1-methylthio-benzyl-2-phenyl<sub>x</sub>chloro<sub>y</sub>stannane (thio<sub>n</sub>, where  $x + y = 3$ ). Exhaustive comparative analyses ascertained the accuracies of the computational optimized models (COMs) generated from each COT relative to experimental data, such as X-ray crystallography (XRC) and solid-state <sup>119</sup>Sn NMR (NMR). Further analyses included: (a) three R<sub>2</sub>SnCl<sub>2</sub> structures, (Me<sub>2</sub>SnCl<sub>2</sub>, MePhSnCl<sub>2</sub>, Ph<sub>2</sub>SnCl<sub>2</sub>) such that R = methyl or phenyl, and (b) MeSnCl<sub>3</sub> and Me<sub>3</sub>SnCl, where Me = methyl, and (c) the bimolecular complex, Ph<sub>2</sub>POCH<sub>2</sub>Cl•Ph<sub>2</sub>SnCl<sub>2</sub>.

This research determined for organotin(IV) molecules, thio<sub>n</sub>: (1) reliable COTs, (2) validation methods, (3) complexities of creating reliable models, (4) hyperconjugation extended to include unexpected thioether OT molecular features, (5) a substitution method

to control intramolecularity and hypercoordination, and (6) pre-optimization COM treatments and pre-optimization conformation changes that may influence final conformations. As external validation of the methodology, research on molecules (a) and (b) (noted above) repeated published research by applying the same COTs to the same organotin(IV) molecules as did the original researchers. A comparison of the current COMs to the original computational values and experimental XRC determined that the current research generated COMs that were at least as reliable as published values. Additionally, it was determined that applying a reliable COT to the bimolecular complex, noted above as (c), enabled the quantification of the dipole moment changes and reduced energy of formation for the complex versus the separated molecules. Examining the combination of molecules listed above, the research methods applied, and the project goals, resulted in a substantially greater understanding of a type of molecule that is becoming increasingly important to materials development.

## Table of Contents

|   |      |
|---|------|
| Acknowledgements.....   | v    |
| Abstract.....   | vi   |
| Table of Contents.....  | viii |
| List of Tables.....   | ix   |
| List of Figures.....  | x    |
| Introduction.....   | 1    |
| Application of Computational Optimization Modeling to Analyze Reactive Organotin(IV)<br>Species (with chapter references).....              | 6    |
| Changing the Bioactivity of Organotin(IV) Thioether Species (with chapter references).....  | 38   |
| Theoretical Computational Analyses of Organotin(IV) Species with Low Steric Hindrances<br>to Ligand Rotation (with chapter references)..... | 63   |
| Conclusions.....  | 79   |
| Future Research.....  | 87   |
| References: Introduction, Conclusion, Future Research.....  | 89   |
| Vita.....   | 94   |

## List of Tables

|  |    |
|--|----|
| Table 2.1.a: Bond data, $\text{Me}_x\text{SnCl}_y$ , XRC versus Computational Modeling.....  | 17 |
| Table 2.1.b: Bond data, original minus present values, $\text{Me}_x\text{SnCl}_y$ , XRC versus Computational Modeling.....                     | 18 |
| Table 2.2.a: Bond data, $\text{MeSnCl}_3$ and $\text{Me}_3\text{SnCl}$ , XRC versus Computational Modeling.....                                | 19 |
| Table 2.2.b: Bond data, original minus present values, $\text{MeSnCl}_3$ and $\text{Me}_3\text{SnCl}$ , XRC versus Computational Modeling..... | 20 |
| Table 2.3: CPU processing time, $\text{thio}_n$ , $\pm$ pretreatment, $\pm$ S-Sn-Cl alignment.....   | 25 |
| Table 2.4: Bond radii, $\text{thio}_n$ .....   | 26 |
| Table 2.5: Electron densities, select atoms, $\text{thio}_n$ , $\pm$ pretreatment.....   | 26 |
| Table 2.6: Energies of formation, select bond data, bimolecular complex.....   | 29 |
| Table 3.1: Computational modeling methods, $\text{thio}_n$ .....   | 45 |
| Table 3.2: Select bond data, $\text{thio}_n$ , $\pm$ pretreatment, $\pm$ S-Sn-Cl alignment.....  | 47 |
| Table 3.3: Energies of formation, dipole moments, $\text{thio}_n$ , $\pm$ pretreatment, $\pm$ S-Sn-Cl alignment.....                           | 51 |
| Table 3.4: Electron densities, $\text{thio}_n$ , select atoms.....   | 52 |
| Table 4.1: Computational modeling methods, $\text{thio}_n$ .....   | 67 |
| Table 4.2: Dipole moments, $\text{thio}_n$ , $\pm$ pretreatment, $\pm$ S-Sn-Cl alignment.....  | 69 |

## List of Figures

|  |    |
|--|----|
| Figure 2.1.a: Thio <sub>0</sub> .....  | 14 |
| Figure 2.1.b: Thio <sub>1</sub> .....  | 14 |
| Figure 2.1.c: Thio <sub>2</sub> .....  | 14 |
| Figure 2.1.d: Thio <sub>3</sub> .....  | 14 |
| Figure 2.2: Energy of formation, thio <sub>2</sub> , compare computational modeling versus XRC.....    | 23 |
| Figure 2.3: Sn-S bond distance, thio <sub>2</sub> , compare computational modeling versus XRC.....     | 24 |
| Figure 2.4: HOMO thio <sub>1</sub> view 1.....   | 27 |
| Figure 2.5: HOMO thio <sub>1</sub> view 2.....   | 27 |
| Figure 3.1.a: Thio <sub>0</sub> , tetrahedral view.....  | 44 |
| Figure 3.1.b: Thio <sub>1</sub> , tetrahedral view.....  | 44 |
| Figure 3.1.c: Thio <sub>2</sub> , tetrahedral view.....  | 44 |
| Figure 3.1.d: Thio <sub>3</sub> , tetrahedral view.....  | 44 |
| Figure 3.2: Energy of formation minus XRC, thio <sub>1</sub> , thio <sub>2</sub> , ± pretreatment..... | 47 |
| Figure 3.3: Bond data, thio <sub>n</sub> , computational modeling versus XRC.....                      | 50 |
| Figure 3.4: Energy of formation, thio <sub>n</sub> , computational modeling versus XRC.....            | 51 |
| Figure 3.5.a: HOMO thio <sub>0</sub> .....   | 56 |
| Figure 3.5.b: HOMO thio <sub>1</sub> .....   | 56 |
| Figure 3.5.c: HOMO thio <sub>2</sub> .....   | 56 |
| Figure 3.5.d: HOMO thio <sub>3</sub> .....   | 56 |
| Figure 4.1.a: Thio <sub>0</sub> , tetrahedral and S-Sn bond view.....                                  | 64 |
| Figure 4.1.b: Thio <sub>1</sub> , tetrahedral and S-Sn bond view.....                                  | 64 |
| Figure 4.1.c: Thio <sub>2</sub> , tetrahedral and S-Sn bond view.....                                  | 64 |

|   |    |
|---|----|
| Figure 4.1.d: Thio <sub>3</sub> , tetrahedral and S-Sn bond view.....                           | 64 |
| Figure 4.2.: Compare S-Sn-Cl bond angles for thio1, pretreatment, over many COTs.....           | 65 |
| Figure 4.3.: Compare S-Sn-Cl bond angles for thio1, no pretreatment, over many COTs.....        | 65 |
| Figure 4.4.: CPU processing time, thio <sub>n</sub> , ± pretreatment, ± S-Sn-Cl alignment ..... | 71 |



## Chapter 1: Introduction

It was particularly complex to generate reliable computational optimization models (COMs) of the molecules listed below, because these organotin(IV) molecules are mono or distannyl (heavy main group metal atoms), larger size, have intramolecular, hyperconjugation, hypercoordination, and correlation effects. Additionally, these molecules have low differences between local and global energies of formation as well as for different conformers due to positioning of freely rotating ligands. Furthermore, these molecules are not well-studied. Therefore, the current research has significant importance for clarifying each complexity. [8, 17, 20, 21, 30, 31, 32, 33, 34, 35, 36, 37, 38, 45, 46]

Research was conducted on:

- a. Four structures of *o*-PhS(CH<sub>2</sub>)(CH<sub>3</sub>)(Ph<sub>x</sub>Cl<sub>y</sub>Sn) (thio<sub>n</sub>, where  $x + y = 3$ ),
- b. Three structures of R<sub>2</sub>SnCl<sub>2</sub> (where R = methyl or phenyl),
- c. One structure each of MeSnCl<sub>3</sub> and Me<sub>3</sub>SnCl (where Me = methyl),
- d. One bimolecular organotin(IV) complex, Ph<sub>2</sub>POCH<sub>2</sub>Cl•Ph<sub>2</sub>SnCl<sub>2</sub>

The present research uses computational optimization treatments (COTs) to generate computational optimization models (COMs) of larger organotin(IV) molecules (identified above). A COT is a combination of selected theoretical computational parameters that guide the determination of the molecular structures and properties and generates a COM. Typical parameters include: quantum mechanical method (semi empirical, *ab initio*, density functional theory, and hybridized theories), basis set (i.e. 3-21G, SDD, LANL2MB, etc.), charge, and spin. An ideal (or reliable) COT would compute a COM that matches either (a) experimental data (e.g. X-ray crystallography), or (b) the global minimum energy of formation. [10, 11, 12, 13, 17, 18, 21, 22, 24]

## 1.1 Research Goals

1. Enabling a broader array of analysis than would otherwise be available. The organotin(IV) molecules identified above included examining experimentally determined COM molecular properties. Developing a method to apply a COT that does not alter the z-matrix of an experimentally determined structure enables modeling software to generate a COM that allows researchers access to a significant range of analytical data. [10, 12, 13, 17]
2. Successful validation of each thio<sub>n</sub> molecule relative to experimentally determined data. Performing a comparative analysis of experimental data (e.g. XRC) versus data from various COMs allows the most reliable COT to be determined. This validation enables future researchers to expand the range of the types of molecules for which the most reliable COT here is applicable. [11, 17, 18, 21, 22, 24]
3. Examination of modeling complexities for thio<sub>n</sub> such as the slight energy of formation difference between conformers that result in significant differences in rotational positions of freely rotating ligands and the strong correlation between energies of formation and dipole moment over conformation changes (without PT). [17, 18, 19, 20]
4. Investigation of hyperconjugation as related to thio<sub>n</sub> and how hyperconjugation of thio<sub>n</sub> may be (a) depicted via computations of HOMO maps and (b) related to bioactivity as chlorine atoms are substituted for ligand phenyl groups. [8, 17, 20, 31, 32, 33]
5. Develop a COT that models the effect on intramolecularity, hyperconjugation, and bioactivity caused by chlorine atoms substituting for ligand phenyl groups. Also,

the COT should reliably model the strength of the S-Sn hyperconjugation and the S-Sn-Cl alignment of thio<sub>n</sub> as the substitutions occur. [1, 3, 5, 7, 8, 9, 10, 17, 35, 36, 41, 42, 43, 45, 46]

6. Determine the validity of using pretreatments (PTs) for larger organotin(IV) molecules. For many types of molecules, such PTs are used commonly by researchers in an attempt to use less CPU time and to generate more reliable COMs. PTs include: preoptimization COTs, sequential layering of COTs (i.e. ONIOM), and conformational PTs. [17, 21, 22, 26, 27, 28, 29]

7. Complete external confirmatory validations of the methodology and conclusions on molecules (c) and (d) (noted above). These validations will repeat published research by applying the same COTs to the same organotin(IV) molecules as did the original researchers. A comparison of the present COMs to the original experimental (XRC) and computational values will determine the potential of the conclusions here to be applied to other organotin(IV) molecules. [1, 17, 26, 27, 28, 29, 43, 44, 57, 65]

8. Lastly, apply a reliable COT to the bimolecular complex noted above as (e) to demonstrate quantification of the dipole moment changes, reduced energy of formation of the bimolecular complex versus the separated molecules, and intramolecularity via relevant bond lengths. [17, 25, 26, 44]

The study of the combination of molecules noted above, and their research methods and goals, will result in a substantially greater understanding of the types of molecules that are becoming increasingly important to materials development.

## 1.2 Why This Research is Important

The research methods, clarifications, and discoveries of the present research will enhance finding methods to harness (understand and control) organotin(IV) species toxicities. Furthermore, being able to rely on the generation of a COM to examine organotin(IV) molecules would facilitate: safer research, the production of new and better applications, a lesser reliance on trial-and-error laboratory experimentation methods, and hastening successful research results. Experimentally examining thio<sub>n</sub> properties *in vivo* or *in situ* and then understanding how to reliably model them establishes that COTs may be applied to engineer COMs of organotin(IV) molecules with many purposeful applications that will affect the numerous industries and applications involved. Future research may affect: medical, anti-cancer, anti-inflammatory, chelation, agriculture, biocides, and as intermediates in the preparation of other organotin species. [1, 2, 3, 4, 5, 7, 8, 9, 10, 12, 13, 36, 41, 42, 43]

Controlling the toxic effects of organotin(IV) compounds involves engineering the molecules for optimized properties. Molecular engineering, coupled with improved capabilities to generate reliable COMs, will enable researchers to have greater success at harnessing the highly specific cytotoxicity of organotins. Bonding various ligands to organotin(IV) compounds, to control structure and electron density, is a significant method of using steric or chemical effects to control the compounds properties. [2, 3, 8, 14, 15, 16, 17, 18, 19, 20]

Specifically, one aspect of this research investigated a COM method to understand and control the bioactivity of the thio<sub>n</sub> molecules. The present research examined the trends of various thio<sub>n</sub> properties as the ligand phenyl groups were replaced with Cl atoms,

resulting in: the S-Sn intramolecularity being strengthened, a decrease in the S-Sn bond distance, and the stannyl tetrahedral structure being deformed from its triphenyl conformation. With each substitution, conformation deformations lowered the molecules damaging bioactivity levels. Hence, a development of understanding of the property trends due to chlorine/ligand phenyl group substitution in larger organotin(IV) molecules, especially as it relates to molecular bioactivity changes. [17, 35, 45, 46]

## Chapter 2: Application of Computational Optimization Modeling to Analyze Reactive Organotin(IV) Species

### 2.1 Abstract

Computational optimization modeling (COM) is a research method that uses advanced computers and specialized software (e.g. Gaussian) to generate extremely detailed analyses of molecular properties and structures with a goal of, depicting molecular properties values to match either (a) experimentation or (b) lowest energies of formation.

Determination and effects of COM treatments of a three series of medium-sized organotin(IV) molecules: (a)  $\text{PhS}(\text{CH}_3)(\text{CH}_2)(\text{Ph}_x\text{Cl}_y\text{Sn})$  (where  $x + y = 3$ ), (b) three  $\text{R}_2\text{SnCl}_2$  structures, ( $\text{Me}_2\text{SnCl}_2$ ,  $\text{MePhSnCl}_2$ ,  $\text{Ph}_2\text{SnCl}_2$ ) such that R = methyl or phenyl, and (c)  $\text{MeSnCl}_3$  and  $\text{Me}_3\text{SnCl}$ , where Me = methyl, were researched relative to X-ray crystallography and solid-state NMR. Also a reliable COM was determined for a bimolecular organotin(IV) complex to compute the energy reduction due to system formation.

In summary, this research determined, for organotin(IV) molecules: (a) reliable COTs (b) validation methods (c) complexities of creating reliable models, (d) comparative analyses of molecular series, (e) hyperconjugation extended to include unexpected thioether OT molecular features (f) a substitution method to control intramolecularity and hypercoordination, and (g) pre-optimization COM treatments and pre-optimization conformation changes that may influence final conformations.

### 2.2 Introduction

Research levels of organotin(IV) molecules are increasing due to significant application developments (i.e. biology, agriculture, construction, and nanotechnology). [1, 2, 3, 4, 5] Hence, being able to rely on the generation of a computational optimization

model (COM) to examine organotin(IV) molecules would facilitate: safer research, the production of new and better applications, a lesser reliance on trial-and-error laboratory experimentation methods, and hastening successful research results. [6]

Modeling of organotin(IV) species is becoming more common because theoretical computational modeling efforts can determine properties, make predictions, help develop methods, allow more researchers to investigate organotin(IV) molecules at the same time in a smaller space, and reduce experimental costs and exposure risks. [6, 7, 8] Software to model molecular properties includes: Gaussian, MOPAC, Chimera, Sirius, Spartan, and many others. Higher-end computers are generally used for molecular modeling of organotin(IV) molecules because of the computational complexity and CPU intensity of the operations involved.

Experimental research of organotin(IV) molecules usually requires careful handling to avoid exposure-related health and environment issues. Unlike other environmental neurotoxins (i.e. Hg, Pb, etc.), organotin molecules have unique toxic actions that are highly targeted. Certain mammalian cells dealkylate organotins. The greatest toxicity seems to occur with highly substituted more lipophilic organotins, because lipophilicity allows easier passage across the cellular membranes than less alkylated types. Polysubstituted organotins show a delayed toxic response due to *in vivo* metabolism into more reactive metabolites. [1, 2, 3, 4, 9]

Significant research investigations are being pursued to harness organotin(IV) molecules properties and highly specific cytotoxicity, catalysis, and many other applications. [3, 5, 10] Much of this is laboratory research, yet, there is significant growth in

the usage and application of computational modeling research of organotin(IV) molecules. [6, 11]

### 2.3 Experimental

The molecular models were assembled, computational optimization treatments (COTs) were selected, and computational optimization models (COMs) were computed using a combination of Gaussian (Gaussian 03w revision c.02 version 6.1 PC) and GaussView (version 3.0, Gaussian's graphical user interface). Gaussian is a premier computational modeling software for applying COTs to generate COMs with extremely detailed analyses per molecule or molecular system. The accuracy, or reliability, of the COMs for the molecules studied in this research were examined in relation to X-ray crystallography (Bruker Apex Small Molecule X-ray Crystallographer) and solid-state  $^{119}\text{Sn}$  NMR (Avance 250 Digital MAS NMR to an SGI 02 Silicone Graphics Computer using xwinnmr version 2.1). [10, 12, 13, 14, 15, 16, 45]

### 2.4 Computational Optimization Treatment (COT)

A computational optimization treatment (COT) is described as the theoretical mathematical parameters that guide the computation of the structures and properties of a molecule or molecular system (molecule plus matrix or solvent) and which result in the generation of a COM. Typical parameters include: quantum mechanical methods (semi empirical, *ab initio*, density functional theory, and hybridized theories), basis sets (i.e. 3-21G, LANL2DZ, LANL2MB, etc.), charge, and spin. Structural computations include: bond lengths, bond angles, and dihedral angles. Molecular properties may include: dipole moment, energy of formation, electron distribution, van der Waals radii, etc. It is the combination of COT parameters that effects structural and molecular conformations. [17]



Until recently, modeling accurately any but the simplest organotin(IV) molecules was particularly difficult because the basis sets were not designed to determine models for organotin(IV) molecules. Recently, Gaussian integrated the Los Alamos basis sets, LANL2MB and LANL2DZ (collectively, LAN), into its modeling software as one of the COT parameters from which researchers could choose. Until the LAN basis sets, no basis set was designed with the goal of accurately computing the structures and properties of molecules such as larger organotin(IV) species. Even with more basis sets available, the lack of validation of COTs for many organotin(IV) molecules remains a limiting factor against generating accurate COMs. An ideal COT would compute a reliable COM. A reliable COM is a molecular model that matches either (a) experimental data, or (b) the global minimum energy of formation. [17, 18, 19, 20]

Gaussian is an excellent software package for using theoretical computational methods to understand organotin(IV) molecules. It is a premier software for implementing complex COT parameters that allow the application of COTs (e.g. LAN) and related methodologies on organotin(IV) molecules. This research was not attempting to evaluate Gaussian. Gaussian showed itself to be a stable substrate upon which reliable research of the COT parameters could be done. [17, 18]

#### **2.4.1 COT Application Methodologies**

A z-matrix is the means used by computational modeling software (Gaussian) to define each molecular structure. The z-matrix includes details regarding atoms, bond angles, bond lengths, etc. An initial z-matrix must be input into the software to create the initial molecular model on which a COT computes a COM. There are three methods for a researcher to define or create a molecular z-matrix: (a) direct input, (b) imported

spreadsheet, or (c) a molecular modeling building interface (e.g. GaussView), which creates the z-matrix while the researcher assembles the molecule via its point-and-click graphical interface on a per atom or per organic subunit basis. Once a complete, non-optimized molecular model has been set-up, the COT may be defined in Gaussian by selecting parameters (e.g. theoretical method, functionals, basis set, etc.) from several pull-down lists. Then, the COT may be applied to generate a reliable COM. [17]

#### **2.4.2 COT Strengths and Weaknesses**

If a molecule is of a type that is well-studied, small, organic, or is made of lighter elements ( $\leq_{36}\text{Kr}$ ), then, typically, applying a COT to compute a reliable COM (described above) has been shown to be more accurate due to more extensive validation, than when compared to molecules that are inorganic, organometallic, not well-studied, or contain at least one heavier molecular element ( $>_{36}\text{Kr}$ ). [17] The present research will show that optimization reliability may be affected by (a) applying COT parameter choices, (b) altering initial molecular ligand orientations, or (c) sequentially applied COTs (defined below). Furthermore, generating COMs for molecules that include heavy atoms (e.g. Sn) or reach a certain level of molecular complexity becomes very difficult relative to generating comparably reliable COMs of lighter, smaller organic, or well-studied molecules.

Sequentially applied COTs is defined here as a process of: (a) assembling an unoptimized model of the molecule of interest (via z-matrix input, as described above), then (b) applying a COT to the unoptimized model, and then (c) computing a first-layer COM, next (d) using the output z-matrix of the first-layer COM as the input z-matrix (e.g. ONIOM) on which a second COT acts, then (e) applying a COT to the first-layer COM, and then (f) computing a second-layer COM, next (g) using the output z-matrix of the second-

layer COM as the input z-matrix on which a third COT may act, and so forth. One may expect that such a sequential layering of optimizations would result in a COM that is even closer to being ideal than any one of the COTs could have computed individually. However, it seems that a compounding of errors, as are endemic to the application of computational modeling theory regarding COTs, causes a COM resulting from sequential layering (as described above) to either (a) drift even further from the ideal, or (b) match the same COM that would have been modeled if the last COT applied was the only COT applied and was applied only once. [11, 21, 22]

If a COT is computationally inadequate for the molecule being studied, then the reliability of the COM suffers. Specifically, even the most reliable COTs for modeling organotin(IV) species (LAN2DZ and LAN2MB) do not fully compute the effects of having a tin(IV) atom in a molecule. This means that Gaussian uses default property values for tin(IV) (bond lengths, bond angles, etc.) for each computational iteration. These default values do not include a complete computational representation of tin(IV)'s properties, especially as each tin(IV) atom relates to the other atoms of the molecule (e.g. correlation effects, packing effects, intramolecularity, etc.), which include intramolecular primary and secondary effects (e.g. primary is an atom being affected by a tin atom directly; secondary is an atom which is being affected by an atom that is being affected by a tin atom directly). The lack of full computational treatment of these properties, as compared to the default values applied, results in a loss of COM accuracy relative to the ideal, as will be seen here. [11, 17, 21, 22]

A significant strength of a reliable COM is being able to learn more about a molecule by modeling a structure that was determined by X-ray Crystallography (XRC), solid-state

$^{119}\text{Sn}$  NMR, or other experimental tools than would otherwise be possible with those tools. The number of properties determined experimentally is expanded by applying a reliable COT to generate a COM of the molecule by Gaussian. Thus, Gaussian computes an expanded range of data about the molecular properties by starting with the structural determinations of the experimental methods. [10, 12, 13, 14, 17]

### **2.4.3 COT Validation**

COT validation is a detailed comparative analysis over a range of COTs that quantifies the range of reliability of each COM per each COT applied to the molecule of interest and relative to ideal values (experimentation or lowest global energy of formation, described above). [11, 18, 21, 22] COTs may be selected to represent the rungs on Perdew's Ladder or other considerations. For more common molecules, there is likely a body of published literature, the combination of which may define adequate COT validation. However, fresh validation becomes especially important if the molecule is inorganic, organometallic, not well-studied, or has heavier atoms (described above). [11, 18]

Once a COT has been validated for particular molecules within a molecular type (e.g. thio<sub>n</sub> species within organotin(IV) molecules), then future researchers seeking to optimize similar molecules may use the same COT as an initial method of computing a reliable COM. [11, 18] Future researchers may have to compare fewer COTs to validate the COT of the prior research as being the most reliable. Thus, a COT may become validated as being able to generate reliable COMs for a broader range of molecules. [11, 17, 18, 21, 22, 24]

However, COTs may become validated for particular molecule types if a significant number of publications apply a non-validated COT to the molecular model and get a reliable COM. If so, then future research of similar molecules may apply the same COT

without further validation. Eventually, enough similar molecules may have been modeled using a non-validated COT that a review of prior research would result in an *ex post facto* validation study. [11, 17, 18, 21, 22, 24]

For each thio<sub>n</sub> molecule, 31 COTs (16 with PT and 15 without PT) generated 31 COMs and were validated against experimental data and a reliable COT was found and detailed below. [11, 17, 18, 21, 22, 24]

A COT validation may be successfully completed and yet the application of the validated COT to model a larger organotin(IV) molecule may result in an erroneous model. A molecular model may depict a different conformation or different energy of formation (especially for molecules with low barriers of energy between conformers) if (a) the starting molecular model is subjected to PT or (b) if the starting conformation is changed (bond lengths, bond angles) prior to applying the COT. If the COT validation method includes the above considerations, then COT reliability would be more comprehensively understood. [17, 26, 27, 28, 29, 39, 40]

## **2.5 COT and COM Analysis of Three Series of Organotin(IV) Species Versus X-ray Crystallography**

### **2.5.1 Comparisons of Thio<sub>n</sub> Bond Angles and Bond Lengths**

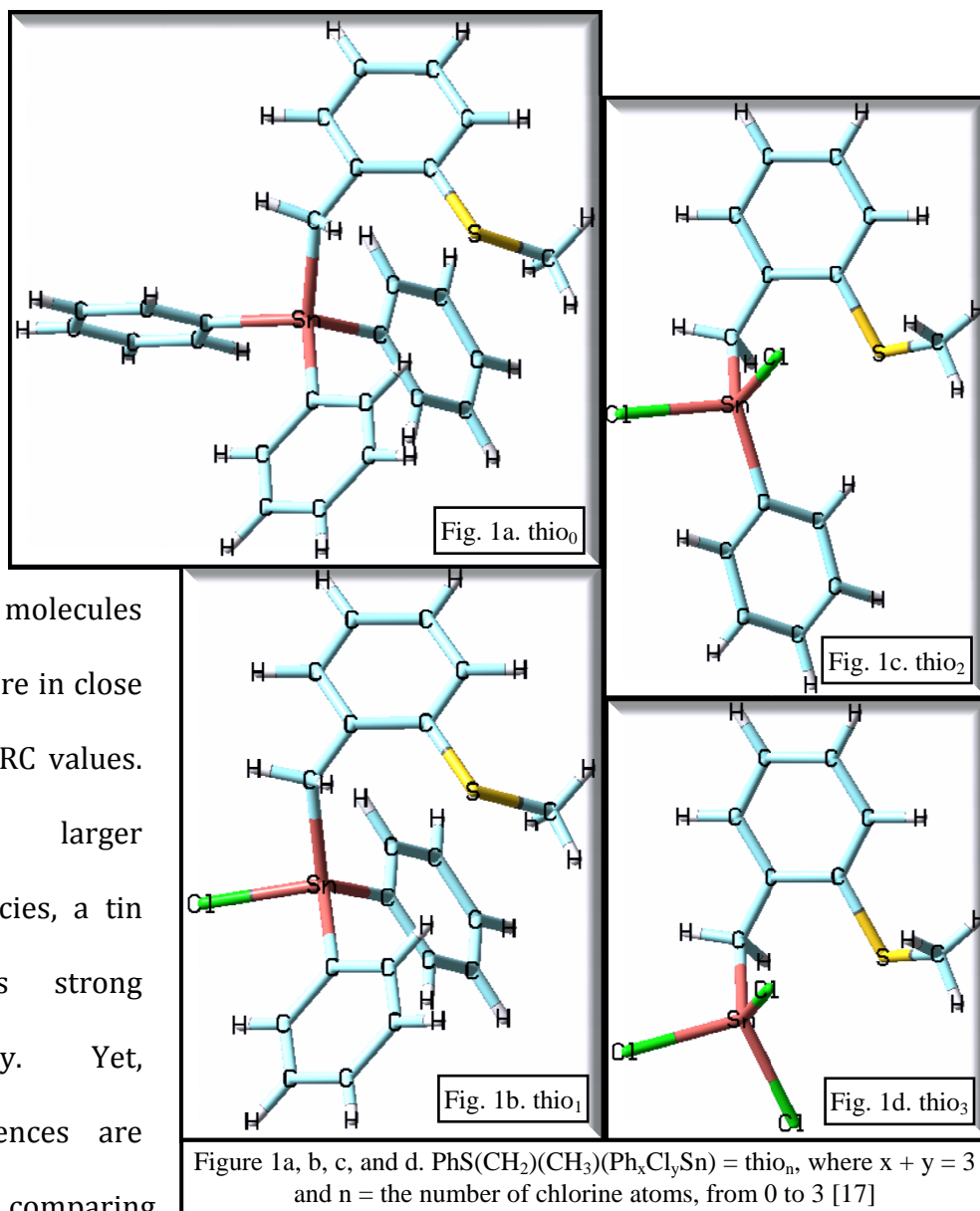
Researched here was a series of medium sized thioether organotin(IV) molecules, PhS(CH<sub>3</sub>)(CH<sub>2</sub>)(Ph<sub>x</sub>Cl<sub>y</sub>Sn), where  $x + y = 3$  (thio<sub>n</sub>, where  $n = 0, 1, 2$ , or  $3$ , equaling the number of chlorine atoms) to find a reliable COT to generate accurate COMs. Figures 1a, 1b, 1c, and 1d depict reliable COMs of thio<sub>n</sub>. COT validation was roughly based on having representation from the various rungs of Jacob's Ladder, via Gaussian. [17, 23, 24] Validation of the thio<sub>n</sub> series was established largely by focusing on thio<sub>2</sub>, because it had

the easiest comparability to published experimental data, including the two most reliable COTs (detailed below). [21, 22, 23, 35, 45, 46] The molecular models generated by COT1 and COT2 were studied relative to experimental data from XRC and solid-state  $^{119}\text{Sn}$  NMR. [10, 12, 13] COT1 is defined as: optimized, density functional theory method, B3LYP (Becke, Lee, Yang, Parr) functional, LANL2DZ (Los Alamos National Laboratories version 2 double-Zeta). COT2 is defined as: optimized, Hartree Fock method, and LANL2DZ basis set.

#### Validation

determined that COT1 is the most reliable COT for thio<sub>n</sub>. [17, 23, 24]

Bond lengths of the organotin(IV) molecules examined here were in close agreement with XRC values. Especially for larger organotin(IV) species, a tin atom introduces strong bond flexibility. Yet, noticeable differences are produced when comparing



highly flexible thio<sub>n</sub> bond angles of a gas phase COM versus a crystalline phase XRC. Also, the overall dipole moment indicates the level to which the molecules are bent (compared to common dipole moment values: CO<sub>2</sub>=0.00D, O<sub>3</sub>=0.53D, and H<sub>2</sub>O<sub>(g)</sub>=1.85D). [10, 12, 15, 17, 25, 35, 45, 46] The current research projects advance the validation of depicting reliable COMs for larger organotin(IV) molecules.

There are differences between the molecular models generated by LANL2MB and LANL2DZ basis sets, even though both are purportedly capable of accounting for the presence of tin. [17] Notably, after applying the basis set, LANL2MB, to thio<sub>n</sub>, the methanethiol sulfur and methyl group are both in the same plane as the central phenyl group, in a neutral ligand conformation; the stannyl ligand forms a mild cis conformation. Whereas, after applying the basis set, LANL2DZ, to thio<sub>n</sub>, the methanethiol sulfur is in the same plane as the central phenyl group and the methyl group juts towards the stannyl ligand, forming a cis conformation.

Thio<sub>n</sub> was examined after applying Hartree Fock, LANL2MB. [17] The methanethiol ligand sets the sulfur in the same plane as the central phenyl group. However, in contrast to the COT, DFT, LANL2MB, the methyl group juts away from the stannyl ligand, forming a trans conformation.

Per XRC and a reliable COM, the thio<sub>n</sub> tetrahedral stannyl structure is not perfect. Further, a ligand chlorine atom assumes an axial position of the tetrahedron opposite sulfur. This conformation seems to be the most logical conformation given the combination of steric effects of the stannyl ligand groups and the intramolecularity of the rest of the molecule (Figures 2, 3, and 4), plus these results agree with experimentally determined values. Seeing the molecular properties (e.g. tetrahedral conformation, S-Sn-Cl alignment,

bond flexibility, etc.) depicted accurately by a COT model increases confidence in the COM it generates. [11, 17, 25, 26, 27, 29, 35, 45, 46]

### **2.5.2 Select Bond Lengths and Bond Angles Compared of $\text{Me}_x\text{Ph}_y\text{SnCl}_2$ , where $x + y = 2$**

Applying COT1 and COT2 to these three molecules of interest yielded reliable results relative to three of the eight molecules from the original research by Buntine, et al.:  $\text{R}_2\text{SnCl}_2$ , where  $\text{R} = x + y = 2$  and  $x = \text{methyl}$  and  $y = \text{phenyl}$ . Of the original molecules, only  $\text{Me}_2\text{SnCl}_2$ ,  $\text{MePhSnCl}_2$ ,  $\text{Ph}_2\text{SnCl}_2$  molecules were researched here so as to examine molecules that had structural similarities to thion. [17, 26, 27, 28]

Tables 1a and 1b show a comparative analysis of two COTs from the original Gaussian 98 data and XRC data (published with the original research) to the current application of the same two COTs Gaussian 03 data. This analysis compared the modeling quality and values of applying COT1 and COT3 to the bond lengths and bond angles of the  $\text{R}_2\text{SnCl}_2$  molecules. Table 1b shows a three-way comparative analysis of current research, the original research, and XRC for COT1 and COT3. This subtractive comparison shows that COT1 yielded the most accurate results relative to the original research. Even so, the current results matched well with original COT results and with the original XRC results. [17, 26, 27, 28]

For all three molecules in the  $\text{R}_2\text{SnCl}_2$  series, the  $\text{R}_2$  components have a smaller R-Sn bond length and a larger R-Sn-R bond angle than do Cl-Sn and Cl-Sn-Cl. The larger bond angle as compared to Cl-Sn-Cl is, at least in part due to steric effects, especially since the R groups are closer to the central tin atom than are the chlorine atoms. However, intramolecularity cannot fully explain why the bond angle difference descends in an order that is the reverse of that expected. The bond angle differences between R-Sn-R from each



molecule's Cl-Sn-Cl is 44° (Me-Sn-Me) to 35° (MePh-Sn-MePh) to 22° (Ph-Sn-Ph). This seems indicative of the energy release due to the polymerization of these molecules noted in the original research. [26]

The COT that yields the best COMs for larger organotin(IV) molecules may also be the best choice for a smaller organotin(IV) molecule. The COT that yielded the best results for thio<sub>n</sub> (a larger organotin(IV) molecular series) was also the best COT for the small R<sub>2</sub>SnCl<sub>2</sub> molecular series relative to X-ray crystallography. Even so, proper validation is needed for future research because the size and type of organotin(IV) molecule may affect which COT will make the best COM, especially for molecules that do not closely resemble an organotin(IV) molecule that has already been validated. [17, 26, 27, 28, 29]

| Table 1a. Shows select bond data of: (a) current research using Gaussian 03 (b) original research using Gaussian 98 and (c) ideal COM values (XRC) after applying COT1 and COT2 to each of these three molecules: Me <sub>2</sub> SnCl <sub>2</sub> , MePhSnCl <sub>2</sub> , and Ph <sub>2</sub> SnCl <sub>2</sub> . [1, 17, 27, 57] |         |               |              |               |              |
|---|---------|---------------|--------------|---------------|--------------|
| Gaussian Parameters Me <sub>2</sub> SnCl <sub>2</sub>   | XRC     | Original COT1 | Current COT1 | Original COT2 | Current COT2 |
| Sn-Cl bond length (Å)   | 2.389   | 2.410         | 2.414        | 2.390         | 2.388        |
| Sn-C bond length (Å)  | 2.120   | 2.120         | 2.116        | 2.110         | 2.106        |
| Cl-Sn-Cl bond angle (°)   | 98.600  | 107.100       | 107.045      | 106.400       | 106.332      |
| C-Sn-C bond angle (°)   | 142.200 | 121.600       | 121.627      | 121.800       | 121.831      |
| Gaussian Parameters MePhSnCl <sub>2</sub>   | XRC     | Original COT1 | Current COT1 | Original COT2 | Current COT2 |
| Sn-Cl bond length (Å)   | 2.335   | 2.410         | 2.412        | 2.390         | 2.385        |
| Sn-C bond length (Å)  | 2.050   | 2.110         | 2.116        | 2.100         | 2.105        |
| Sn-C bond length (Å)  | 2.200   | 2.120         | 2.110        | 2.110         | 2.095        |
| Cl-Sn-Cl bond angle (°)   | 98.600  | 108.800       | 108.799      | 107.700       | 107.669      |
| C-Sn-C bond angle (°)   | 133.000 | 121.200       | 121.223      | 121.200       | 121.150      |
| Gaussian Parameters Ph <sub>2</sub> SnCl <sub>2</sub>   | XRC     | Original COT1 | Current COT1 | Original COT2 | Current COT2 |
| Sn-Cl bond length (Å)   | 2.336   | 2.410         | 2.411        | 2.380         | 2.382        |
| Sn-C bond length (Å)  | 2.105   | 2.110         | 2.108        | 2.090         | 2.092        |
| Cl-Sn-Cl bond angle (°)   | 101.700 | 105.200       | 105.199      | 104.200       | 105.010      |
| C-Sn-C bond angle (°)   | 123.900 | 117.600       | 117.663      | 117.600       | 118.190      |

| Table 1b. Shows a three-way comparative analysis from (a) current research using Gaussian 03 to (b) original research using Gaussian 98 to (c) ideal COM values (XRC) for select data after applying COT1 and COT2 to each of these three molecules: Me <sub>2</sub> SnCl <sub>2</sub> , MePhSnCl <sub>2</sub> , and Ph <sub>2</sub> SnCl <sub>2</sub> . [1, 17, 27, 57] |                                      |   |  |                                      |   |  |
|--|--------------------------------------|---|--|--------------------------------------|---|--|
| Gaussian Parameters<br>Me <sub>2</sub> SnCl <sub>2</sub> Molecular<br>Feature  | Original<br>minus<br>Current<br>COT1 | Original<br>XRC minus<br>Original<br>COT1 | Original<br>XRC minus<br>Current<br>COT1 | Original<br>minus<br>Current<br>COT2 | Original<br>XRC minus<br>Original<br>COT2 | Original<br>XRC minus<br>Current<br>COT2 |
| Sn-Cl bond length (Å)  | -0.0038                              | -0.0210                                   | -0.0248                                  | 0.0017                               | -0.0010                                   | 0.0007                                   |
| Sn-C bond length (Å)   | 0.0039                               | 0.0000                                    | 0.0039                                   | 0.0044                               | 0.0100                                    | 0.0144                                   |
| Cl-Sn-Cl bond angle (°)  | 0.0554                               | -8.5000                                   | -8.4446                                  | 0.0678                               | -7.8000                                   | -7.7322                                  |
| C-Sn-C bond angle (°)  | -0.0272                              | 20.6000                                   | 20.5728                                  | -0.0310                              | 20.4000                                   | 20.3690                                  |
|  |                                      |   |  |                                      |   |  |
| Gaussian Parameters<br>MePhSnCl <sub>2</sub> Molecular<br>Feature  | Original<br>minus<br>Current<br>COT1 | Original<br>XRC minus<br>Original<br>COT1 | Original<br>XRC minus<br>Current<br>COT1 | Original<br>minus<br>Current<br>COT2 | Original<br>XRC minus<br>Original<br>COT2 | Original<br>XRC minus<br>Current<br>COT2 |
| Sn-Cl bond length (Å)  | -0.0024                              | -0.0750                                   | -0.0774                                  | 0.0047                               | -0.0550                                   | -0.0503                                  |
| Sn-C bond length (Å)   | -0.0058                              | -0.0600                                   | -0.0658                                  | -0.0049                              | -0.0500                                   | -0.0549                                  |
| Sn-C bond length (Å)   | 0.0100                               | 0.0800                                    | 0.0900                                   | 0.0148                               | 0.0900                                    | 0.1048                                   |
| Cl-Sn-Cl bond angle (°)  | 0.0013                               | -10.2000                                  | -10.1987                                 | 0.0306                               | -9.1000                                   | -9.0694                                  |
| C-Sn-C bond angle (°)  | -0.0230                              | 11.8000                                   | 11.7770                                  | 0.0497                               | 11.8000                                   | 11.8497                                  |
|  |                                      |   |  |                                      |   |  |
| Gaussian Parameters<br>Ph <sub>2</sub> SnCl <sub>2</sub> Molecular<br>Feature  | Original<br>minus<br>Current<br>COT1 | Original<br>XRC minus<br>Original<br>COT1 | Original<br>XRC minus<br>Current<br>COT1 | Original<br>minus<br>Current<br>COT2 | Original<br>XRC minus<br>Original<br>COT2 | Original<br>XRC minus<br>Current<br>COT2 |
| Sn-Cl bond length (Å)  | -0.0011                              | -0.0740                                   | -0.0751                                  | -0.0020                              | -0.0440                                   | -0.0460                                  |
| Sn-C bond length (Å)   | 0.0022                               | -0.0050                                   | -0.0028                                  | -0.0021                              | 0.0150                                    | 0.0129                                   |
| Cl-Sn-Cl bond angle (°)  | 0.0010                               | -3.5000                                   | -3.4990                                  | -0.8097                              | -2.5000                                   | -3.3097                                  |
| C-Sn-C bond angle (°)  | -0.0628                              | 6.3000                                    | 6.2372                                   | -0.5898                              | 6.3000                                    | 5.7102                                   |

### 2.5.3 Select Bond Lengths and Bond Angles Compared of MeSnCl<sub>3</sub> and Me<sub>3</sub>SnCl

Tables 2a and 2b show a comparative analysis of two COTs from the original Gaussian 98 data and XRC data to the current application of the same two COTs Gaussian 03 data. This analysis compared the modeling quality and values of applying COT1 and COT2 to the bond lengths and bond angles of: MeSnCl<sub>3</sub> and Me<sub>3</sub>SnCl. The current application of COT1 and COT2 yielded accurate results relative to the original research published by Buntine, et al. [17, 29] Table 2b shows a three-way comparative analysis of

current research, the original research, and XRC for COT1 and COT2. This subtractive comparison shows that current COT2 data more closely matches the original research values than XRC. However, current COT1 data is more closely matches XRC. [1, 17, 29]

| Table 2a. Shows select bond data after applying COT1 and COT2 to each of the two molecules: MeSnCl <sub>3</sub> and Me <sub>3</sub> SnCl: (a) current research using Gaussian 03 (b) original research using Gaussian 98 and (c) ideal COM values (XRC) [17, 29] |         |               |              |               |              |
|--|---------|---------------|--------------|---------------|--------------|
| Gaussian Bond Length and Bond Angle Parameters for MeSnCl <sub>3</sub>   | XRC     | Original COT1 | Current COT1 | Original COT2 | Current COT2 |
| Sn-C bond length (Å)   | 2.074   | 2.110         | 2.109        | 2.098         | 2.097        |
| Sn-Cl bond length (Å)  | 2.283   | 2.388         | 2.388        | 2.358         | 2.358        |
| Sn-Cl bond length (Å)  | 2.318   | 2.388         | 2.388        | 2.358         | 2.358        |
| Sn-Cl bond length (Å)  | 2.318   | 2.388         | 2.388        | 2.358         | 2.358        |
| C-Sn-Cl bond angle (°)   | 120.300 | 111.200       | 111.265      | 111.800       | 111.744      |
| C-Sn-Cl bond angle (°)   | 113.500 | 111.200       | 111.265      | 111.800       | 111.744      |
| C-Sn-Cl bond angle (°)   | 113.500 | 111.200       | 111.265      | 111.800       | 111.744      |
| Cl-Sn-Cl bond angle (°)  | 103.580 | 107.700       | 107.619      | 107.100       | 107.106      |
| Cl-Sn-Cl bond angle (°)  | 103.580 | 107.700       | 107.619      | 107.100       | 107.106      |
| Cl-Sn-Cl bond angle (°)  | 99.780  | 107.700       | 107.619      | 107.100       | 107.106      |
| Gaussian Bond Length and Bond Angle Parameters for Me <sub>3</sub> SnCl  | XRC     | Original COT1 | Current COT1 | Original COT2 | Current COT2 |
| Sn-Cl bond length (Å)  | 2.430   | 2.444         | 2.444        | 2.424         | 2.424        |
| Sn-C bond length (Å)   | 2.121   | 2.130         | 2.129        | 2.121         | 2.120        |
| Sn-C bond length (Å)   | 2.126   | 2.130         | 2.129        | 2.121         | 2.120        |
| Sn-C bond length (Å)   | 2.109   | 2.130         | 2.129        | 2.121         | 2.120        |
| Cl-Sn-C bond angle (°)   | 100.600 | 104.700       | 104.661      | 104.600       | 104.587      |
| Cl-Sn-C bond angle (°)   | 99.100  | 104.800       | 104.661      | 104.600       | 104.587      |
| Cl-Sn-C bond angle (°)   | 100.100 | 104.700       | 104.661      | 104.600       | 104.587      |
| C-Sn-C bond angle (°)  | 119.800 | 113.800       | 113.823      | 113.900       | 113.882      |
| C-Sn-C bond angle (°)  | 116.300 | 113.700       | 113.823      | 113.900       | 113.882      |
| C-Sn-C bond angle (°)  | 115.200 | 113.800       | 113.823      | 113.900       | 113.882      |

| Table 2b. A three-way comparative analysis of (a) current research using Gaussian 03 to (b) original research using Gaussian 98 to (c) ideal COM values (XRC) to select data by applying COT1 and COT2 to each of the two molecules: MeSnCl <sub>3</sub> and Me <sub>3</sub> SnCl. [1, 17, 43, 65] |                             |                                  |                                 |                             |                                  |                                 |
|--|-----------------------------|----------------------------------|---------------------------------|-----------------------------|----------------------------------|---------------------------------|
| Gaussian Bond Length and Bond Angle Parameters for MeSnCl <sub>3</sub>   | Original minus Current COT1 | Original XRC minus Original COT1 | Original XRC minus Current COT1 | Original minus Current COT2 | Original XRC minus Original COT2 | Original XRC minus Current COT2 |
| Sn-C bond length (Å)   | 0.0009                      | -0.0360                          | -0.0351                         | 0.0009                      | -0.0240                          | -0.0231                         |
| Sn-Cl bond length (Å)  | -0.0003                     | -0.1050                          | -0.1053                         | 0.0001                      | -0.0750                          | -0.0749                         |
| Sn-Cl bond length (Å)  | -0.0003                     | -0.0700                          | -0.0703                         | 0.0001                      | -0.0400                          | -0.0399                         |
| Sn-Cl bond length (Å)  | -0.0003                     | -0.0700                          | -0.0703                         | 0.0001                      | -0.0400                          | -0.0399                         |
| C-Sn-Cl bond angle (°)   | -0.0650                     | 9.1000                           | 9.0350                          | 0.0560                      | 8.5000                           | 8.5560                          |
| C-Sn-Cl bond angle (°)   | -0.0650                     | 2.3000                           | 2.2350                          | 0.0560                      | 1.7000                           | 1.7560                          |
| C-Sn-Cl bond angle (°)   | -0.0650                     | 2.3000                           | 2.2350                          | 0.0560                      | 1.7000                           | 1.7560                          |
| Cl-Sn-Cl bond angle (°)  | 0.0807                      | -4.1200                          | -4.0393                         | -0.0059                     | -3.5200                          | -3.5259                         |
| Cl-Sn-Cl bond angle (°)  | 0.0807                      | -4.1200                          | -4.0393                         | -0.0059                     | -3.5200                          | -3.5259                         |
| Cl-Sn-Cl bond angle (°)  | 0.0807                      | -7.9200                          | -7.8393                         | -0.0059                     | -7.3200                          | -7.3259                         |
| Gaussian Bond Length and Bond Angle Parameters for Me <sub>3</sub> SnCl  | Original minus Current COT1 | Original XRC minus Original COT1 | Original XRC minus Current COT1 | Original minus Current COT2 | Original XRC minus Original COT2 | Original XRC minus Current COT2 |
| Sn-Cl bond length (Å)  | 0.0000                      | -0.0140                          | -0.0140                         | 0.0001                      | 0.0060                           | 0.0061                          |
| Sn-C bond length (Å)   | 0.0009                      | -0.0090                          | -0.0081                         | 0.0006                      | 0.0000                           | 0.0006                          |
| Sn-C bond length (Å)   | 0.0009                      | -0.0040                          | -0.0031                         | 0.0006                      | 0.0050                           | 0.0056                          |
| Sn-C bond length (Å)   | 0.0009                      | -0.0210                          | -0.0201                         | 0.0006                      | -0.0120                          | -0.0114                         |
| Cl-Sn-C bond angle (°)   | 0.0386                      | -4.1000                          | -4.0614                         | 0.0131                      | -4.0000                          | -3.9869                         |
| Cl-Sn-C bond angle (°)   | 0.1386                      | -5.7000                          | -5.5614                         | 0.0131                      | -5.5000                          | -5.4869                         |
| Cl-Sn-C bond angle (°)   | 0.0386                      | -4.6000                          | -4.5614                         | 0.0131                      | -4.5000                          | -4.4869                         |
| C-Sn-C bond angle (°)  | -0.0226                     | 6.0000                           | 5.9774                          | 0.0177                      | 5.9000                           | 5.9177                          |
| C-Sn-C bond angle (°)  | -0.1226                     | 2.6000                           | 2.4774                          | 0.0177                      | 2.4000                           | 2.4177                          |
| C-Sn-C bond angle (°)  | -0.0226                     | 1.4000                           | 1.3774                          | 0.0177                      | 1.3000                           | 1.3177                          |

## 2.5 Pretreatments

### 2.6.1 Pretreatments Affecting COM Conformations

Application of a pretreatment (PT) accomplishes modeling results that are similar to the often-used method of randomly altering pre-optimization bond angles and bond lengths. However, PT COTs were used here because the effects of PT COTs (as defined here) are reproducible. For consistency of comparability among pretreated molecules, the same PT COT was used for all PT COTs. In the present research, a PT COT includes: optimization,

ground state calculation, semi empirical theoretical method, and AM1 basis set. [17, 26-29, 39, 40]

The purpose of PT, including random alterations, is to arrange the molecular components so that applying a COT generates a COM with a lower total CPU time and greater accuracy of determining the molecular properties than would be achieved without the PT. Furthermore, the intent of random altering is to manually alter the atomic coordinates of the input z-matrix from the pre-optimization molecular bond measurements into atomic coordinates that are supposed to help the COT avoid determining that a conformation is globally optimized when it is only caught in a localized minimum. [17, 26-29, 39, 40] Specifically, “For models having or approximating symmetrical structures, starting models were deliberately perturbed from a symmetric arrangement and allowed to optimize freely. This was done in order to confirm that the optimized structure was indeed the global energy minimized structure.” [17] Random altering is a form of PT and PT is a form of sequential layering of COTs (see above). [21, 22]

#### **2.6.2 R<sub>2</sub>SnCl<sub>2</sub> and MeSnCl<sub>3</sub>/Me<sub>3</sub>SnCl Molecular Series**

As indicated in Tables 1 and 2, two research projects involving computational modeling of organotin(IV) molecules were completed. The projects compared the present COM values, obtained by applying the same two COTs to five molecules of interest to generate COMs, to the values obtained by the original research groups: COT1 (optimized, DFT, B3LYP, LANL2DZ) and COT2 (optimized, HF, LANL2DZ), to the values generated by original research groups. The original research groups examined a total of five organotin(IV) species. Tables 1a and 1b investigate select COM values of three of the molecules of interest: Me<sub>2</sub>SnCl<sub>2</sub>, MePhSnCl<sub>2</sub>, and Ph<sub>2</sub>SnCl<sub>2</sub>. [17, 26, 27, 28, 29, 57] Tables 2a

and 2b investigate select COM values of the remaining two molecules of interest:  $\text{MeSnCl}_3$  and  $\text{Me}_3\text{SnCl}$ . [1, 17, 26, 29, 43, 65] Relative to the prior section on COT validation, comparing the reliability of two COMs was the extent of each original research group's validation.

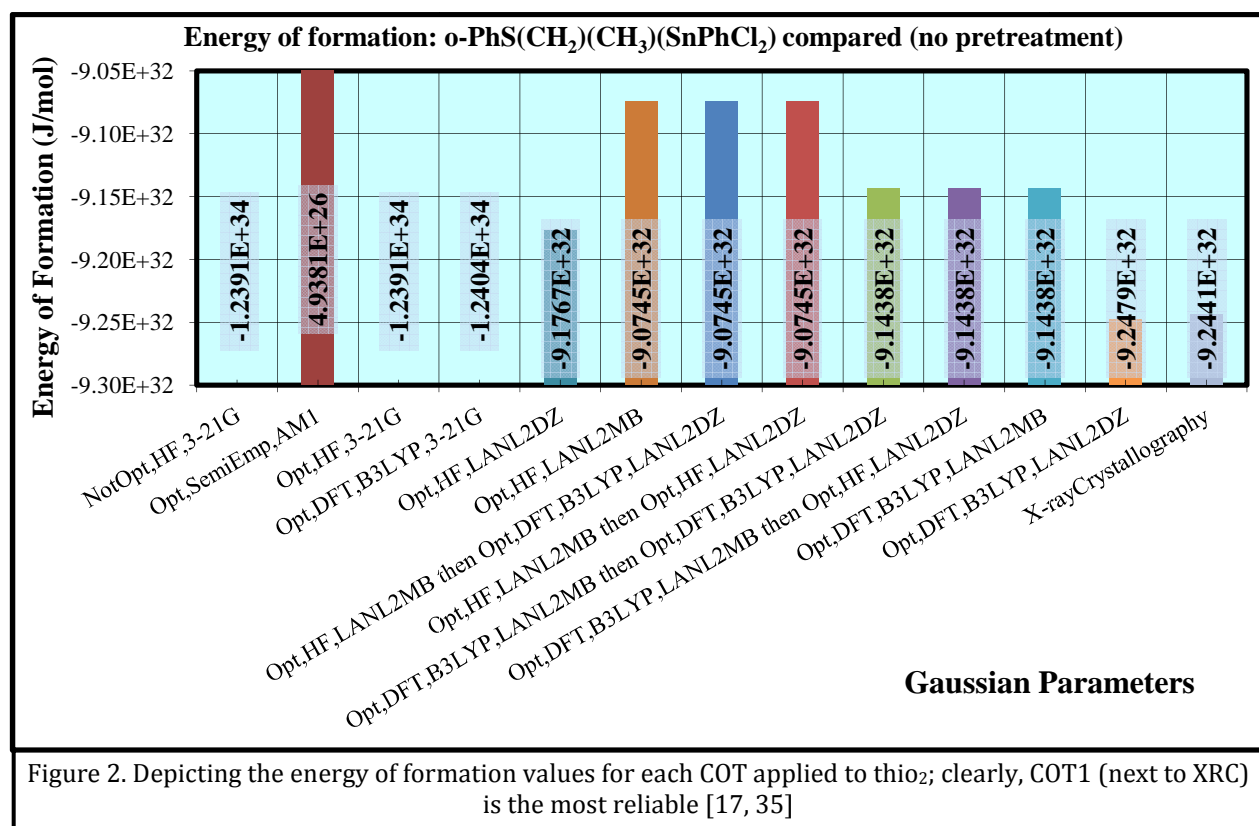
In each project, the original researchers stated that they made preoptimization adjustments to the bond angles and bond lengths of the molecules of interest prior to running the selected COT. [17, 26, 27, 28, 29] The present research ran the original projects selected COT on the same molecules with and without PT (defined above) instead of random adjustments. An analysis revealed that the reliability of the present COM data matched or exceeded those of the original researchers, relative to ideal data. The COT of the current research produced the most reliable COMs, in the least amount of CPU time, without PT or random adjustments.

### 2.6.3 Thio<sub>n</sub> Molecular Series

None of the COT models for thio<sub>2</sub> started or ended in a trans conformation. Even so, seven of the COTs generated COMs that had no ligand aligned with sulfur and tin. Yet, seven of the COTs generated COMs with ligand phenyl groups aligned with sulfur and tin, rather than the chlorine atom that was indicated would be aligned per XRC. [35, 45, 46] Of those seven, six were pretreated models. Only eight of the COTs generated COMs with the S-Sn-Cl alignment and none of them were pretreated models.

Compared to computed XRC values for energy of formation [17], the most reliable COT to generate a COM for thio<sub>2</sub> was COT1 without any PT. As seen in Figure 2, four of the twelve COTs applied were unable to compute a reliable energy of formation value. Of the remaining eight COTs, COT1 was significantly closer to the XRC values. Furthermore, in

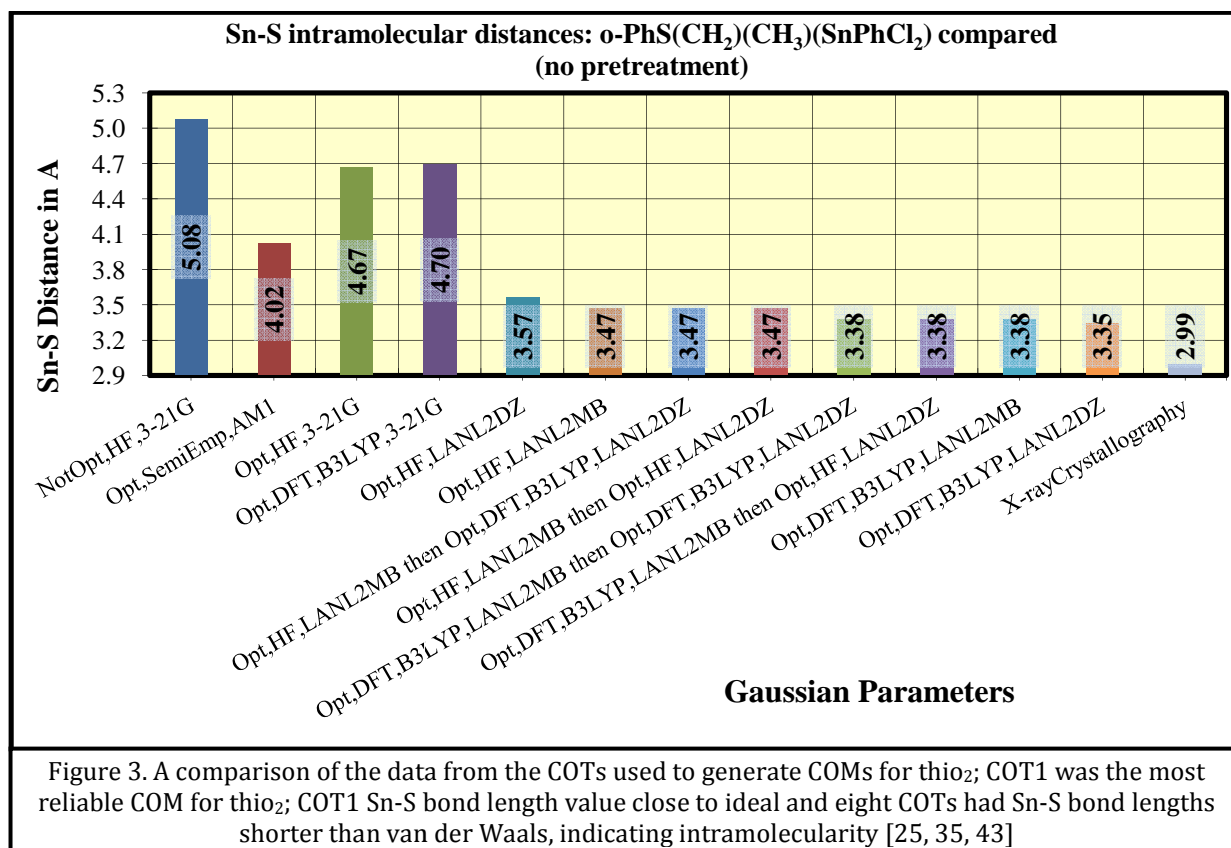
Figure 3, the same eight COTs computed bond lengths that were less than the van der Waals limit. [25, 35, 45, 46] This clearly indicates intramolecular bonding between S and Sn and that COT1 is the most reliable for these types of molecules. Eight of the COTs were identified as generating less accurate, but similar data. It is necessary, especially for larger organotin(IV) models, to consider the reliability of the COMs and the amount of CPU time involved. For these types of molecules, COT1 was determined to generate the most reliable values, without excess CPU time.



## 2.6.4 Pretreatments Affecting CPU Time Requirements

In addition to accuracy issues regarding the research projects noted above, for a COT to compute a reliable COM, Gaussian states that applying a PT is likely to cause the greatest decrease in the total amount of CPU time required as compared to applying (a) random bond adjustments or (b) neither a PT nor adjustments. [17] Table 3 shows a small

sample of the total data obtained, comparing the CPU time required by two COTs to compute COMs for each thio<sub>n</sub>. One column shows the total CPU time required for molecules with PT and another column shows the time required without PT.



Only thio<sub>1</sub> required conformational alignment. Alignment was done by switching the ligand phenyl group with a ligand chlorine atom because the most reliable COT calculated the COM as having a ligand phenyl group in the site known to be occupied by the chlorine atom (per XRC). [10, 12, 13, 17, 35, 45, 46] In Table 3, subsection thio<sub>1</sub>: (a) row one shows the CPU time required for computation of the first COM, (b) the next row shows the time required, after manually adjusting the ligand groups to establish the S-Sn-Cl alignment, to recalculate the COM values, then (c) the third row shows the total CPU time required for determining COM with no PTs for the aligned thio<sub>1</sub> molecule.



Surprisingly, and consistently across all data collected, the results indicate that generating a COM by applying a PT followed by a COT to a z-matrix defined molecule required from two to five times more total CPU time than was required without PT. Plus, PT does not increase the accuracy of the COM values relative to ideal values. This research indicates that PTs do not accomplish the desired goals for these types of molecules.

## 2.6 COT Structural Effects: Hyperconjugation, Hypercoordination, Intramolecularity

### 2.7.1 Hyperconjugation

The present research shows that hyperconjugation-like stabilities are effectual forces in thio<sub>n</sub> molecules. [8, 20, 31, 32, 33, 35, 45, 46] This is evidenced when applying the PT COT to thio<sub>n</sub> because Gaussian states, at the end of each of the PT COT iterations, that the sulfur atom may be hyperconjugated. [17] According to Figures 4 and 5, sulfur is hyperconjugated to tin.

Quantum mechanical modeling proposed that hyperconjugation is the correct explanation for the preference of the staggered conformation, when viewing a molecule per a Newman-like projection, rather than steric hindrance. It is the vicinal attractive and geminal repulsive hyperconjugative effects that keep the molecule in the staggered conformation. [30, 31, 32, 33, 34] Hyperconjugation is a stabilizing interaction between sigma bond electrons and an adjacent non-bonding p-orbital that is at least partially empty, or has an antibonding  $\pi$  orbital or

| Table 3. Total CPU processing times for each thio <sub>n</sub> (a) with and without PT, and (b) before and after thio <sub>1</sub> S-Sn-Cl alignment [17, 35] |                    |                       |
|---|--------------------|-----------------------|
| Total CPU Processing Time (COT1)  | Total Time with PT | Total Time with No PT |
| thio <sub>0</sub> optimized; S-Sn-Cl not misaligned   | 24 hr 37 min       | 9 hr 55 min           |
| thio <sub>1</sub> optimized; S-Sn-Cl misaligned   | 48 hr 50 min       | 5 hr 0 min            |
| thio <sub>1</sub> optimized; S-Sn-Cl aligned and reoptimized  | 64 hr 32 min       | 14 hr 12 min          |
| thio <sub>2</sub> optimized; S-Sn-Cl not misaligned   | 10 hr 24 min       | 1 hr 56 min           |
| thio <sub>3</sub> optimized; S-Sn-Cl not misaligned   | 2 hr 40 min        | 1 hr 44 min           |

filled  $\pi$  orbital. This stabilizing interaction causes the molecule to extend its molecular orbitals, thereby resulting in increased molecular stability over an increased number of bonds. As seen in Figure 4, hyperconjugation is not restricted against organotin(IV) molecules (e.g. thio<sub>n</sub>). Even so, it is a term that is used most often for organic molecules.

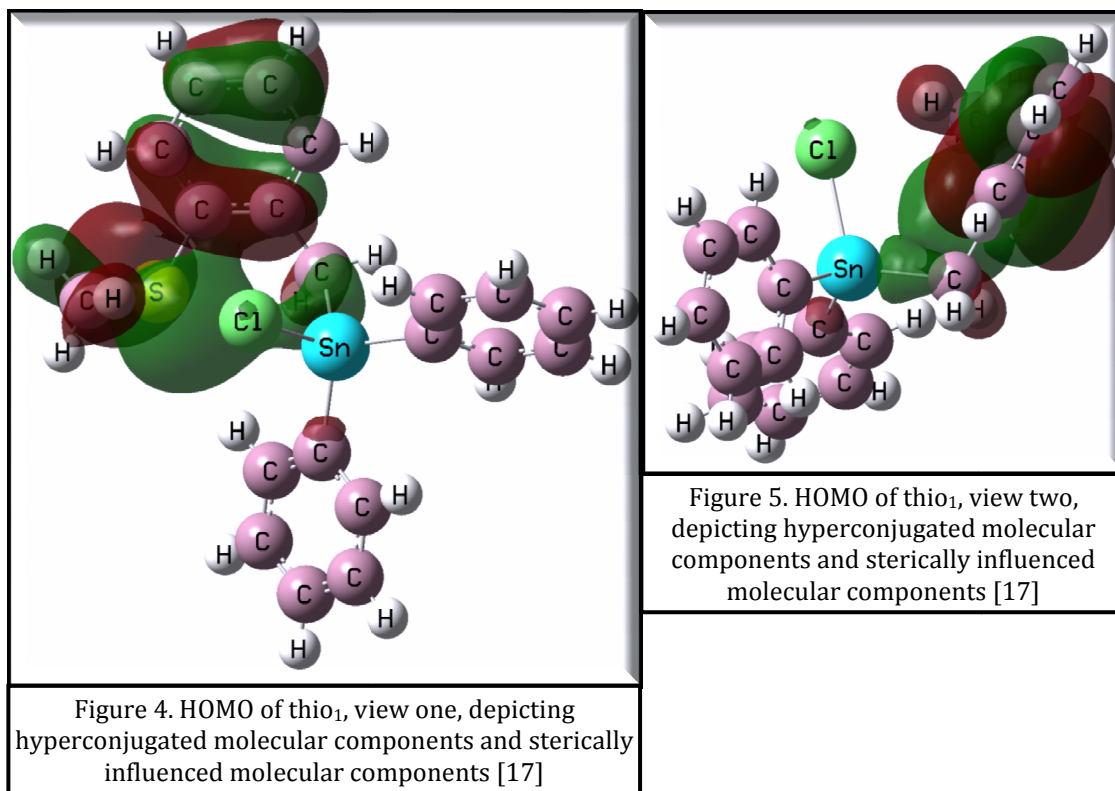
| Table 4. Properties related to bond radii of thio <sub>n</sub> atoms [25] |                           |                      |
|---|---------------------------|----------------------|
| 100 pm = 1 Å  |                           |                      |
| Bond Type   | van der Waals radius (pm) | covalent radius (pm) |
| C-H   | 290                       | 197                  |
| C-S   | 350                       | 179                  |
| Sn-C  | 387                       | 222                  |
| Sn-Cl   | 392                       | 244                  |
| Sn-S  | 397                       | 247                  |

[17, 31, 32, 33]

Thio<sub>n</sub> does not have a carbocation, which is present often for a hyperconjugated molecule. [31, 32, 33, 34] However, a reliable COT has determined (per Gaussian) that Sn in thio<sub>n</sub> has almost a +1 positive charge and is well

within the van der Waals radii for forming an intramolecular bond with sulfur and methylene carbon (Table 4). Furthermore, the calculated electron densities of the thio<sub>n</sub> atoms (a selected few are shown in Table 5) reveal an intramolecular charge imbalance strong enough to expect a hyperconjugation-like effect (Figures 4 and 5). Hyperconjugation typically requires a  $\beta$  relationship between the positively charged atom (Sn) and the atom forming a hyperconjugation bond in order for the positively charged atom to be stabilized. Although tin is not  $\beta$  to sulfur, tin and sulfur share an intramolecular bond, making them  $\alpha$  to each other via that bond (vicinal). Sulfur has two available sigma bonds (filled) and tin is able to receive one of the sigma bonds because of unfilled d orbitals. [8, 20, 31, 32, 33, 34]

| Table 5. Thio <sub>n</sub> Electron Densities for Selected Atoms, Indicators of Hyperconjugation [17] |                   |                   |                   |                   |                   |                   |                   |                   |
|---|-------------------|-------------------|-------------------|-------------------|-------------------|-------------------|-------------------|-------------------|
| Electron Density (Mulliken)   |                   | Pretreated        |                   | Pretreated        |                   | Pretreated        |                   | Pretreated        |
| Thio <sub>n</sub>   | Thio <sub>0</sub> | Thio <sub>0</sub> | Thio <sub>1</sub> | Thio <sub>1</sub> | Thio <sub>2</sub> | Thio <sub>2</sub> | Thio <sub>3</sub> | Thio <sub>3</sub> |
| Sulfur  | 0.138             | 0.138             | 0.124             | 0.170             | 0.111             | 0.173             | 0.163             | 0.163             |
| Tin   | 1.186             | 1.188             | 1.089             | 1.070             | 1.042             | 1.061             | 1.051             | 1.051             |
| Ligand phenyl C (averaged)  | -0.169            | -0.169            | -0.179            | -0.165            | -0.187            | -0.205            | n/a               | n/a               |
| Methylene carbon  | -0.935            | -0.986            | -0.791            | -0.912            | -0.937            | -0.929            | -0.927            | -0.927            |
| Methyl carbon   | -0.803            | -0.803            | -0.939            | -0.808            | -0.784            | -0.797            | -0.788            | -0.788            |
| Chlorine (averaged)   | n/a               | n/a               | -0.402            | -0.396            | -0.386            | -0.376            | -0.346            | -0.346            |



Figures 4 and 5 clearly depict the hyperconjugation of the HOMO electron density of thio<sub>1</sub> to include the central phenyl group, sulfur atom, methyl group, methylene group, and one side of the tin atom. Also depicted, both of the ligand phenyl groups and the chlorine atom are almost completely uninvolved in the HOMO hyperconjugation system of thio<sub>1</sub> (Cl not shown clearly in Figure 4). This indicates that the conformation of lowest energy for the ligand groups is almost entirely decided by steric forces as the ligand rotates about its Sn-methylene C bond. This combination of hyperconjugation and steric influences makes the stannyl ligand more vulnerable to hypercoordination (Figure 4). [8, 17, 20, 31-40]

Each chlorine atom has three available sigma bonds (filled), likely contributing to packing effects and solvent effects for thio<sub>n</sub>. [25, 35, 45, 46] Additionally, each of thio<sub>n</sub>'s methylene and methyl electron acceptor groups has almost a -1 charge. Experimental

evidence found that molecular stability increases with the number of alkyl groups bonded to the charge-bearing atom. [9] Interestingly, ranking the stability of thio<sub>n</sub> COMs, from lowest to highest, would be: thio<sub>3</sub> > thio<sub>2</sub> > thio<sub>1</sub> > thio<sub>0</sub>, which is the inverse of the strength of hyperconjugation, perhaps indicating 1,3 repulsive interactions. [31, 32, 33, 34, 39, 40]

### 2.7.2 Hypercoordination

Researchers claim that much of the attraction between the two ligands is S-Sn hypercoordination in thio<sub>1</sub> and thio<sub>2</sub> (Figures 3 and 5). [35, 36, 45, 46] Although thio<sub>3</sub> has not yet been examined experimentally, based on the present COT research, thio<sub>3</sub> is expected to follow the trend set by thio<sub>1</sub> and thio<sub>2</sub> regarding an expectation of increased hypercoordination bond strength. Also, thio<sub>0</sub> has no chlorine atoms to perform an electron withdrawing function. Hence, thio<sub>3</sub> should form the weakest of the S-Sn hypercoordination bonds in the series and set control values. [35, 36, 37, 38, 39, 40, 45, 46]

Hypercoordinated molecules use electronegative ligands (e.g. methanethiol) to pull enough electron density away from the hypercoordinated atom (e.g. Sn) so that its net electron density is again eight electrons or fewer, thus allowing the hypercoordinated atom to form more than four bonds (in the case of Sn) that are each slightly weaker and longer than typical covalent bonds. Yet, the amount of bond weakening due to hypercoordination varies per molecule. [20, 31, 32, 33, 36, 37, 38]

Prior researchers found that hypercoordination effects of thio<sub>1</sub> and thio<sub>2</sub> were insufficient to explain all of the attraction between the ligands [35, 45, 46]. The current research indicates that the remainder could be: (a) an inductive effect (-I), (b) hyperconjugation, (c) an accumulation of computational errors affecting the depiction of a

reliable COM, where error sources could include per-iteration or pre-treatment. [11, 21, 22, 31, 37, 38, 39, 40]

### 2.7.3 Intramolecularity

| Table 6. Energies of formation and select bond lengths indicate intramolecularity for the bimolecular complex, $\text{Ph}_2\text{POCH}_2\text{Cl} \cdot \text{Ph}_2\text{SnCl}_2$ , determined by COM [16, 17, 25, 26] |                                    |                                 |
|--|------------------------------------|---------------------------------|
| Bimolecular complex energy savings versus each individual molecule   | Energy of formation, COT, (J/mol)  | Molecular dipole moment (Debye) |
| Intact bimolecular complex   | $-2.29283 \times 10^{10}$          | 11.954                          |
| $\text{Ph}_2\text{POCH}_2\text{Cl}$ component  | $-3.58792 \times 10^{10}$          | 6.891                           |
| $\text{Ph}_2\text{SnCl}_2$ component   | $-1.93404 \times 10^{10}$          | 7.942                           |
| Difference due to intramolecular effects   | $-3.22913 \times 10^{10}$          | -2.879                          |
| XRC versus sigma bond lengths (Å); Showing intramolecularity   | Bond length, experimental, XRC (Å) | Bond length, standard (Å) [CRC] |
| Sn-Cl bond length  | 2.523                              | 2.39                            |
| Sn-Cl bond length  | 2.488                              | 2.39                            |
| O-P bond length  | 1.608                              | 1.76                            |
| Sn-O bond length van der Waals versus covalent   | 2.213                              | 2.06                            |
| C-Cl bond length   | 1.883                              | 1.76                            |

Table 6 depicts data from the COMs of a bimolecular complex,  $\text{Ph}_2\text{POCH}_2\text{Cl} \cdot \text{Ph}_2\text{SnCl}_2$  and each of its molecular components. The COMs were created in Gaussian using XRC unit cell data. The COT applied via Gaussian (energy, Hartree Fock, 3-21G) depicted, but did not alter, the XRC conformational data. [16, 17, 26] This COT modeling method makes

significant research data available for bimolecular components and for the combined bimolecular complex.

As computed in Table 6, intramolecularity caused this bimolecular complex to have a lower energy of formation than did the sum of each of the two individual molecular components. Gaussian computes COT energies of formation in a.u. per molecule, conversion to match standard values is: 1 a.u./molecule =  $2.624568 \times 10^6$  J/mole. [25] Analysis of the COT models, XRC values, and CRC Handbook values determined: (a) an intramolecular bond is present between Sn and O, (b) each XRC bond length nearly matches each established single bond length (including Sn-O), and (c) the bimolecular complex is at a lower energy state than are each component calculated separately. [16, 17, 25, 26]

Regarding optimization calculations, in cases where two independent molecules comprise an asymmetrical unit (i.e.  $\text{Ph}_2\text{SnCl}_2 \cdot \text{Me}(\text{Ph})\text{SnCl}_2$ ), there may be no inherent chemical (e.g. kinetic) reasons for multiple conformers in the solid state. So, without crystal packing effects, all molecules (i.e.  $\text{R}_2\text{SnCl}_2$ ) adopt symmetric conformations in their calculated gas-phase structures. Thus, non-systemic solid-state differences in bond distances, typically, are not depicted in the optimized structures. [16, 17, 26, 27, 28, 29]

The above paragraph clearly supports packing effects as an explanation for multiple conformations in the solid state for asymmetrical molecules such as the bimolecular complex or thio<sub>n</sub>. [16, 21, 30, 35, 39, 40, 45, 46] Typically, molecules studied via Gaussian are modeled in the gas phase at 0 K, where they are likely to only display systematic differences. Hence, Gaussian would model intramolecular effects only if such effects are included in the computational considerations. Thus, for asymmetrical molecules, intramolecular and packing effects could apply and yet may not be modeled properly by Gaussian. [17]

## 2.8 Discussion

Below are examples of a few of the types of organotin(IV) research efforts that would likely benefit from developing COTs that are able to generate reliable COMs.

1. Several organotin(IV) thiolates exhibited high *in vitro* levels of antitumor and anti-parasite bioactivity, relative to traditional chemotherapy arsenic derivatives. Yet, the *in vitro* bioactive organotin(IV) thiolates were not as bioactive *in vivo* due to low water solubility. A reliable COM would be helpful towards identifying water soluble, bioactive thiolates based on chemical

properties (e.g. structural geometry, dipole moment, energies of formation, etc.).

[1, 3, 5, 7, 8, 9]

2. 3-methoxypropyl stannanes show promising anti-parasite activity. Conditions determinable by a reliable COM, such as solvents and temperature, are likely influences on which of two conformations are favored: linear monodentate, or cyclic bidentate. The cyclic conformation has a C-O bidentate chelating ligand, which forms an intramolecular partial scorpionate-like bond with the Sn(IV) atom. [10, 36, 41] A reliable COT that may distinguish between the properties of the two conformations would benefit this research.

3. A reliable COM may have anticipated or confirmed the molecular properties of a diethyltin(IV) antitumor agent,  $\text{Ph}_2\text{SnCl}_2(\text{phen})$  as it interacted with DNA. Experimental investigation included using biologically relevant conditions, which indicated that  $\text{Ph}_2\text{SnCl}_2(\text{phen})$  reacts with DNA by electrostatically causing DNA conformation changes, and intercalating and unwinding DNA's double-helix. [5, 42]

4. Reliable COMs may have helped resolve conflicting analytical results of six novel triorganotin(IV) antibiotic complexes (e.g. solvent effects, coordinations, polymerizations, etc.). The complexes were penicillin derivatives that were synthesized and investigated in solid and solution states. [43]

## 2.9 Conclusions

This research has shown that an extensive hyperconjugation system is present in the  $\text{thio}_n$  molecular series. Because this system included molecular components that are not typically considered capable of participating in hyperconjugation, a new aspect of research is opened. Furthermore, the  $\text{thio}_n$  molecules exhibit hyperconjugation and

molecular bond angles that demonstrate strong bending flexibility. [15, 17, 31, 32, 33, 35, 39, 40, 45, 46]

This research has also established that PTs are not recommended for larger organotin(IV) molecules. PTs cause a COT to use more CPU time without generating a better COM. Also, PTs often cause COTs to compute less reliable COMs than would have been generated had the only one COT layer been applied. [17, 21, 22, 26, 27, 28, 29, 39, 40]

Organotin(IV) molecules have many interesting and useful properties that need further COT and COM research. The value of COT and COM research will increase as its usefulness towards developing new applications and understanding existing products increases. Improving the ability of researchers to predict accurately the properties of organotin(IV) molecules, enables an increasing number of research advances regarding the many applications being developed.

One such advance is helping researchers determine which molecules may have the most promise for particular experimental investigations. Another advance is to determine methods to make conducting organotin(IV) research safer for researchers and the environment. As was shown here, regardless of which method is used to input the z-matrix or whether: (a) a layered sequence of COTs (i.e. ONIOM), (b) validation, or (c) PTs were used, developing a reliable COM for the molecule of interest would likely enable faster analyses because the model should indicate the molecular properties that could guide more focused experimental research. As described above, using structural data for a molecule obtained experimentally to enter a z-matrix into molecular modeling software, such as Gaussian, allows Gaussian to model that molecule as though it were *in situ*, such that the number of experimental properties able to be examined is greatly expanded. [17]



## References

1. Buck, Bethany; Mascioni, Alessandro; Que, Lawrence, Jr.; Veglia, Gianluigi (2003) J. Am. Chem. Soc. 125:13316.
2. Buck-Koehntop, Bethany A.; Mascioni, Alessandro; Buffy, Jarrod J.; Veglia, Gianluigi (2005) Journal of Molecular Biology 354:3:652.
3. Pellerito, Claudia; Nagy, Laszlo; Pellerito, Lorenzo; Szorcsik, Attila (2006) Journal of Organometallic Chemistry 691:8:1733.
4. Atanasov, Atanas G.; Nashev, Lyubomir G.; Tam, Steven; Baker, Michael E.; Odermatt, Alex (2005) Environmental Health Perspective 113:11:1600.
5. Chasapis, Christos T.; Hadjikakou, Sotiris K.; Garoufis, Achilles; Hadjiliads, Nick; Bakas, Thomas; Kubicki, Maciej; Ming, Yang (2004) Bioinorganic Chemistry and Applications 2:1:43.
6. Rocha, Willian R.; De Almeida, Katia J.; De Almeida, Wagner B. (2000) Chemical Physics Letters 316:5:510.
7. Bulaj, G.; Kortemme, T.; Goldenberg, D. (1998) Biochemistry 37:25:8965.
8. Billingsley, M. L.; Yun, J.; Reese, B. E.; Davidson, C. E.; Buck-Koehntop, B. A.; Veglia, G. (2006) Journal of Cellular Biochemistry 98:2:243.
9. Davidson, Collin E.; Reese, Brian E.; Billingsley, Melvin L.; Yun, Jong K. (2004) Molecular Pharmacology 66:855.
10. Ruzicka, Ales (2001) Chemicke Listy 95:807.
11. Williams, T. Gavin; DeYonker, Nathan J.; Wilson, Angela K (2008) Journal of Chemical Physics 128:04:4101.

12. Lycka, Antonin; Micák, D.; Holecek, J.; Biesemans, M.; Martins, J. C.; Willem, R. (2000) *Organometallics* 19:703.
13. Harris, R.K. (1996) *Encyclopedia of Nuclear Magnetic Resonance*, D. M. Granty and R. K. Harris editors, v5, John Wiley & Sons, Chichester, UK.
14. Martins, José C.; Mercier, Frédéric A. G.; Vandervelden, Alexander; Biesemans, Monique; Wieruszeski, Jean-Michel; Humpfer, Eberhard; Willem, Rudolph; Lippens, Guy (2002) *Chemistry – A European Journal* 8:15:3431.
15. Engelhardt, Lutz M.; Leung, Wing-Por; Raston, Colin L.; White, Allan H. (1982) *Australian Journal of Chemistry* 35:11:2383.
16. Samskog, Olof; Lee, i Su-hwa; Arroyo, Carmen M.; Kispert, Lowell D.; Geoffrey, Michael (1984) *J. Phys. Chem.* 88:1804.
17. Gaussian 03, Revision C.02, M. J. Frisch, G. W. Trucks, H. B. Schlegel, G. E. Scuseria, M. A. Robb, J. R. Cheeseman, J. A. Montgomery, Jr., T. Vreven, K. N. Kudin, J. C. Burant, J. M. Millam, S. S. Iyengar, J. Tomasi, V. Barone, B. Mennucci, M. Cossi, G. Scalmani, N. Rega, G. A. Petersson, H. Nakatsuji, M. Hada, M. Ehara, K. Toyota, R. Fukuda, J. Hasegawa, M. Ishida, T. Nakajima, Y. Honda, O. Kitao, H. Nakai, M. Klene, X. Li, J. E. Knox, H. P. Hratchian, J. B. Cross, C. Adamo, J. Jaramillo, R. Gomperts, R. E. Stratmann, O. Yazyev, A. J. Austin, R. Cammi, C. Pomelli, J. W. Ochterski, P. Y. Ayala, K. Morokuma, G. A. Voth, P. Salvador, J. J. Dannenberg, V. G. Zakrzewski, S. Dapprich, A. D. Daniels, M. C. Strain, O. Farkas, D. K. Malick, A. D. Rabuck, K. Raghavachari, J. B. Foresman, J. V. Ortiz, Q. Cui, A. G. Baboul, S. Clifford, J. Cioslowski, B. B. Stefanov, G. Liu, A. Liashenko, P. Piskorz, I. Komaromi, R. L. Martin, D. J. Fox, T. Keith, M. A. Al-Laham, C. Y. Peng, A. Nanayakkara, M.

- Challacombe, P. M. W. Gill, B. Johnson, W. Chen, M. W. Wong, C. Gonzalez, and J. A. Pople, Gaussian, Inc., Wallingford CT (2004).
18. Hannachi, Yacine; Barthelat, Jean-Claude; Jolly, Luc-Henry; Silvi, Bernard; Bouteiller, Y. (2004) *International Journal of Quantum Chemistry* 42:3:509.
19. Wann, Derek A. (2005) *Gas-Phase Structures of Molecules Containing Heavy P-Block Elements*, PhD Dissertation, University of Edinburgh.
20. Chen, De-Li; Quan Tian, Wei; Feng, Ji-Kang; Sun, Chia-Chung (2007) *The Journal of Physical Chemistry A* 111:33:8277.
21. Crespo-Otero, Rachel; Montero, Luis Alberto (2005) *Journal of Chemical Physics* 123:13:4107.
22. Hladyszowski, Jerzy (2001) *Cell. Biol. Mol. Letters* 6:2A:398.
23. Perdew, John P.; Schmidt, Karla (2001) *Density Functional Theory and Its Applications to Materials*, V.E. Van Doren, C. Van Alsenoy, and P. Geerlings, editors, American Institute of Physics Conference Proceedings 577 pp 1-20.
24. Mann, J. B. (1968) *Atomic Structure Calculations II. Hartree-Fock Wave Functions and Radial Expectation Values: Hydrogen to Lawrencium*, Report LA-3691, Los Alamos Scientific Laboratory.
25. CRC Handbook of Chemistry and Physics, 74<sup>th</sup> edition, Special Student Edition (1993-94) David R. Lide, Editor-in-Chief, CRC Press, Inc.
26. Buntine, Mark A.; Kosovel, Frances J.; Tiekink, Edward R. T. (2003) *CrystEngComm* 5:58:331.
27. Cox, M. J.; Tiekink, Edward Richard Tom (1997) *Zeitschrift für Kristallographie - New Crystal Structures* 212:351.

28. Dakternieks, D.; Farhangi, Y.; Tiekink, Edward Richard Tom (1998) *Zeitschrift für Kristallographie - New Crystal Structures* 213:397.
29. Buntine, Mark A.; Hall, Veronica J.; Kosovel, Frances J.; Tiekink, Edward R. T. (1998) *J. Phys. Chem. A* 102:2472.
30. Gielen, Marcel (2003) *Journal of the Brazilian Chemical Society* 14:6.
31. McMurry, John (1988) *Organic Chemistry*, 2<sup>nd</sup> edition, Pacific Grove, Calif.: Brooks/Cole.
32. Pophristic, V.; Goodman, L. (2001) *Nature* 411:565.
33. Weinhold, Frank (2001) *Nature* 411:539.
34. Ingold, K.U.; Dilabio, G.A. (2006) *Org. Lett.* 8:592.
35. Munguia, Teresita; Lopez-Cardoso, Marcela; Cervantes-Lee, Francisco; Pannell, Keith H. (2007) *Inorg. Chem.* 46:4:1305.
36. Lebl, Thomas; Zoufalá, Petra; Brun, Clemens (2005) *European Journal of Inorganic Chemistry* 2536.
37. Mitchell, Tracy A.; Finocchio, Debbie; Kua, Jeremy (2007) *J. Chem. Educ.* 84:629.
38. Beckmann, Jens; Dakternieks, Dainis; Duthie, Andrew; Mitchell, Cassandra (2003) *Dalton Transactions* 3258.
39. Gillespie, R. J.; Silvi, B. (2002) *Coord. Chem. Rev.* 233:53.
40. IUPAC Compendium of Chemical Terminology, The Gold Book, 2<sup>nd</sup> Edition (1997) compiled by Alan D. McNaught and Andrew Wilkinson, Blackwell Science, Royal Society of Chemistry, Cambridge, UK.
41. Lebl, Tomas; Smicka, Ales; Brus, Jirí; Bruhn, Clemens (2003) *European Journal of Inorganic Chemistry* 1:143.
42. Li, Q.; Yang, P.; Wang, H.; Guo, M. (1996) *Journal of Inorganic Biochemistry* 64:3:181.

43. Di Stefano, R.; Scopelliti, M.; Pellerito, C.; Fiore, T.; Vitturi, R.; Colomba, M. S.; Gianguzza, P.; Stocco, G. C.; Consiglio, M.; Pellerito, L. (2002) *Journal of Inorganic Biochemistry* 89:3:279.
44. XWINNMR 2.6 is software provided by Bruker for managing NMR spectra.
45. Munguia, Teresita; Pavel, Ioana S.; Kapoor, Ramesh N.; Cervantes-Lee, Francisco; Párkányi, László; Pannell, Keith H., Lewis Acidity of Group 14 Elements Toward Intramolecular Sulfur in Ortho-aryl-thioanisoles *Can. J. Chem.* (2003) 81 11 1388 - 1397.
46. Munguia, Teresita; Cervantes-Lee, Francisco; Parkanyi, Laszlo; Pannell, Keith H., Organotin - Sulfur Intramolecular Interactions: Overview of Current and Past Compounds and the Biological Implications of Sn - S Interactions *ACS Symposium Series* (2006) 917 422 - 435.

## Chapter 3: Changing the Bioactivity of Organotin(IV) Thioether Species

### 3.1 Abstract

Controlling the damaging bioactivity of each molecule of a series of four medium-sized thioether organotin(IV) molecules,  $\text{PhS}(\text{CH}_3)(\text{CH}_2)(\text{Ph}_x\text{Cl}_y\text{Sn})$  (where  $x + y = 3$ ), was researched using computational optimization models (COMs). [30, 37] COMs were evaluated relative to XRC and solid-state NMR as well as a molecular properties comparative analysis. [24, 25, 26] Research of these thioether organotin molecules identified (a) the computational optimization treatment (COT) that generates a reliable COM, (b) complexities of generating reliable COMs for molecules having low energy barriers between conformers, (c) a substitution method to control bioactivity and intramolecularity, and (d) issues influencing COMs, e.g. PTs and pre-optimization conformation changes. [13, 21, 30, 37]

As the thioether organotin(IV) ligand phenyl groups were replaced with Cl atoms, the S-Sn intramolecularity was strengthened and the S-Sn distance decreased and the stannyl tetrahedral structure was deformed from its triphenyl conformation. With each substitution, conformation deformations lowered the molecules damaging bioactivity levels. [13, 17, 21, 37]

### 3.2 Introduction

As their properties *in vivo* are increasingly understood, the structures of bioactive organotin(IV) molecules is being engineered for many purposeful applications. Animals, fungi, and bacteria are highly responsive to bioactive organotin(IV) molecules. Often the biological response to an organotin(IV) species is more efficient and stronger than may be expected from other molecular species with the same effect (e.g. anti-cancer treatments).

Hence, applications of the organotin(IV) molecules are being developed with greater frequency and over a broader range of applications, including: medical, anti-cancer, anti-inflammatory, chelation, agriculture, and biocides. [1, 2, 3, 4, 5, 6, 7, 8, 9, 10]

### **3.3 Bioactivity Discussion of Organotin I, II, III, and IV**

#### **3.3.1 Organotin Toxicities**

Most organotin(IV) compounds are toxic towards animals, fungi, and bacteria. Additionally, the maximum toxic response can be delayed after exposure while the host metabolizes some organotin(IV) compounds. Organotin(III) compounds include the most toxic of all organotin forms. Organotin(II) compounds have very low toxicities. However, organotin(II) species are far more readily absorbed via the intestinal tract than are organotin(IV) species. Organotin(I) compounds have virtually no toxicity. [2, 4, 5, 11, 12]

Controlling the toxic effects of organotin(IV) compounds involves engineering the molecules for optimized properties. Bonding various ligands to organotin(IV) compounds is a significant method of using steric or chemical effects to control the compounds properties. For maximum stability, bioactive organotin(IV) compounds should have available coordination positions around Sn, a relatively stable Sn-ligand bond (e.g. Sn-N and Sn-S), and low hydrolytic decomposition. [4, 5]

#### **3.3.1 Organotin(IV) Toxicities**

Experimental research of organotin(IV) molecules usually requires careful handling to avoid exposure-related health and environment issues. Unlike other environmental neurotoxins (i.e. Hg, Pb, etc.), organotin molecules have unique toxic actions that are highly targeted. Certain mammalian cells dealkylate organotins. The greatest toxicity seems to occur with highly substituted more lipophilic organotins, because lipophilicity allows

easier passage across the cellular membranes than less alkylated types. Polysubstituted organotins show a delayed toxic response due to *in vivo* metabolism into more reactive metabolites. [1, 2, 5, 9, 11] Furthermore, organotin(IV) molecules are used as intermediates in the preparation of other organotin compounds. [12]

### 3.3.2 Organotin(III) Toxicities

The organotin(III) group includes compounds that are tri-coordinated and include the most toxic of all the organotin species (tributyltin and triphenyltin). Unlike other environmental neurotoxins (e.g. methylmercury, lead, etc.), heavy metals, and organometallic compounds, organotin compounds display highly selective activity, damaging specific areas of the neurological system. [1, 2, 5] For example, trimethyltin chloride causes lesions in specific hippocampus and neocortex regions. Yet, triethyltin chloride damages the spinal cord. [2] Dithiols appear to facilitate the selective neurotoxic activity of trimethyltin (TMT) in mammals by triggering neuronal apoptosis in the hippocampus. [5] Even incidental exposure to organotin(III) compounds in humans can cause severe problems, ranging from severe behavioral changes (e.g. disorientation, seizures, and aggressiveness) to death. Such significant specificity is not experienced with the other neurotoxins. [2, 5]

### 3.3.3 Organotin(II) Toxicities

Organotin(II) molecules have no antifungal activity, low toxicity, and low antibacterial activity. They are used in polymer manufacturing, as PVC heat stabilizers, catalysts, in the manufacturing of polyurethane and silicone curing. [1, 5, 13]

For example, organotin(II) molecules may leach from food packaging or water pipes. However, leeching results in concentrations of organotin(II) molecules in food and water



that generally are very low. Hence, it has been concluded that PVC results in a small exposure to organotin(II) molecules. [1, 5, 13]

### **3.3.4 Organotin(I) Toxicities**

Organotin(I) molecules have no biocidal activity and their toxicity to mammals is very low. Methyltin, butyltin, monoestertins, etc. are used as PVC heat stabilizers. [1, 13]

### **3.3.5 Summary of Toxicity Threat Source Vectors**

Organotin(IV) molecules are becoming highly significant in a wide array of industries, such as: cancer treatments, anti-parasites, catalysis, polymers, agriculture, construction, chelation, nanowires, etc. Molecular engineering coupled with molecular models is enabling researchers to harness the highly specific cytotoxicity of organotins. The level of toxicity of alkyltins correlates inversely with the number and length of the alkyl groups bound directly to tin. Unlike other environmental neurotoxins (i.e., methylmercury, lead, *m*-dinitrobenzene, etc.), toxic organotins such as trimethyltin chloride cause lesions in specific hippocampus and neocortex regions and triethyltin chloride damages the spinal cord. [2, 3, 8, 14, 15, 16, 17, 18, 19, 20]

Mammalian organs (i.e. brain, liver, and kidneys) dealkylate organotins to inorganic Sn(IV). Dealkylation causes less stable less harmful alkyltins to break down into more stable more toxic alkyltins. Furthermore, the breakdown rate increases as the alkyltins become more toxic. Ergo, polysubstituted organotins show a toxic action that is delayed by the rate of *in vivo* metabolization. [2, 3, 5, 8, 14, 15, 16, 17, 18, 19, 20]

Cysteine and histidine amino acids appear to be the primary biological ligands for organotin molecules and vicinal dithiols are a main target for organotins. This dithiol preference seems related to toxicity because a small membrane protein, stannin (SNN),

contains vicinal dithiols at the membrane interface. Dithiols appear to facilitate the selective neurotoxic activity of trimethyltin in mammals by triggering neuronal apoptosis in the hippocampus. [2, 3, 7, 8, 14, 15, 16, 17, 18, 19, 20, 21]

An example of organotin(IV) bioactivity includes cellular proteins called stannins. Stannins have amino acid residues (cysteine and cystine), with thiol (cysteines) and dithiol (cystines) moieties. [1, 2, 5, 7, 9, 22] These moieties are concentrated in mitochondria and cellular membrane systems. Although not yet fully understood, these thiol moieties enable highly alkylated organotin molecules to traverse bi-lipid membrane systems (including crossing the blood-brain barrier). Then, stannins of mitochondria attract the organotin(IV) molecules, where the mitochondria significantly dealkylate and thereby bioactivate the molecules. Once bioactive, the organotin molecules cause a cellular apoptosis cascade. [2, 3, 5, 7, 11] Therefore, the cellular presence of stannin thiols are used as indicators that those cells are potentially vulnerable to organotin biological activity. [1, 2, 4, 5, 11, 23]

As explained above, organotin(IV) molecules tend to be very reactive and highly selectively damaging towards certain types of cells *in vivo*. Deliberately building ligands onto an organotin(IV) molecule(s) to control the function of the assembled molecule has enabled great advances in many applications of these molecules (i.e. catalysis, anti-tumor, anti-trypanosome, nanotechnology). A potential source of organotin(III) molecules in food and beverages arises from the use of organotin(III) agricultural biocides and organotin(II) as heat stabilizers in PVC packaging materials. Normally, food does not contain any detectable organotin(III) molecules. In any case, normal processing (i.e. cooking) of food would largely degrade most organotin species that may contaminate food. [1, 12, 13] The amount of organotin molecules necessary to cause damage to a susceptible life form

(mammal, bacteria, etc.) is very low. There are several sources that cause a susceptible life form to be exposed to small amounts of various organotin species. Therefore, it is the accumulated exposure to organotin species from these many small sources that may result in a toxic biological response. [12, 13]

### **3.4 Experimental**

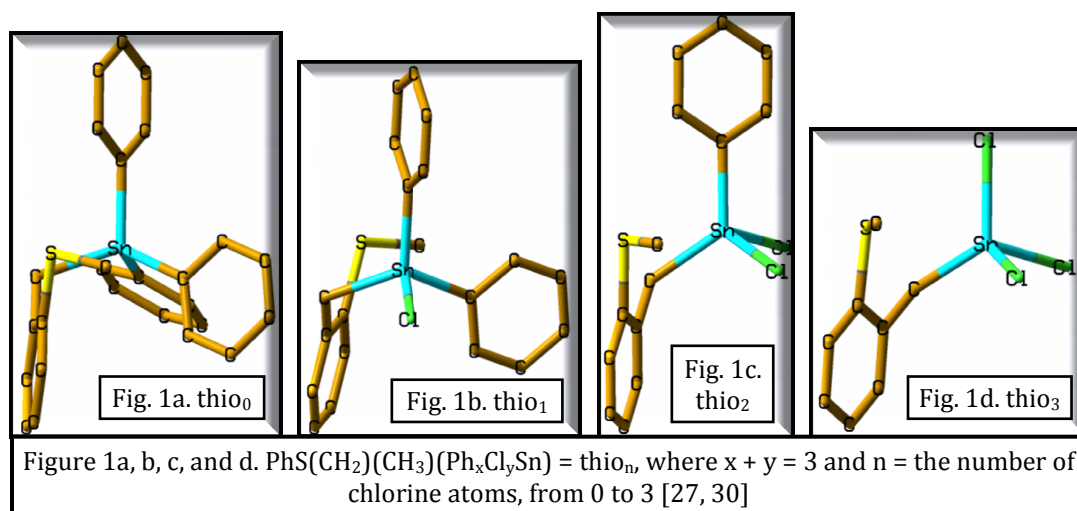
The molecular models were assembled, computational optimization treatments (COTs) were selected, and computational optimization models (COMs) were computed using a combination of Gaussian (Gaussian 03w revision c.02 version 6.1 PC) and GaussView (version 3.0, Gaussian's graphical user interface). Gaussian is a premier computational modeling software for applying COTs to generate COMs with extremely detailed analyses per molecule or molecular system. The accuracy, or reliability, of the COMs for the molecules studied in this research were examined in relation to X-ray crystallography (Bruker Apex Small Molecule X-ray Crystallographer) and solid-state  $^{119}\text{Sn}$  NMR (Avance 250 Digital MAS NMR to an SGI 02 Silicone Graphics Computer using xwinnmr version 2.1). [24, 25, 26, 27, 28, 29, 30]

### **3.5 Introduction to Computational Optimization Treatments (COT)**

A computational optimization treatment (COT) is comprised of the theoretical mathematical parameters that guide the computation of the structures and properties of a molecule and generates a computational optimization model (COM). Typical parameters include: quantum mechanical method (semi empirical, *ab initio*, density functional theory, and hybridized theories), basis set (i.e. 3-21G, SDD, LANL2MB, etc.), charge, and spin. An ideal (or reliable) COT would compute a COM that matches either (a) experimental data, or (b) the global minimum energy of formation. [24, 25, 26, 27, 28, 29]

Such computations, because of their complexity, are normally conducted using high-end computers with advanced modeling software. Recently, Gaussian made available two basis sets, LANL2MB and LANL2DZ. These were the first basis sets designed to accurately compute the structures and properties of molecules such as medium to large organotin(IV) molecules. [30, 31, 32, 33] For the present research, Gaussian was chosen as the most appropriate software for modeling the bioactive thio<sub>n</sub> organotin(IV) molecular series. [30]

### 3.5.1 COTs Applied to a Thioether Organotin(IV) Series (thio<sub>n</sub>)



The present research examined a series of medium sized thioether organotin(IV) molecules, thio<sub>n</sub>,  $\text{PhS}(\text{CH}_3)(\text{CH}_2)(\text{Ph}_x\text{Cl}_y\text{Sn})$  (depicted in Figures 1a, 1b, 1c, and 1d), where  $x + y = 3$  and  $n =$  equals the number of Cl atoms = 0, 1, 2, or 3. The most reliable COT for thio<sub>n</sub> (COT1), relative to XRC, included: Opt (Optimized), LANL2DZ (Los Alamos National Laboratories version 2 double-Zeta), and B3LYP (Becke, Lee, Yang, Parr) without PT (defined below). [30]

Table 1 indicates which COTs were applied to each thio<sub>n</sub> molecule. For nomenclature consistency and clarity, Table 1 COT descriptions include all significant selected parameters. For example, because B3LYP is a subtype of DFT, it may be considered

to be redundant to designate them both. Yet, for completeness in identifying each choice a researcher must make when designating a particular COT, applications of DFT and B3LYP COT parameters are each specified. [30]

Table 1 identifies each of the COTs (including: point source energy, semi-empirical, *ab initio*, and DFT) was applied to thio<sub>n</sub> (with and without PT) so as to identify the most reliable COT relative to XRC and NMR for the thio<sub>n</sub> series. [24, 25, 26, 30, 37] For validation, 12 COTs without PT (PT) and 10 COTs with PT were applied to thio<sub>2</sub>. Also, a subset of these COTs was applied to thio<sub>1</sub> (7 without PT and 11 with PT) to further validate the most

reliable COT for the thio<sub>n</sub>

series. After validation

that COT1 was the most

reliable for thio<sub>n</sub>, only

two of these COTs were

applied to thio<sub>3</sub> (with

and without PT).

Furthermore, after

validation, three COTs

without PT and two

COTs with PT (including

COT1) were applied to

thio<sub>3</sub> to predict XRC. [21,

30, 31, 34, 35, 37]

An example of the

| Table 1. COTs used to generate COMs of thio <sub>n</sub> to identify the most reliable COM relative to XRC [24, 25, 26, 30, 37] |  |
|---|--|
| COT Reference Number  | COTs used to generate COMs of thio <sub>n</sub> molecules  |
| COT1  | Optimized + Density Functional Theory + B3LYP + LANL2DZ  |
| COT2  | Optimized + Density Functional Theory + B3LYP + SDD  |
| COT3  | Optimized + Density Functional Theory + B3LYP + LANL2MB  |
| COT4  | Optimized + Density Functional Theory + B3LYP + 3-21G  |
| COT5  | Optimized + Hartree Fock + LANL2DZ   |
| COT6  | Optimized + Hartree Fock + LANL2MB   |
| COT7  | Optimized + Hartree Fock + 3-21G   |
| COT8  | Energy (Not Optimized) + Hartree Fock + 3-21G  |
| COT9  | (1) Optimized + Density Functional Theory + B3LYP + LANL2MB<br>(2) Optimized + Density Functional Theory + B3LYP + LANL2DZ |
| COT10   | (1) Optimized + Density Functional Theory + B3LYP + LANL2DZ<br>(2) Optimized + Hartree Fock + LANL2DZ                      |
| COT11   | (1) Optimized + Density Functional Theory + B3LYP + LANL2MB<br>(2) Optimized + Hartree Fock + LANL2MB                      |
| COT12   | (1) Optimized + Density Functional Theory + B3LYP + LANL2MB<br>(2) Optimized + Hartree Fock + LANL2DZ                      |
| COT13   | (1) Optimized + Hartree Fock + LANL2MB<br>(2) Optimized + Density Functional Theory + B3LYP + LANL2DZ                      |
| COT14   | (1) Optimized + Hartree Fock + LANL2MB<br>(2) Optimized + Density Functional Theory + B3LYP + LANL2MB                      |
| COT15   | (1) Optimized + Hartree Fock + LANL2MB<br>(2) Optimized + Hartree Fock + LANL2DZ   |
| COT16   | Optimized + Semi-Empirical + AM1   |
| XRC   | X-ray Crystallography  |

comparative analysis for validation is seen in Figure 2. Figure 2 shows the difference between each of the COT applications noted above and XRC values for thio<sub>n</sub> energies of formation. Figure 2 shows that 3-21G basis set fails to model the energy of formation whether using *ab initio* or DFT methods. The DFT method with SDD basis set was also inadequate in Figure 2, as was the semi-empirical method AM1 basis set. [24, 25, 26, 30, 31, 32, 33, 37]

COTs that can generate reliable COMs for thio<sub>n</sub> molecules are especially complex. For the present research, a reliable COT must compute COMs that depict thio<sub>n</sub> molecules experiencing a combination of: intramolecularity, larger size, hyperconjugation, hypercoordination, heavy metal atoms, correlation effects, etc. [21, 30, 34, 35] The COTs applied to thio<sub>n</sub> were chosen to be computationally representative of some of the COTs that are commonly used in the literature to model organotin(IV) molecules. [6, 21, 24] Furthermore, the current research determined that optimization reliability may be affected by (a) the chosen COT parameters (b) series of COTs (layers of COTS and PTs, a.k.a. ONIOM), or (c) the initial conformation of the molecular model.

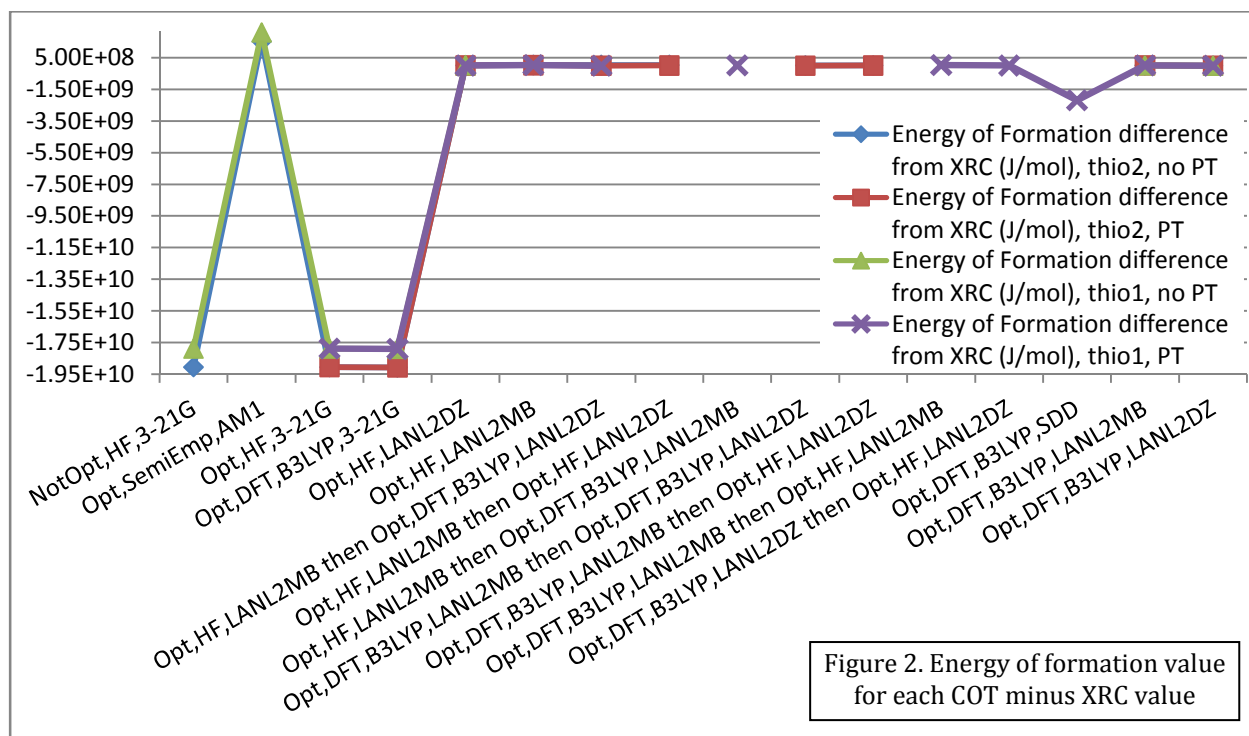


| Table 2. Select bond angles and bond lengths of thio <sub>n</sub> , values as described for Table 1 |                        |                        |                       |                       |                      |                      |
|---|------------------------|------------------------|-----------------------|-----------------------|----------------------|----------------------|
| Bond Angles and Bond Lengths Using COT1   | PT                     | No PT                  | PT                    | No PT                 | PT                   | No PT                |
| Optimized Values for <i>o</i> -PhS(CH <sub>2</sub> )(CH <sub>3</sub> )(Ph <sub>3</sub> Sn)          | Ph-Sn-S Bond Angle (°) | Ph-Sn-S Bond Angle (°) | Ph-Sn Bond Length (Å) | Ph-Sn Bond Length (Å) | S-Sn Bond Length (Å) | S-Sn Bond Length (Å) |
| no S-Sn-Cl realignment  | 155.91                 | 156.35                 | 2.143                 | 2.143                 | 3.906                | 3.900                |
| Optimized Values for <i>o</i> -PhS(CH <sub>2</sub> )(CH <sub>3</sub> )(Ph <sub>2</sub> ClSn)        | Cl-Sn-S Bond Angle (°) | Cl-Sn-S Bond Angle (°) | Cl-Sn Bond Length (Å) | Cl-Sn Bond Length (Å) | S-Sn Bond Length (Å) | S-Sn Bond Length (Å) |
| S-Sn-Cl realignment   | 96.08                  | 73.92                  | 2.437                 | 2.44070               | 3.918                | 3.970                |
| S-Sn-Cl realigned, reoptimized  | 158.86                 | 158.50                 | 2.453                 | 2.454                 | 3.535                | 3.537                |
| Optimized Values for <i>o</i> -PhS(CH <sub>2</sub> )(CH <sub>3</sub> )(PhCl <sub>2</sub> Sn)        | Cl-Sn-S Bond Angle (°) | Cl-Sn-S Bond Angle (°) | Cl-Sn Bond Length (Å) | Cl-Sn Bond Length (Å) | S-Sn Bond Length (Å) | S-Sn Bond Length (Å) |
| no S-Sn-Cl realignment  | 76.49                  | 164.51                 | 2.416                 | 2.435                 | 3.602                | 3.346                |
| Optimized Values for <i>o</i> -PhS(CH <sub>2</sub> )(CH <sub>3</sub> )(Cl <sub>3</sub> Sn)          | Cl-Sn-S Bond Angle (°) | Cl-Sn-S Bond Angle (°) | Cl-Sn Bond Length (Å) | Cl-Sn Bond Length (Å) | S-Sn Bond Length (Å) | S-Sn Bond Length (Å) |
| no S-Sn-Cl realignment  | 169.86                 | 169.88                 | 2.413                 | 2.413                 | 3.190                | 3.189                |

### 3.6 Pretreatment

The COTs noted in Table 1 were used to generate thio<sub>n</sub> models with and without PT (PT). The application of a PT COT effectively accomplishes similar results as the often-applied random shifting of bond angles and bond lengths, but with reproducibility. PT changes the input z-matrix of the molecular components from its original values so that applying the COT: (a) generates a reliable COM with a lower total CPU time, (b) determines more accurate molecular properties than would be found without PT, and (c) avoids misidentifying localized minima as a globally optimized conformation. PT parameters are usually less rigorous than non-PT COTs. PT for the present research: optimization, ground state calculation, semi empirical theoretical method, and AM1 basis set. [21, 30, 35, 37, 41]

Applying PTs does not accomplish the desired goals for these types of molecules, with only one exception, as seen in Table 2. The realignment and reoptimization for thio<sub>1</sub> indicated in Table 2 (may be considered as a COT layering or PT) was done so that each of the COMs may more reliably match the ideal S-Sn-Cl alignments as per XRC. This was necessary to study the bioactivity of thio<sub>1</sub>. [2, 3, 4, 5, 6, 8, 9, 21, 23, 24, 25, 30, 35, 37, 40, 41]

### 3.7 Validation

One goal of the present research is to validate a reliable COT for each molecule in the thio<sub>n</sub> series from among the numerous COTs in Table 1. For more common molecules, there is likely a body of literature, the combination of which may adequately validate a particular COT as generating a reliable COM. However, thio<sub>n</sub> molecules are di-stannyl, not well-studied, and have other complexities (described above) that make validating a COT for thio<sub>n</sub> via literature sources inadequate. Validation was done by generating a COM by applying each of the COTs to an unoptimized model of each assembled thio<sub>n</sub> that was or



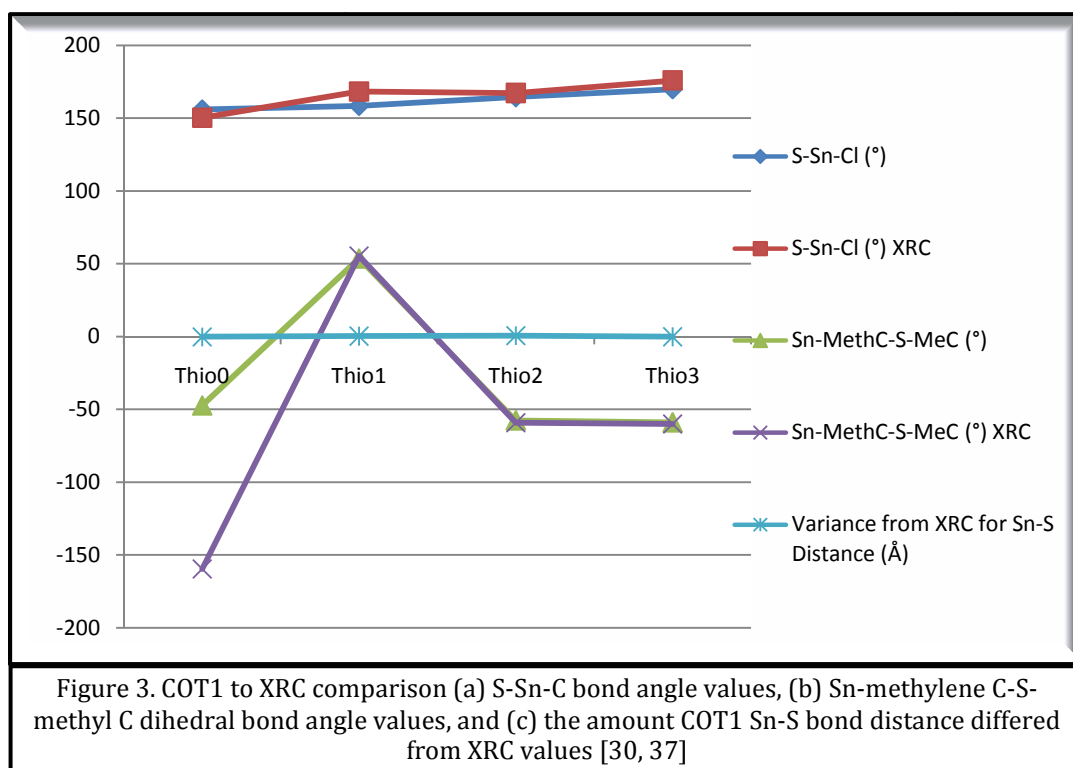
was not pretreated. All of the values from the COMs were then comparatively analyzed relative to experimental values (XRC) and a reliable COT was found (identified above). [21, 24, 25, 30, 31, 34, 35, 36, 37]

### 3.8 Structural Changes Affecting Bioactivity

When examining the starting versus ending conformations of each thio<sub>n</sub>, the differences in the behavior of the molecules as chlorine atoms are substituted for ligand phenyl groups becomes evident. Figures 1a, 1b, 1c, and 1d depict the changes in the stannyl tetrahedral moiety as the substitutions occur. There are two most important measures for thio<sub>n</sub> to determine accuracy of each COM relative to the ideal. The first is the S-Sn-Cl bond angle (Figure 3), which is directly related to the conformations bioactivity capability. The second is the Sn-methylene C-S-methyl C dihedral angle (also in Figure 3), which is a significant measure of the tetrahedral moiety. For thio<sub>n</sub>, a change in this dihedral angle indicates loss of bioactivity. Therefore, validation of COT1 was confirmed through analyzing these two measures for thio<sub>1</sub> and thio<sub>2</sub>. Also, these measures for thio<sub>3</sub> were validated relative to XRC. However, the large set of COTs (see Table 1 and its discussion) was not applied to thio<sub>3</sub>. Furthermore, these measures for thio<sub>3</sub> were not validated because there has not yet been any published XRC analysis on this molecule. The data presented here for thio<sub>3</sub> is predictive. [24, 25, 30, 37]

Analysis of Figure 3 indicates excellent agreement for thio<sub>0</sub>, <sub>2</sub>, and <sub>3</sub> for the S-Sn-Cl bond angle. There was very good agreement for thio<sub>1</sub>. The small difference was likely due to the substitution/realignment method applied to thio<sub>1</sub> (described above). It is possible that energy of formation values with better agreement to XRC would be found if the other ligand phenyl group had been used for substitution. Further, there was excellent agreement

for thio<sub>1</sub>, <sub>2</sub>, and <sub>3</sub> for the dihedral angle indicated. The significant difference for thio<sub>0</sub> is unknown at this time (perhaps the COT under-computed the effects of having the extra ligand phenyl group). Figure 4 displays an overlay of COT1 with XRC values of actual energies of formation for each thio<sub>n</sub>. Furthermore, Figure 4 shows the difference between the energies of formation calculated for each thio<sub>n</sub> using COT1 and experimentally determined by XRC. Analysis of Figure 4 reveals excellent agreement for each thio<sub>n</sub>. [24, 25, 30, 31, 32, 33, 37]



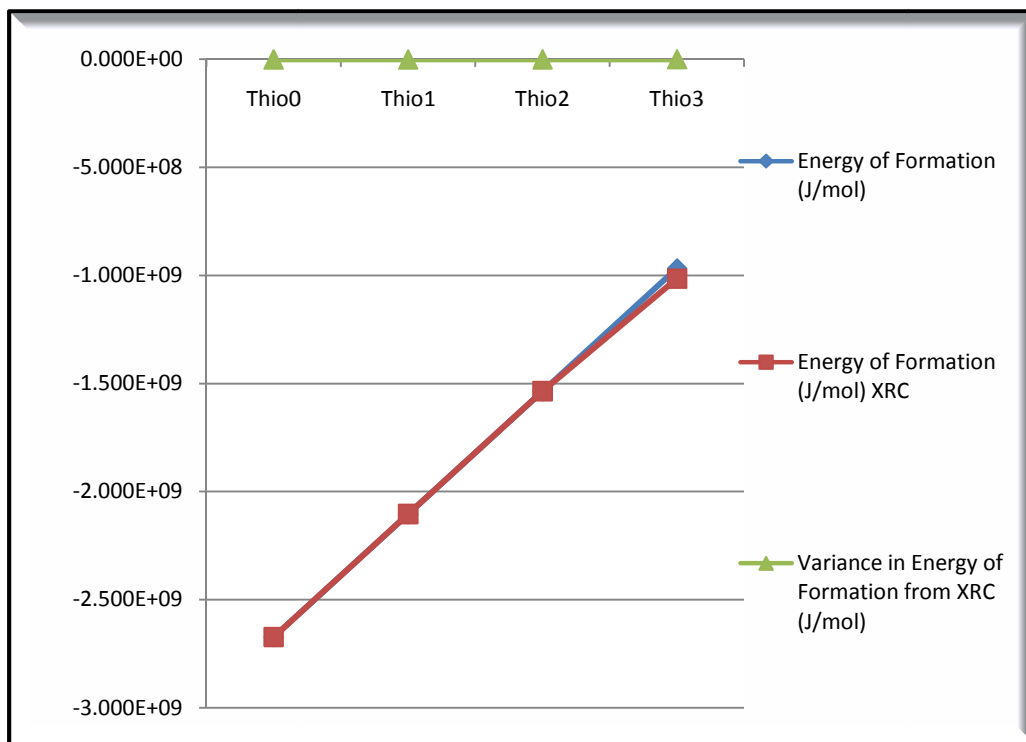


Figure 4. COT1 to XRC comparison of (a) the energy of formation values, (b) the amount of difference in energy of formation [30, 37]

| Table 3. COT1 energies of formation and dipole moments for each thio <sub>n</sub> , with and without pretreatment and for thio <sub>1</sub> , data before and after the substitution realignment of a chlorine atom and ligand phenyl group [30] |                             |                             |                       |                       |
|--|-----------------------------|-----------------------------|-----------------------|-----------------------|
| thio <sub>0</sub>  | PT                          | No PT                       | PT                    | No PT                 |
| COT1 Values for o-PhS(CH <sub>2</sub> )(CH <sub>3</sub> )(Ph <sub>3</sub> Sn)  | Energy of Formation (J/mol) | Energy of Formation (J/mol) | Dipole Moment (Debye) | Dipole Moment (Debye) |
| COT1 values; no S-Sn-Cl realignment  | -2.6816E+09                 | -2.6816E+09                 | 1.61                  | 1.63                  |
| thio <sub>1</sub>  | PT                          | No PT                       | PT                    | No PT                 |
| COT1 values; S-Sn-Cl realignment needed  | -2.1113E+09                 | -2.1113E+09                 | 5.36                  | 2.36                  |
| COT1 values; S-Sn-Cl realigned and reoptimized   | -2.1113E+09                 | -2.1113E+09                 | 5.13                  | 5.14                  |
| thio <sub>2</sub>  | PT                          | No PT                       | PT                    | No PT                 |
| COT1 values; no S-Sn-Cl realignment needed   | -1.5410E+09                 | -1.5410E+09                 | 4.22                  | 5.22                  |
| thio <sub>3</sub>  | PT                          | No PT                       | PT                    | No PT                 |
| COT1 values; no S-Sn-Cl realignment needed   | -9.7066E+08                 | -9.7066E+08                 | 7.12                  | 7.11                  |

As seen in Table 1, approximately sixteen COTs were applied without pretreatment (non-PT) and fifteen COTs were applied with pretreatment (PT) to generate a total of thirty-one COMs for thio<sub>n</sub>. Seven of the thirty-one ending COT model conformations (PT and non-PT) had no ligand aligned with sulfur and tin. Furthermore, seven of the thirty-one ending COT model conformations had the ligand phenyl group aligned with sulfur and tin, rather than the chlorine atom that was indicated would be aligned per XRC. Of those seven, six were from PT COT models. Only eight of the thirty-one ending COT model conformations had the chlorine atom aligned with sulfur and tin and all eight of them were from non-PT COT models. None of the COT models for thio<sub>3</sub> started or ended in a trans conformation. Further, all five of the five ending COT model conformations had a chlorine atom aligned with sulfur and tin. This thio<sub>3</sub> organotin(IV) species has never been analyzed experimentally. The present COT results for thio<sub>3</sub> are anticipatory, based on the accuracy of the results from the other thio<sub>n</sub> species. [21, 30, 35, 41]

| Table 4. Thio <sub>n</sub> Electron Densities for Selected Atoms, Indicators of Hyperconjugation [30] |                   |                   |                   |                   |                   |                   |                   |                   |
|---|-------------------|-------------------|-------------------|-------------------|-------------------|-------------------|-------------------|-------------------|
|   |                   | Pretreated        |                   | Pretreated        |                   | Pretreated        |                   | Pretreated        |
| Electron Density (Mulliken)   | Thio <sub>0</sub> | Thio <sub>0</sub> | Thio <sub>1</sub> | Thio <sub>1</sub> | Thio <sub>2</sub> | Thio <sub>2</sub> | Thio <sub>3</sub> | Thio <sub>3</sub> |
| S   | 0.138             | 0.138             | 0.124             | 0.170             | 0.111             | 0.173             | 0.163             | 0.163             |
| Sn  | 1.186             | 1.188             | 1.089             | 1.070             | 1.042             | 1.061             | 1.051             | 1.051             |
| Ph C (aligned with S-Sn)  | -0.153            | -0.153            | -0.191            | -0.137            | n/a               | n/a               | n/a               | n/a               |
| Ph C (co-planar with S-Sn)  | -0.174            | -0.174            | -0.166            | -0.193            | n/a               | n/a               | n/a               | n/a               |
| Ph C  | -0.180            | -0.179            | n/a               | n/a               | -0.187            | -0.205            | n/a               | n/a               |
| Methylene C   | -0.935            | -0.986            | -0.791            | -0.912            | -0.937            | -0.929            | -0.927            | -0.927            |
| Methyl C  | -0.803            | -0.803            | -0.939            | -0.808            | -0.784            | -0.797            | -0.788            | -0.788            |
| Cl (aligned with S-Sn)  | n/a               | n/a               | n/a               | n/a               | n/a               | n/a               | -0.368            | -0.368            |
| Cl (co-planar with S-Sn)  | n/a               | n/a               | n/a               | n/a               | -0.408            | -0.374            | -0.340            | -0.340            |
| Cl  | n/a               | n/a               | -0.402            | -0.396            | -0.363            | -0.378            | -0.330            | -0.330            |

### 3.9 Intramolecularity and Bioactivity of Organotin(IV)

Specifically, the thio<sub>n</sub> organotin(IV) molecules demonstrated damaging bioactivity in biological systems when the S-Sn intramolecular bond is not present. [37] Furthermore, the S-Sn intramolecularity was strengthened by replacement of ligand phenyl groups with Cl atoms, which moved S and Sn closer together. The sum of the covalent radii of tin and chlorine is normally considered to be 2.44Å° and the sum of the van der Waals radii for these elements is at least 3.92Å°. [38] As the phenyl groups were substituted with Cl, the bioactivity levels of the thio<sub>n</sub> molecules dropped. There is a plane created by the methylene carbon, either one of the ligand phenyl carbons, and chlorine atoms. If there were no intramolecularity between tin and sulfur, then the tin atom would also be in the aforementioned plane. However, intramolecularity with sulfur pulls tin up above the plane. [13, 21, 37]

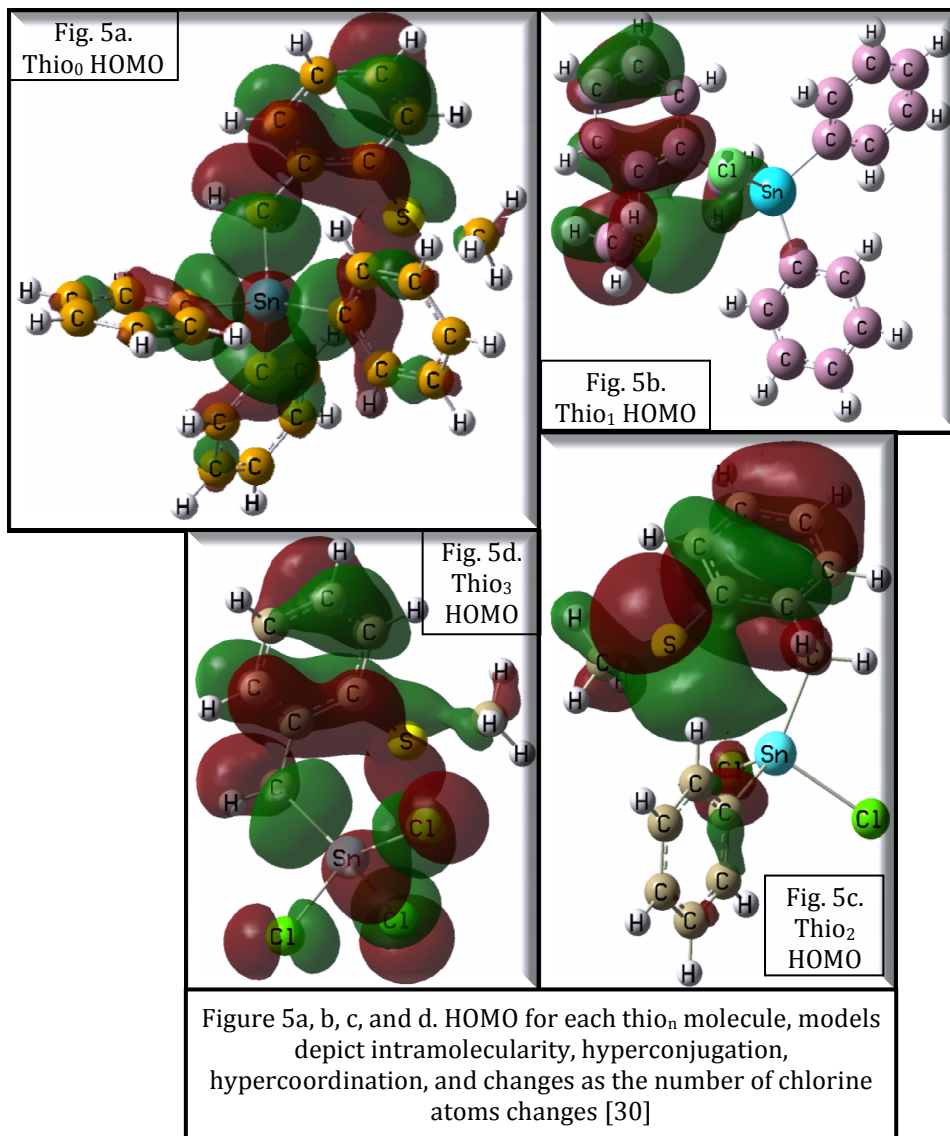
When running the PT that was applied to thio<sub>n</sub>, Gaussian states, at the end of each of the PT computational iterations, that the sulfur atom may be hyperconjugated. Although often used as a term for organic species, hyperconjugation is a stabilizing interaction between sigma bond electrons and an adjacent non-bonding p-orbital that is at least partially empty, or has an antibonding  $\pi$  orbital or filled  $\pi$  orbital. This interaction causes an extension of the molecular orbitals, resulting in an increase of the molecular stability. [23, 30, 33, 37, 39] However, hyperconjugation typically requires a beta relationship. Tin and sulfur are beta to each other through the dihedral described in Figure 3. Other researchers claimed that much of the attraction between the two ligands was S-Sn hypercoordination in thio<sub>1-2</sub>. But, that they were unable to explain all of the attraction

between the ligands [37]. The remaining attraction may be: (a) hyperconjugation of thio<sub>n</sub> that includes sulfur with tin, or (b) a PT error carried forward by the COTs. [23, 30, 33, 39]

To consider hyperconjugation, PT, and electron density, COMs for the present research were computed with and without PT (Table 4). These COMs enable examination of the data in Table 4, which shows the electron densities of select atoms compared with the values of each thio<sub>n</sub> and with PT or non-PT. However, there seem to be no overall trends. Even so, values for thio<sub>1</sub> tend to be strikingly different from thio<sub>0</sub>, <sub>2</sub>, and <sub>3</sub>, especially for PT and especially for S, Sn, and methylene C. The lack of trends makes it impossible to draw conclusions linking structure or behavior to electron density, as computed per Mulliken. Even so, the calculated electron densities of the thio<sub>n</sub> atoms reveal an intramolecular charge imbalance strong enough to expect a hyperconjugation-like effect. [13, 21, 23, 30, 33, 37, 39]

Figures 5a, b, c, and d explain the remaining, unaccounted for S-Sn attraction by depicting the HOMO for each thio<sub>n</sub> molecule. The HOMO electron density of each thio<sub>n</sub> includes extended hyperconjugation with an increasing involvement of the central phenyl group, sulfur atom, methyl group, methylene group, and one side of the tin atom as thio<sub>n</sub> has more chlorine atoms. The molecular structures displaying the least extensive low energy signature as the hyperconjugated area are, in increasing order of HOMO character, the ligand phenyl group that is part of the tetragonal stannyl base, chlorine atom, and the ligand phenyl group that is an apex longitudinally opposite the central phenyl group. Hyperconjugation of thio<sub>n</sub> decreases as the number of chlorine atoms decreases. [13, 21, 23, 30, 33, 37, 39]

Depicted in Figures 5b and 5c, the ligand phenyl groups and chlorine atoms are almost completely uninvolved in the HOMO hyperconjugation system of thio<sub>1</sub> and only slightly more involved in thio<sub>2</sub>. The HOMO hyperconjugation for thio<sub>3</sub> expands to include all molecular components. Yet, the HOMO hyperconjugation of thio<sub>0</sub> only barely includes the thiomethyl ligand and lacks the coherent flow of electron density between its molecular components. This coherent flow (directly related to hyperconjugation) is increasingly present, such that thio<sub>0</sub> < thio<sub>1</sub> < thio<sub>2</sub> < thio<sub>3</sub>. Hence, the conformation of lowest energy of formation has the positioning of the ligand groups decided largely by steric forces as the ligand rotates about its Sn-methylene C bond (Table 3). [13, 21, 23, 30, 31, 32, 33, 37, 39]





### 3.10 Conclusion

This research examined a series of medium sized thioether organotin(IV) molecules,  $\text{PhS}(\text{CH}_3)(\text{CH}_2)(\text{Ph}_x\text{Cl}_y\text{Sn})$ , by applying COTs via Gaussian, as related to XRC and solid-state NMR. Performing a validation for thio<sub>n</sub> molecules revealed one COT that generates the most reliable COMs for these types of molecules. The bond lengths of the organotin(IV) molecules examined here were in close agreement with X-ray crystallographic values. Yet, the high flexibility of thio<sub>n</sub> becomes evident when examining the sometimes noticeable difference between modeled bond angles and X-ray spectra values. [24, 25, 26, 28, 30, 37]

This research has shown that substituting a chlorine atom for a ligand phenyl group alters the conformation of bioactive thioether organotin(IV) molecules. This alteration causes the bioactivity to decrease in strength with each substitution. COT1 generated the best COMs in which the proper Cl-Sn-S alignment occurs, matching XRC. This alignment is one of the crucial molecular features for this species to be bioactive. Generally, COT1 generated the COM that most accurately reflected XRC.

Additionally, this research has shown that thioether organotin(IV) molecules are able to have extended hyperconjugated systems, hypercoordination, and intramolecularity. The hyperconjugated systems may include methyl and methylene groups, which traditionally do not become involved in such systems.

It has been widely believed that applying a PT to a molecular model, before applying a (usually more rigorous) COT, helps to more closely match the above stated ideal criteria. However, it has been established here that the application of a PT does not allow the resultant COMs to more closely match an ideal of either experimental values or the globalized minimum.

Furthermore, having the ability to predict accurately the properties of organotin(IV) species would enable research regarding the many applications of those species. Specifically, there are many examples of types of research efforts that would benefit, by increased efficiency, time saved, and lowered exposure risk, from reliable COT modeling methods for organotin(IV) species. [2, 3, 4, 5, 6, 8, 23, 24, 34, 40, 41, 42]

## References

1. Atanasov, Atanas G.; Nashev, Lyubomir G.; Tam, Steven; Baker, Michael E.; Odermatt, Alex, *Environmental Health Perspective* 113 (2005) 11 1600 - 1606.
2. Buck, Bethany; Mascioni, Alessandro; Que, Lawrence, Jr.; Veglia, Gianluigi, *J. Am. Chem. Soc.* 125 (2003) 13316 - 13317.
3. Bulaj, G.; Kortemme, T.; Goldenberg, D., *Biochemistry* 37 (1998) 25 8965 - 8972.
4. Chasapis, Christos T.; Hadjikakou, Sotiris K.; Garoufis, Achilles; Hadjiliads, Nick; Bakas, Thomas; Kubicki, Maciej; Ming, Yang, *Bioinorganic Chemistry and Applications* 2 (2004) 1 - 2 43 - 54.
5. Davidson, Collin E.; Reese, Brian E.; Billingsley, Melvin L.; Yun, Jong K., *Molecular Pharmacology* 66 (2004) 855 - 863.
6. Di Stefano, R.; Scopelliti, M.; Pellerito, C.; Fiore, Tiziana; Vitturi, R.; Colomba, M. S.; Gianguzza, P.; Stocco, Gian Carlo; Consiglio, Mario; Pellerito, Lorenzo, *Journal of Inorganic Biochemistry* 89 (2002) 3 - 4 279 - 292.
7. Gennari, Alessandra, *Mechanisms of Immunosuppression by Organotin(IV) Species, Apoptosis vs. Proliferative Arrest*, PhD Dissertation (2000) Utrecht University.
8. Lebl, Thomas; Zoufalá, Petra; Brun, Clemens, *Eur. J. Inorg. Chem.* (2005) 2536 - 2544.

9. Pellerito, Claudia; Nagy, Laszlo; Pellerito, Lorenzo; Szorcsik, Attila, Journal of Organometallic Chemistry 691 (2006) 8 1733 - 1747.
10. Shahid, Khadija; Shahzadi, Saira; Ali, Saqib; Mazhar, M., Bulletin of the Korean Chemical Society 27 (2006) 1 44 - 52.
11. Buck-Koehntop, Bethany A.; Mascioni, Alessandro; Buffy, Jarrod J.; Veglia, Gianluigi, Journal of Molecular Biology 354 (2005) 3 652 – 665.
12. International Health Council, Environmental Health Criteria 15, Tin and Organotin Compounds, World Health Organization, Geneva (1980).
13. Gielen, Marcel, Journal of the Brazilian Chemical Society 14 (2003) 6.
14. Keppler, Bernhard K.; Silvestru, Cristian; Haiduc, Ionel, Antitumour Organometallics 1 (1993) 1 73 - 77.
15. Nath, Mala; Yadav, Rakesh; Eng, G.; Nguyen, Thanh-Truc; Kumar, Ashok, Journal of Organometallic Chemistry 577 (1999) 1 1 - 8.
16. Karaoglanidis, G. S.; Karadimos, D. A.; Ioannidis, P. M.; Ioannidis, P. I., Crop Protection 22 (2003) 5 735 - 740.
17. Kinart, Wojciech J.; Kinart, Cezary M., Journal of Organometallic Chemistry 691 (2006) 8 1441 - 1451.
18. Choffat, Fabien, Polystannanes, PhD Thesis (2007) ETH Zurich.
19. Ramirez, A. R.; Parvez, M.; Ahmad, V. U.; Hussain, J.; Hussain H., Acta Cryst. E 58 (2002) 6 278 - 280.
20. Ibach, Rebecca E.; Rowell, Roger M., Holzforschung 55 (2001) 4 358 - 364.
21. Crespo-Otero, Rachel; Montero, Luis Alberto, Journal of Chemical Physics 123 (2005) 13 4107.

22. Mosberg, Henry; Murzin, Aleksey; Henrick, Kim, Orientations of Proteins in Membranes, University of Michigan, <http://opm.phar.umich.edu/protein.php?pdbid=1zza> (2008).
23. Billingsley, M. L.; Yun, J.; Reese, B. E.; Davidson, C. E.; Buck-Koehntop, B. A.; Veglia, G., *Journal of Cellular Biochemistry* 98 (2006) 2 243 – 250.
24. Ruzicka, Ales, *Chemicke Listy* 95 (2001) 807 – 808.
25. Lycka, Antonin; Micák, D.; Holecek, J.; Biesemans, M.; Martins, J. C.; Willem, R., *Organometallics* 19 (2000) 703 - 706.
26. Harris, R.K. (1996) *Encyclopedia of Nuclear Magnetic Resonance*, D. M. Granty and R. K. Harris, editors, v 5, John Wiley & Sons, Chichester, UK.
27. Martins, José C.; Mercier, Frédéric A. G.; Vandervelden, Alexander; Biesemans, Monique; Wieruszeski, Jean-Michel; Humpfer, Eberhard; Willem, Rudolph; Lippens, Guy, *Journal of Chemistry* 8 (2002) 15 3431 - 3441.
28. Engelhardt, Lutz M.; Leung, Wing-Por; Raston, Colin L.; White, Allan H., *Australian Journal of Chemistry* 35 (1982) 11 2383 – 2384.
29. XWINNMR 2.6 is software provided by Bruker for managing NMR spectra.
30. Gaussian 03, Revision C.02, M. J. Frisch, G. W. Trucks, H. B. Schlegel, G. E. Scuseria, M. A. Robb, J. R. Cheeseman, J. A. Montgomery, Jr., T. Vreven, K. N. Kudin, J. C. Burant, J. M. Millam, S. S. Iyengar, J. Tomasi, V. Barone, B. Mennucci, M. Cossi, G. Scalmani, N. Rega, G. A. Petersson, H. Nakatsuji, M. Hada, M. Ehara, K. Toyota, R. Fukuda, J. Hasegawa, M. Ishida, T. Nakajima, Y. Honda, O. Kitao, H. Nakai, M. Klene, X. Li, J. E. Knox, H. P. Hratchian, J. B. Cross, C. Adamo, J. Jaramillo, R. Gomperts, R. E. Stratmann, O. Yazyev, A. J. Austin, R. Cammi, C. Pomelli, J. W. Ochterski, P. Y. Ayala, K. Morokuma, G. A. Voth, P. Salvador, J. J. Dannenberg, V. G. Zakrzewski, S. Dapprich, A. D. Daniels, M. C. Strain, O.

- Farkas, D. K. Malick, A. D. Rabuck, K. Raghavachari, J. B. Foresman, J. V. Ortiz, Q. Cui, A. G. Baboul, S. Clifford, J. Cioslowski, B. B. Stefanov, G. Liu, A. Liashenko, P. Piskorz, I. Komaromi, R. L. Martin, D. J. Fox, T. Keith, M. A. Al-Laham, C. Y. Peng, A. Nanayakkara, M. Challacombe, P. M. W. Gill, B. Johnson, W. Chen, M. W. Wong, C. Gonzalez, and J. A. Pople, Gaussian, Inc., Wallingford CT (2004).
31. Hannachi, Yacine; Barthelat, Jean-Claude; Jolly, Luc-Henry; Silvi, Bernard; Bouteiller, Y., International Journal of Quantum Chemistry 42 (2004) 3 509 – 521.
32. Wann, Derek A., Gas-Phase Structures of Molecules Containing Heavy P-Block Elements, PhD Dissertation (2005) University of Edinburgh.
33. Chen, De-Li; Quan Tian, Wei; Feng, Ji-Kang; Sun, Chia-Chung, The Journal of Physical Chemistry A 111 (2007) 33 8277.
34. Williams, T. Gavin; DeYonker, Nathan J.; Wilson, Angela K, Journal of Chemical Physics 128 (2008) 04 4101.
35. Hladyszowski, Jerzy, Cell. Biol. Mol. Letters 6 (2001) 2A 398.
36. Rocha, Willian R.; De Almeida, Katia J.; De Almeida, Wagner B., Chemical Physics Letters 316 (2000) 5 – 6 510 – 516.
37. Munguia, Teresita; Lopez-Cardoso, Marcela; Cervantes-Lee, Francisco; Pannell, Keith H., Inorg. Chem. 46 (2007) 4 1305 - 1314.
38. CRC Handbook of Chemistry and Physics, 74<sup>th</sup> edition, Special Student Edition (1993-94) David R. Lide, Editor-in-Chief, CRC Press, Inc.
39. McMurry, John (1988) Organic Chemistry, 2<sup>nd</sup> edition, Pacific Grove, Calif.: Brooks/Cole.
40. Li, Qingshan; Yang, Pin; Wang, Hongfei; Guo, Maolin, Journal of Inorganic Biochemistry 64 (1996) 3 181 - 195.

41. Buntine, Mark A.; Kosovel, Frances J.; Tiekink, Edward R. T., CrystEngComm 5 (2003) 58  
331 - 336.
42. Beckmann, Jens; Dakternieks, Dainis; Duthie, Andrew; Mitchell, Cassandra, Dalton  
Transactions (2003) 3258 - 3263.

## Chapter 4: Theoretical Computational Analyses of Organotin(IV) Species with Low Steric Hindrances to Ligand Rotation

### 4.1 Abstract

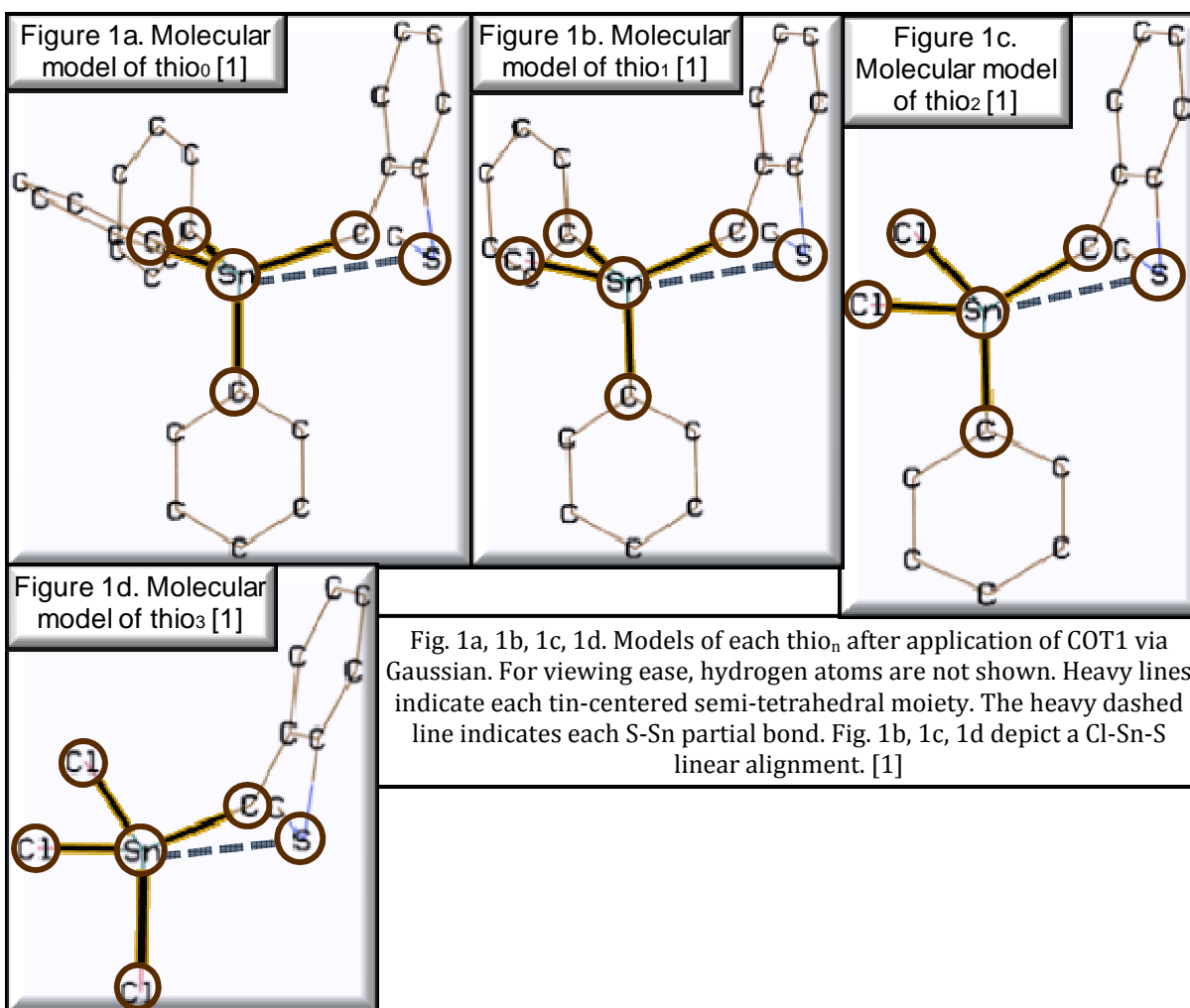
Numerous computational optimization treatments were applied to *o*-1-methylthio-benzyl-2-phenyl<sub>x</sub>chloro<sub>y</sub>stannane (thio<sub>n</sub>). Exhaustive comparative analyses ascertained the accuracies of the models generated from each computational optimization treatment (COT) relative to experimental data (X-ray crystallography and solid-state <sup>119</sup>Sn NMR). Molecular models from such validated COTs may be used as predictive tools for researching properties of organotin(IV) species.

Thio<sub>n</sub> had significant theoretical computational modeling issues. For example, low barriers to ligand rotation caused significant difficulty in accurately modeling thio<sub>n</sub> relative to experimental data. Thio<sub>n</sub> were highly sensitive to initial theoretical modeling conditions, such that the molecular models were often affected.

Establishing which COT generated the most accurate models for each thio<sub>n</sub> molecule was particularly difficult due to the complexities of both species. These complexities included: (a) ligands with very low rotational steric hindrances, (b) strong intramolecularity, (c) large molecules, (d) strong aromaticity with hyperconjugation-like effects, (d) low differences in energies of formation between certain localized and global minima, and (e) conformational sensitivity to initial modeling conditions. However, theoretical computations should consider such complexities, especially in larger organometallic compounds, so that a validated molecular model is a reliable tool, adjunct to experimentation.

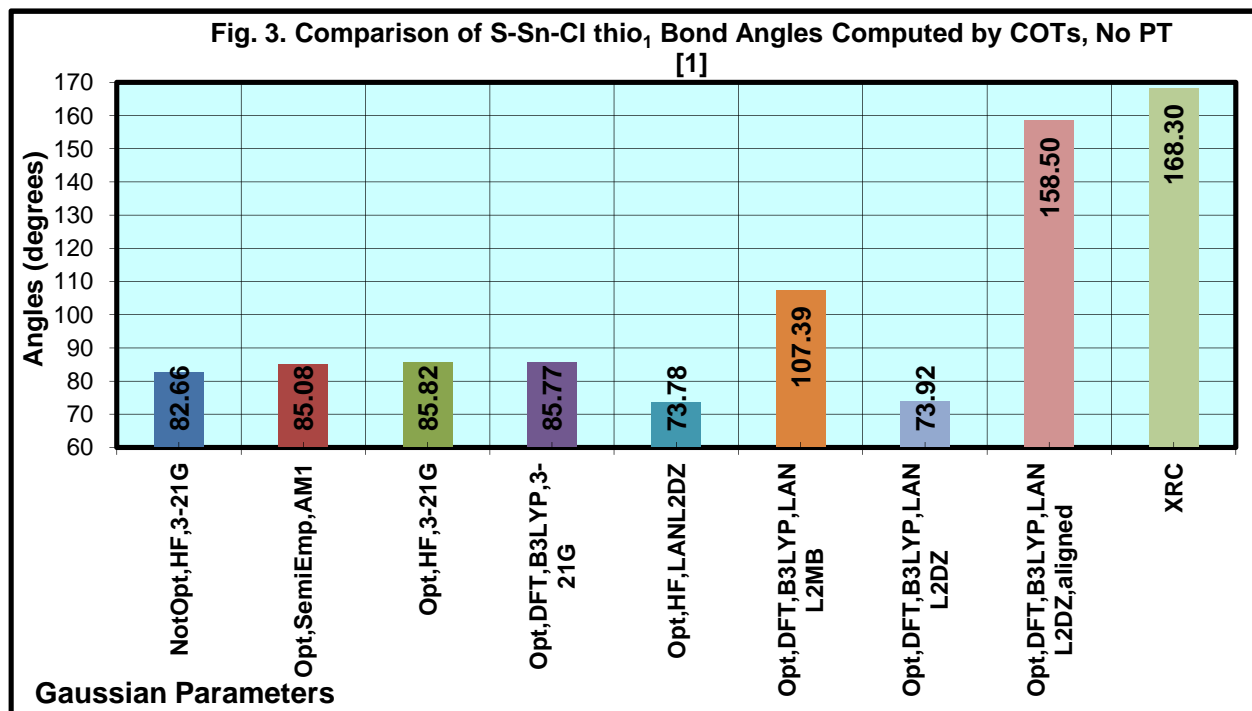
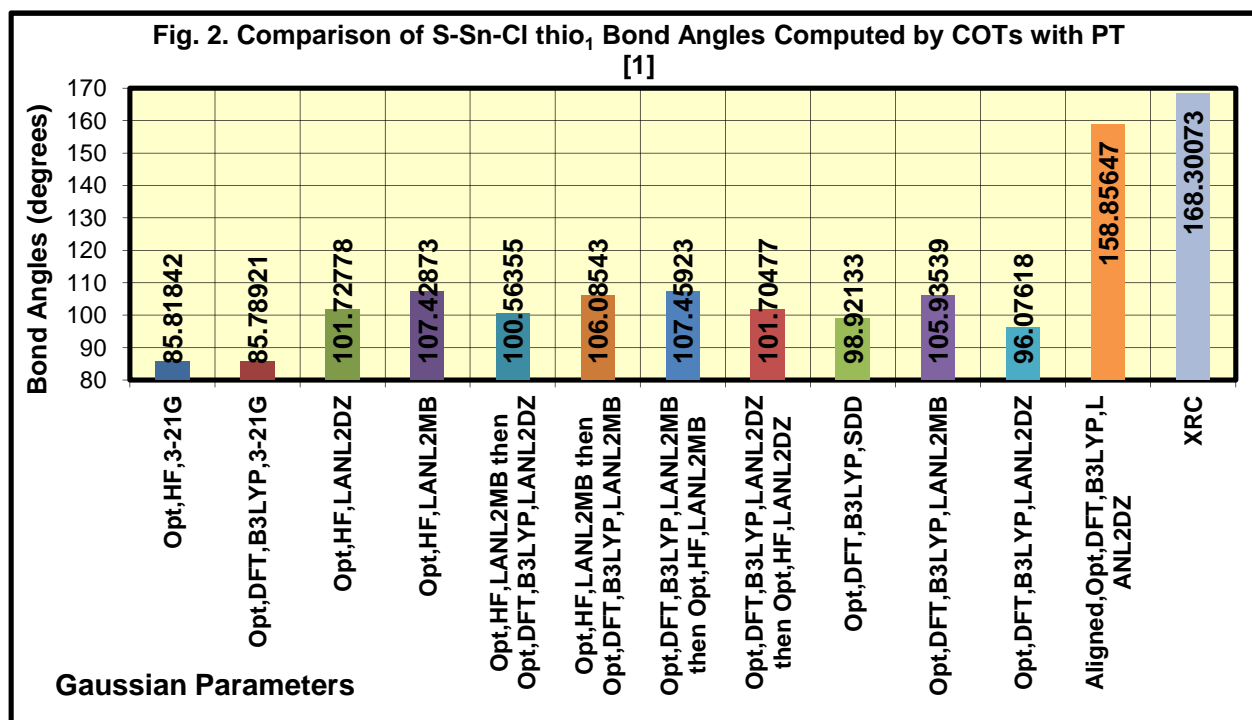
## 4.2 Introduction

Theoretical computational models of the following series of organotin(IV) species was determined to be highly sensitive to (a) pre-optimization conformations of molecular ligands, (b) pre-optimization PTs, and (c) low steric hindrances to rotation. The molecular series investigated was: *o*-1-methylthio-benzyl-2-phenyl<sub>x</sub>chloro<sub>y</sub>stannane (thio<sub>n</sub>) where  $x + y = 3$ ,  $n = 0, 1, 2$ , and  $3$ , and  $n$  equals the number of chlorine atoms (Fig. 1a, 1b, 1c, and 1d). [3, 4, 8]





Indicated in Fig. 2 and Fig. 3, numerous computational optimization treatments (COT) (e.g. semi-empirical, Hartree Fock (HF), density functional theory (DFT), and their



relative basis sets and functionals, as applicable) were selected to represent the most commonly applied (literature) and the most recommended (Gaussian). [1, 19, 22, 23]

Once the selected COTs were applied and a COM was computed for each molecule, then the values were comparatively analyzed against each other and against XRC. As supported by Figure 2 and Figure 3, this research has determined that COT1 generates the most reliable COMs for thio<sub>n</sub>. Using Gaussian 03, COT1 is: optimization, DFT, B3LYP (Becke, Lee, Yang, and Parr), LANL2DZ (Los Alamos National Laboratories version 2 double-Zeta, an Effective Core Potential (ECP) basis set). [1, 19, 22, 23]

### **4.3 Experimental**

Depicted in Table 1 is each computational optimization treatment (COT) (COT numbers 1 through 16 plus XRC as the standard) that was applied to each thio<sub>n</sub> through Gaussian (Gaussian 03w molecular modeling software revision c.02 version 6.1 PC) to generate computational optimization models (COMs). Highly detailed comparative analyses were then done on the resultant data, which identified the relative ability of each COT to generate reliable COMs of each thio<sub>n</sub> conformational structure, relative to X-ray crystallography (Bruker Apex Small Molecule X-ray Crystallographer) and solid-state <sup>119</sup>Sn NMR (Avance 250 Digital MAS NMR to an SGI 02 Silicone Graphics Computer using xwinnmr version 2.1). [1, 5, 6, 10]

| Table 1. COTs used to model thio <sub>n</sub> via Gaussian (with and without PT) to identify COT reliability relative to X-ray crystallography and solid-state <sup>119</sup> Sn NMR [1, 3, 4, 8] |  |
|---|--|
| COT Reference Number  | COTs used to generate COMs of thio <sub>n</sub> molecules  |
| COT1  | Optimized + Density Functional Theory + B3LYP + LANL2DZ  |
| COT2  | Optimized + Density Functional Theory + B3LYP + SDD  |
| COT3  | Optimized + Density Functional Theory + B3LYP + LANL2MB  |
| COT4  | Optimized + Density Functional Theory + B3LYP + 3-21G  |
| COT5  | Optimized + Hartree Fock + LANL2DZ   |
| COT6  | Optimized + Hartree Fock + LANL2MB   |
| COT7  | Optimized + Hartree Fock + 3-21G   |
| COT8  | Energy (Not Optimized) + Hartree Fock + 3-21G  |
| COT9  | (1) Optimized + Density Functional Theory + B3LYP + LANL2MB<br>(2) Optimized + Density Functional Theory + B3LYP + LANL2DZ |
| COT10   | (1) Optimized + Density Functional Theory + B3LYP + LANL2DZ<br>(2) Optimized + Hartree Fock + LANL2DZ                      |
| COT11   | (1) Optimized + Density Functional Theory + B3LYP + LANL2MB<br>(2) Optimized + Hartree Fock + LANL2MB                      |
| COT12   | (1) Optimized + Density Functional Theory + B3LYP + LANL2MB<br>(2) Optimized + Hartree Fock + LANL2DZ                      |
| COT13   | (1) Optimized + Hartree Fock + LANL2MB<br>(2) Optimized + Density Functional Theory + B3LYP + LANL2DZ                      |
| COT14   | (1) Optimized + Hartree Fock + LANL2MB<br>(2) Optimized + Density Functional Theory + B3LYP + LANL2MB                      |
| COT15   | (1) Optimized + Hartree Fock + LANL2MB<br>(2) Optimized + Hartree Fock + LANL2DZ   |
| COT16   | Optimized + Semi-Empirical + AM1   |
| XRC   | X-ray Crystallography  |

#### 4.4 Steric Hindrance, Intramolecularity, and Hyperconjugation Regarding Ligand Rotation for Thio<sub>n</sub>

##### 4.4.1 Steric Hindrance

Common to the molecules in the thio<sub>n</sub> series (Fig. 1a, 1b, 1c, and 1d), each thio<sub>n</sub> has two ligands, and each ligand is singly bonded onto a central phenyl group. Therefore, unless a ligand is limited rotationally by an external force, the ligands would have very low rotational steric hindrances. None of the molecules in this series was sterically prevented from rotating about their single bonds. [1, 3, 4, 8, 13, 15, 16, 19]

#### 4.5.2 Intramolecularity

COMs based on the most reliable COT indicate that the thio<sub>n</sub> ligands have intramolecular interactions with one another that influences which molecular conformations have the lowest energies of formation (Table 2). Energies of formation were determined for each COT1 model of thio<sub>n</sub> (with and without COT PTs). [1] Even so, the calculated differences in energies of formation is very small as the ligands rotate, even though these are larger organotin(IV) compounds with differences in other properties. [1, 3, 4, 8, 12, 13, 14, 15, 16, 19]

#### 4.6 Treatment Layering and CPU Time

The Gaussian online users manual states that applying a COT PT and then applying the COT (resulting in a dual treatment) would help model a molecule with a final conformation that is an even more reliable model than would be obtained with only running the target COT. Furthermore, the Gaussian online users manual states that applying a dual treatment would require less total CPU time than would be required by only running the target COT. However, this research determined that larger organotin(IV) molecules, such as thio<sub>n</sub>, have no improvement in the accuracy of COMs generated by COT PT values relative to the increase in CPU time (PT methods detailed below). Many researchers conducting molecular modeling perform some form of PT (i.e. layering, ONIOM). Yet, other researchers make the common statement that doing so results in valid results while using less CPU time. Although this may be true for other molecule types, this research indicates that it is not true for larger organotin(IV) species. Applying PT to thio<sub>n</sub> caused a two to ten-fold increase in the overall CPU time required for COT1 to compute COMs and a decrease in accuracy for some COTs. [1, 3, 4, 8, 12, 13, 14, 15, 16, 19]

#### 4.7 Thio<sub>n</sub> Conformation, Energy of Formation, and Dipole Moment

| Table 2. Comparative analysis of data from application of COT1 to thio <sub>n</sub> (with and without PT), specifically to compare energies of formation to dipole moments as ligand phenyl groups are substituted with chlorine atoms [1] |                              |                              |                       |                       |
|--|------------------------------|------------------------------|-----------------------|-----------------------|
| Energy of Formation, Dipole Moment thio <sub>n</sub>   | PT                           | No PT                        | PT                    | No PT                 |
| COM values for thio <sub>0</sub>   | Energy of Formation (J/mole) | Energy of Formation (J/mole) | Dipole Moment (Debye) | Dipole Moment (Debye) |
| Cl-Sn-S aligned, no alignment needed   | -2.6742x10 <sup>9</sup>      | -2.6742x10 <sup>9</sup>      | 1.6136                | 1.6305                |
| COM values for thio <sub>1</sub>   | Energy of Formation (J/mole) | Energy of Formation (J/mole) | Dipole Moment (Debye) | Dipole Moment (Debye) |
| Optimized & Misaligned   | -2.1055x10 <sup>9</sup>      | -2.1055x10 <sup>9</sup>      | 5.3648                | 2.3591                |
| Cl-Sn-S Aligned, ReOptimized   | -2.1054x10 <sup>9</sup>      | -2.1054x10 <sup>9</sup>      | 5.1326                | 5.1431                |
| COM values for thio <sub>2</sub>   | Energy of Formation (J/mole) | Energy of Formation (J/mole) | Dipole Moment (Debye) | Dipole Moment (Debye) |
| Cl-Sn-S aligned with no realignment needed   | -1.5367x10 <sup>9</sup>      | -1.5367x10 <sup>9</sup>      | 4.2202                | 5.2168                |
| COM values for thio <sub>3</sub>   | Energy of Formation (J/mole) | Energy of Formation (J/mole) | Dipole Moment (Debye) | Dipole Moment (Debye) |
| Cl-Sn-S aligned with no realignment needed   | -9.6797x10 <sup>8</sup>      | -9.6797x10 <sup>8</sup>      | 7.1159                | 7.1147                |

Regarding Table 2, the energies of formation indicate that there is little difference between the various thio<sub>n</sub> molecules and between different conformers of thio<sub>1</sub>. Furthermore, dipole moments vary significantly between the various thio<sub>n</sub> molecules, as expected.

Also, there is a surprisingly significant variation of dipole moments between the thio<sub>1</sub> conformers and show that the misaligned thio<sub>1</sub> was conformationally incorrect (no PT). As chlorine atoms are substituted for ligand phenyl groups, the energy of formation drops and the dipole moment rises. This is expected because hyperconjugation increases in strength with increased chlorine substitutions and therefore the energy of formation would drop as hyperconjugation increases in strength. Also, as expected, the polarity of thio<sub>n</sub> decreases from thio<sub>3</sub> to thio<sub>0</sub> (no PT). [1, 3, 4, 8, 12, 13, 14, 15, 16, 19]

## **4.8 Pretreatment versus No Pretreatment**

### **4.8.1 Dual COT PT**

As stated above, the issue of whether a COT PT would generate a more reliable model versus only applying a COT was researched. COT PT refers to a pre-COT optimization that often (but, not always) occupies a lower rung on Perdew's Ladder than the COT and then applying the COT. To examine this issue, two sets of sixteen identical initial molecular conformations were built using GaussView (version 3.0, Gaussian's graphical user interface). One set was pretreated by applying the COT PT: optimized, semi-empirical, AM1, and then one each of COT1-16 was applied to each molecule in the set (dual treatment). Also, the other set was not pretreated and one each of COT1-16 was applied to each molecule in the set (single treatment). [1, 20]

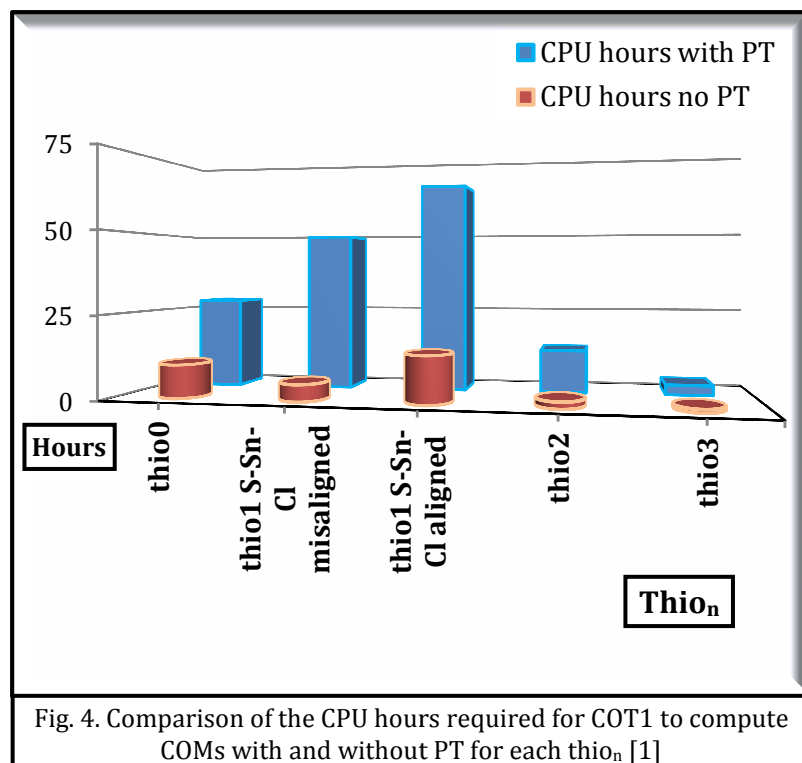
Comparing dual treatment versus single treatment, the post-COT conformations for thio<sub>n</sub> showed moderate to mild differences. Surprisingly, in all cases, the dual COT treatment yielded less reliable COMs than the single COT treatment and required more CPU time to complete computations. [1, 19, 22, 23]

### **4.8.2 Effects of Varying Starting Conformations**

Another type of PT involves the common practice among researchers of randomly adjusting bond angles and bond lengths prior to applying COT. The stated premise of this approach is ostensibly to avoid causing the COM to display a localized minima or other molecular structure that does not match the global minimum or experimental results, because the structure becomes stuck in a non-optimal energy well. This premise was examined here. Specifically, each of the thio<sub>n</sub> molecules was built using GaussView to be modeled by applying the same COT. Applying a reliable COT with and without PT resulted

in the structure of thio<sub>1</sub> not matching experimental values. The optimized structure had to have its larger ligand repositioned to cause the expected Cl-Sn-S alignment, and then COT1 could be reapplied. In order to minimize the number of atoms that were manually repositioned, the positions of a ligand chlorine atom and the ligand phenyl group that was located almost exactly in the position expected for the chlorine atom were switched (alignment). This alignment was accomplished and resulted in a COM with a slightly lower energy of formation than it had before alignment. [1, 3, 4, 8, 12, 13, 14, 15, 16, 19, 22, 23]

A reliable COT is expected to compute a reliable COM for molecules over which the COT is computationally valid. Thus, a reliable COM is expected to have values very near or at either: its energetically lowest conformation or the values of the experimental analysis being modeled. COTs that reliably model larger organotin(IV) molecules, such as COT1 for



thio<sub>n</sub>, complete highly complex computations to define an optimized model. Yet, the computations to model these types of molecules are sensitive to pre-COT conditions. As determined by examining thio<sub>1</sub>, applying a reliable COT may result a significantly

different conformation depending on the relative positioning of ligands, especially for molecules having low conformational energy barriers. [1, 19, 22, 23]

#### 4.8.3 Issues Affecting Dipole Moments and CPU Processing Duration

Fig. 4 depicts comparative effects on dipole moments and total CPU processing times for models of thio<sub>n</sub> when two assembly methods were used. Both methods (defined above) are graphically depicted in Fig. 4, which depicts a comparative examination of the dipole moments of thio<sub>n</sub> COM, computed with and without PT relative to CPU processing time. The dipole moment comparison in Table 2 shows that thio<sub>0, 2, 3</sub> needed no alignment and thio<sub>1</sub> data from before and after alignment. This research indicates that PT significantly affects model values. [1, 3, 4, 8, 12, 13, 14, 15, 16, 19, 22, 23]

- a. As discussed above, the data resulting from the models of thio<sub>1</sub> are more complicated than and have unique differences from those of the other thio<sub>n</sub> COMs (e.g. thio<sub>1</sub> was the only thio<sub>n</sub> requiring alignment).
  - i. Table 2 indicates that the PT model of thio<sub>1</sub> resulted in a dipole moment that was approximately 3 D higher than the no PT model for the most reliable COT. This difference in dipole moment is almost twice the order of magnitude as that of water vapor [11], which means the dipole shift from no PT to PT was very high.
  - ii. Once the Cl-Sn-S alignment was completed for thio<sub>1</sub>, the dipole moment of the aligned model, without PT was ~1.4 D higher and with PT was ~1.1 D lower than pre-alignment values.
  - iii. Finally, of the aligned models, the dipole moment for the model without PT was ~1.4 D higher and with PT was ~0.9 D higher than the non-reoptimized values.



b. The thio<sub>2</sub> conformation generated by COT1 revealed that the no PT model had a much higher dipole moment than the PT model (~1.0 D).

c. Finally, Gaussian modeled the conformation for thio<sub>0</sub> and thio<sub>3</sub>. As expected, the no PT models for both had almost identical dipole moments to their PT models.

Dipole moments for thio<sub>n</sub> seem to coincide with expectations. As indicated in Fig. 1a, 1b, 1c, 1d, dipole moment is also an indication of molecular bending. As the ligand phenyl groups were substituted with chlorine atoms, the intramolecular Sn-S bond became shorter, thus indicating a stronger bond. Therefore, thio<sub>0</sub> should be less bent than thio<sub>1</sub>, than thio<sub>2</sub>, than thio<sub>3</sub>. The data from Table 2 confirm this expectation. [1, 3, 4, 8, 13, 15, 16, 19, 22, 23]

#### **4.9 Mulliken Charges and Electron Densities**

For thio<sub>n</sub>, Gaussian computed each atomic electron density for each molecule as a Mulliken Charge (nominal charge). For a given atom, the Mulliken charge describes electronic density and is based on the decomposition of Kohn-Sham eigenstates into localized atomic orbitals. In contrast, the effective charge describes vibrational properties and thereby molecular chemical bonding. [1, 18] Electron density influences the reactivity levels of active sites, which may affect intramolecularity. [9, 13, 15, 16, 19] Hypercoordinated organotin compounds tend to extend their coordination sphere when bound to electronegative atoms or groups. [11, 12, 13, 14, 15]

Intramolecular Mulliken charges for thio<sub>n</sub> showed a high electron density (charge) range of approximately  $\pm 1$ . There were electron density similarities, even though molecular sizes ranged from medium to large. Tin atoms showed the greatest positive charges and methylene carbon atoms showed greatest negative charges in each thio<sub>n</sub> molecule. As

chlorine atoms substituted for phenyl groups in thio<sub>n</sub>, the tin atoms showed only a slight increase in electron density. The molecules in these series are very polar. [1, 3, 4, 8, 12, 13, 14, 15, 16, 18, 19]

#### 4.10 X-ray Crystallography

As stated in the Experimental section, X-ray crystallographic data were generated by the single crystal method. [5, 6, 12] Gaussian significantly enhanced the analytical utility of X-ray crystallography by generating data using the exact X-ray crystallographic structures. [1, 3, 4, 5, 6, 8, 12] Note, the COT model of thio<sub>3</sub> is predictive because it lacks X-ray crystallography (or other experimental data, such as solid-state <sup>119</sup>Sn NMR). [1]

#### 4.11 Conclusions

A result of the COT analyses is that reliable organotin(IV) models may be made with predictive capabilities (thio<sub>3</sub>, for example). Even so, analyses show that the COT output characteristics of each thio<sub>n</sub> molecule can be affected by varying the input conformations. Such considerations could alter a researcher's conclusions and the lack of such considerations could introduce error, which may be significant, depending upon the possibility that the amount that the COT results could be affected.

Dissimilar COMs were computed for the same thio<sub>n</sub> molecule, as evidenced by the differences in energies of formation between different initial ligand conformations and between PT or no PT (Table 2). This difference is significant because, if differences are computed for thio<sub>n</sub>, which are larger organotin(IV) molecules with essentially unhindered ligand rotations, then computational models of other organotin(IV) molecules may unknowingly experience differences that may affect research and influence conclusions.

The thio<sub>n</sub> Sn-S intramolecular moiety must maintain a certain structural conformation for the molecules to be bioactive. Replacing ligand phenyl groups with chlorine atoms causes the intramolecular moieties of the thio<sub>n</sub> molecules to deform slightly with each replacement, deactivating the molecular bioactivity (Fig. 1a, 1b, 1c, and 1d). [1, 3, 4, 8, 13] By developing the application of theoretical computational methods, short-cuts with greater accuracy and less exposure risk may be developed. These methods may allow molecules to be deliberately crafted with predetermined levels and forms of bioactivity control.

COT1 models the molecular conformations to match the structure obtained by XRC, as evidenced by Fig. 2 and Fig. 3. The thio<sub>n</sub> ligands have levels of intramolecularity (or hyperconjugation) that are responsive to the numbers of chlorine atoms present in the molecule. However, not all bioactive organotin(IV) compounds have hyperconjugation and not all hyperconjugated organotin compounds are bioactive. [1, 3, 4, 8, 13, 14, 15, 16]

For thio<sub>n</sub>, COT and XRC structural data, such as energies of formation, dipole moments, and electron densities were used to help determine the amount of intramolecular bonding. The phenyl groups represent potential steric hindrances. A user may mitigate the aforementioned steric problems by adjusting the starting conformation of the molecule to minimize atomic overlap. Hence, *in situ*, the ligands of thio<sub>n</sub> would rotate at a rate that is largely related to the temperature and in a manner that would require little coordination between the ligands. In all cases, a dual or triple COT treatment yielded less reliable results than a single COT treatment. Selecting the best COT (Table 1) for modeling thio<sub>n</sub> molecules was based largely on rigorous comparative validation methods. [1, 3, 4, 8, 12, 13, 14, 15, 16, 19, 22, 23]

## References

1. Gaussian 03, Revision C.02, M. J. Frisch, G. W. Trucks, H. B. Schlegel, G. E. Scuseria, M. [A. Robb, J. R. Cheeseman, J. A. Montgomery, Jr., T. Vreven, K. N. Kudin, J. C. Burant, J. M. Millam, S. S. Iyengar, J. Tomasi, V. Barone, B. Mennucci, M. Cossi, G. Scalmani, N. Rega, G. A. Petersson, H. Nakatsuji, M. Hada, M. Ehara, K. Toyota, R. Fukuda, J. Hasegawa, M. Ishida, T. Nakajima, Y. Honda, O. Kitao, H. Nakai, M. Klene, X. Li, J. E. Knox, H. P. Hratchian, J. B. Cross, C. Adamo, J. Jaramillo, R. Gomperts, R. E. Stratmann, O. Yazyev, A. J. Austin, R. Cammi, C. Pomelli, J. W. Ochterski, P. Y. Ayala, K. Morokuma, G. A. Voth, P. Salvador, J. J. Dannenberg, V. G. Zakrzewski, S. Dapprich, A. D. Daniels, M. C. Strain, O. Farkas, D. K. Malick, A. D. Rabuck, K. Raghavachari, J. B. Foresman, J. V. Ortiz, Q. Cui, A. G. Baboul, S. Clifford, J. Cioslowski, B. B. Stefanov, G. Liu, A. Liashenko, P. Piskorz, I. Komaromi, R. L. Martin, D. J. Fox, T. Keith, M. A. Al-Laham, C. Y. Peng, A. Nanayakkara, M. Challacombe, P. M. W. Gill, B. Johnson, W. Chen, M. W. Wong, C. Gonzalez, and J. A. Pople, Gaussian, Inc., Wallingford CT (2004).
2. IUPAC Compendium of Chemical Terminology, The Gold Book, 2<sup>nd</sup> Edition (1997) compiled by Alan D. McNaught and Andrew Wilkinson, Blackwell Science, Royal Society of Chemistry, Cambridge, UK.
3. Teresita Munguia, Ioana S. Pavel, Ramesh N. Kapoor, Francisco Cervantes-Lee, László Párkányi and Keith H. Pannell, *Can. J. Chem.* 81 11 (2003) 1388-1397.
4. Teresita Munguia, Marcela Lopez-Cardoso, Francisco Cervantes-Lee and Keith H. Pannell, *Inorg. Chem.* 46 4 (2007) 1305-1314.
5. Gang Wu, Boqin Sun, Roderick E. Wasylshen and Robert G. Griffen, *Journal of Magnetic Resonance* 124 (1997) 366-371.

6. HBA 1.5, K. Eichele, R. E. Wasylishen, Dalhousie University. Copyright © 1995, (2005) by Klaus Eichele.
7. F. W. B. Einstein, C. H. W. Jones, T. Jones and R. D. Sharma, *Can. J. Chem.* 61 11 (1983) 2611-2615.
8. Teresita Munguia, Francisco Cervantes-Lee, Laszlo Parkanyi and Keith H. Pannell, *ACS Symposium Series* 917 (2006) 422-435.
9. Hong-Wen Liu, Wen-Guan Lu and Jia-Xun Tao, *Chinese Journal of Chemistry* 22 (2004) 109-113.
10. XWINNMR 2.6 is software provided by Bruker for managing NMR spectra.
11. *CRC Handbook of Chemistry and Physics*, 74<sup>th</sup> edition, Special Student Edition, David R. Lide, Editor-in-Chief, CRC Press, Inc. (1993-94).
12. A. R. Ramirez, M. Parvez, V. U. Ahmad, J. Hussain and H. Hussain, *Acta Cryst. E* 58 6 (2002) 278-280.
13. Jens Beckman, Institute of Chemistry and Biochemistry University of Berlin, 2006.
14. J. Beckmann, D. Dakternieks, A. Duthie and C. Mitchell, *Dalton Trans.* 16 (2003) 3258-3263.
15. Carlos Camacho-Camacho, Hugo Tlahuext, Heinrich Nöth and Rosalinda Contreras, *Heteroatom Chemistry* 9 3 (1998) 321-326.
16. P. J. Cox, S. M. S. V. Doidge-Harrison, I. W. Nowell, R. A. Howie, J. L. Wardell and J. McM. Wigzell, *Acta Crystallographica Section C* 46 6 (1990) 1015-1017.
17. Andrew R. Gibbs, Hiromi Morimoto, Henry F. VanBrocklin and Philip G. Williams, Lawrence Berkeley National Laboratory, LBNL-48958, eScholarship Repository (2001).
18. R. S. J. Mulliken, *Chem. Phys.* 23 (1955) 1833-1840.

19. Kevin E. Riley and Kenneth M. Merz, Jr., J. Phys. Chem. A 111 27 (2007) 6044-53.
20. John P. Perdew and Karla Schmidt, Density Functional Theory and Its Applications to Materials edited by V.E. Van Doren, C. Van Alsenoy, and P. Geerlings AIP Conference Proceedings American Institute of Physics 577 (2001) 1-20.
21. J. Susperregui, M. Bayle, J. M. Léger and G. Déléris, Journal of Organometallic Chemistry 556 1-2 (1998) 105-110.
22. Julien Toulouse and Andreas Savin, Journal of Molecular Structure: THEOCHEM 762 (2006) 147-150.
23. J. B. Mann, Report LA-3691, Los Alamos Scientific Laboratory (1968) 271.

## Chapter 5: Conclusion

A result of the COT analyses is that reliable organotin(IV) models may be made with predictive capabilities (e.g., thio<sub>3</sub>). This research may help researchers determine which molecules may have the most promise for particular experimental investigations. Another advance is to determine methods to make organotin(IV) research safer for researchers and the environment. In all cases, regardless of which method is used to input the z-matrix or whether: (a) a layered sequence of COTs (i.e. ONIOM), (b) validation, or (c) PTs were used, developing a reliable COM for the molecule of interest would likely enable faster analyses because the model should indicate the molecular properties that could guide more focused experimental research.

This research examined a series of medium sized thioether organotin(IV) molecules, PhS(CH<sub>3</sub>)(CH<sub>2</sub>)(Ph<sub>x</sub>Cl<sub>y</sub>Sn), thio<sub>n</sub>, by applying COTs via Gaussian, as related to XRC. For each thio<sub>n</sub> molecule, approximately 31 COTs (16 with PT and 15 without PT) generated 31 COMs and were validated against experimental data and a reliable COT was found. [11, 17, 18, 21, 22, 24] Performing a validation, COT1 was determined to generate the most reliable COM for these types of molecules. The bond lengths of the organotin(IV) molecules examined here were in close agreement with X-ray crystallographic values. Yet, the high flexibility of thio<sub>n</sub> became evident when examining the sometimes noticeable difference between modeled bond angles and X-ray spectra values.

Regarding the completion of the research goals stated earlier:

1. A broader array of analysis has been enabled than would otherwise be available, the organotin(IV) molecules identified above included examining experimentally determined COM molecular properties. Applying a COT that does not alter the z-

matrix of an experimentally determined structure enables modeling software to generate a COM that allows researchers access to a significant range of analytical data. [10, 12, 13, 17]

This research has established the significant utility of using structural data for a molecule obtained experimentally to enter its z-matrix into molecular modeling software, such as Gaussian. The generated COM allows Gaussian to model a molecule as though it were *in situ*, such that the number of properties able to be examined for the conformation determined experimentally is greatly expanded. [10, 12, 13, 17]

2. Successful validation involved a comparative analysis of experimental data (e.g. XRC) versus the theoretical computational modeling of each thio<sub>n</sub> molecule to determine the COT that generates the COM that most reliably models experimental data. Experimentally determined data was compared to the data of various COMs that were generated by applying COTs of varying reliability. For each thio<sub>n</sub> molecule, 31 COTs (16 with PT and 15 without PT) generated 31 COMs and were validated against experimental data and a reliable COT was found. [11, 17, 18, 21, 22, 24]
3. Thio<sub>n</sub> displayed complexities that affected creating reliable models, such as the slight energy of formation difference between conformers that have significant differences in rotational positions of freely rotating ligands and the strong correlation between energies of formation and dipole moment over conformation changes (without PT). [17, 18, 19, 20]



This research has shown that steric problems may be mitigated by adjusting the starting conformation of the molecule to minimize atomic overlap. Hence, *in situ*, the ligands of thio<sub>n</sub> would rotate at a rate that is largely related to the temperature and in a manner that would require little coordination between the ligands. In all cases, a dual or triple COT treatment yielded less reliable results than a single COT treatment. [17]

4. Hyperconjugation is a stabilizing interaction that causes an extension of the molecular orbitals. Specifically, the hyperconjugation effect for thio<sub>n</sub> was determined to extend to include unexpected methyl and methylene groups, which traditionally do not become involved in such systems. Furthermore, hyperconjugation is typically noted as requiring a beta relationship. Tin and sulfur are beta to each other through the dihedral angle (Sn-methylene C-S-methyl C) that is structurally significant towards examining the strength of bioactivity for these molecules. This research computed the HOMO electron density for thio<sub>n</sub> and was able to show that hyperconjugation of thio<sub>n</sub> decreases as the number of chlorine atoms decreases. [8, 17, 20, 31, 32, 33]

This research has shown that thioether organotin(IV) molecules are able to have extended hyperconjugated systems, hypercoordination, and intramolecularity. The hyperconjugated systems include the methyl and methylene groups, which traditionally do not become involved in such systems. Because the thio<sub>n</sub> molecular system included molecular components that are not typically considered capable of participating in hyperconjugation, a new aspect of research is opened. Furthermore, the same molecules exhibit hyperconjugation.

For thio<sub>n</sub>, COT and X-ray crystallographic structural data, such as energies of formation, dipole moments, and electron densities were used to help determine the amount of intramolecular bonding. [17, 18, 19, 20, 31, 32, 33, 35, 40]

5. This research has shown that substituting a chlorine atom for a ligand phenyl group alters the conformation of bioactive thioether organotin(IV) molecules. This alteration causes the S-Sn hypercoordination to increase and bioactivity to decrease in strength with each substitution. A reliable COT and a substitution method to control intramolecularity and hypercoordination was determined. This COT generated the best COMs for larger organotin(IV) molecules. Further, this COT generated a reliable COM in which the proper Cl-Sn-S alignment occurs, matching XRC. This alignment is one of the crucial molecular features for this species to be bioactive. Generally, COT1 generated the COM that most accurately reflected XRC. [1, 3, 5, 7, 8, 9, 10, 17, 35, 36, 41, 42, 43, 45, 46]

The thio<sub>n</sub> Sn-S intramolecular moiety must maintain a certain structural conformation for the molecules to be bioactive. Replacing ligand phenyl groups with chlorine atoms causes the intramolecular moieties of the thio<sub>n</sub> molecules to deform slightly with each replacement, deactivating their bioactivity (Fig. 1). This alteration causes the bioactivity to decrease in strength with each substitution. COT1 generated the best COMs in which the proper Cl-Sn-S alignment occurs, matching XRC. This alignment is one of the crucial molecular features for this species to be bioactive. By developing the application of theoretical computational methods, short-cuts with greater accuracy and less exposure risk may be developed. These methods may allow molecules to be

deliberately crafted with predetermined levels and forms of bioactivity control.  
[17, 21, 30, 34, 35, 42, 43]

6. PTs are commonly used by researchers generating COMs in an attempt to use less CPU time and to generate more reliable COMs. PTs are defined as including: preoptimization COT applications, sequential layering of COTs (a.k.a. ONIOM), and preoptimization conformation changes. An analysis of the PTs applied to the molecules studied here established that PTs do not accomplish the purposes typically sought by researchers. [17, 21, 22, 26, 27, 28, 29]

It has been established here that the application of a PT does not allow the resultant COMs to more closely match an ideal of either experimental values or the globalized minimum. Actually, PTs use more CPU time and they often get less reliable results than they would have generated had the researcher applied only one COT. Therefore, this research has established that PTs are not recommended for larger organotin(IV) molecules.

7. As external confirmatory validation of the methodology, research on molecules (c) and (d) (noted above) repeated published research by applying the same COTs to the same organotin(IV) molecules as did the original researchers. A comparison of the present COMs to the original experimental (XRC) and computational values determined that the present research generated COMs that matched or exceeded published values. These two research projects were chosen because each used the COT determined to be most reliable for larger organotin(IV) species. [1, 17, 26, 27, 28, 29, 43, 44, 57, 65]

8. Lastly, a reliable COT was applied to the bimolecular complex noted above as (e). The goal was to demonstrate that quantification of the dipole moment changes and reduced energy of formation of the bimolecular complex versus the separated molecules and validating intramolecularity via relevant bond lengths. [17, 25, 26, 44]

Analyses here have shown that the COT output characteristics of each thio<sub>n</sub> molecule can be affected by varying the input conformations. Furthermore, varying the positions of the ligands and varying the number and type of COT applied caused significant structural effects. Shown here, these effects may introduce error, which can be significant, depending upon the amount that the COT results could be affected by the input data for the molecules being studied.

Selecting the best COT (Table 1) for modeling the thio<sub>n</sub> molecules was based largely on rigorous comparative validation methods using Gaussian. COT1 was verified to be the most accurate of the COTs applied. [10, 14, 15, 16] Many types of research efforts that would benefit, by increased efficiency, time saved, and lowered exposure risk, from reliable COT modeling methods for organotin(IV) species. [2, 3, 4, 5, 6, 8, 23, 24, 34, 40, 41, 42]

The current research of these molecules and development of reliable modeling methods has increased the global knowledge base upon which the development of more targeted organotin(IV) applications may stand. Gaining a better understanding of these organotin(IV) compounds through theoretical modeling may ultimately lead to a lower exposure risk, and hence, fewer occurrences of unintended harmful biological damage. Accurate modeling of these molecules was developed through coordinated refinements

between modeling and experimentation and ultimately facilitated a degree of bioactivity prediction (thio<sub>3</sub>).

Regarding thio<sub>n</sub>, the ligand phenyl groups and Cl atoms act as electron withdrawers, C atoms are amphoteric but act as electron withdrawers here, Sn atoms are also amphoteric, but act as electron donors here, and S atoms act as electron donors. Thio<sub>n</sub> are highly polarized molecules with many single bonded sites with free rotation. Interference with bioactivity ensues the substitution of ligand phenyl groups with chlorine atoms in bioactive organotin(IV) compounds. The chlorine atoms alter the molecular conformation. As substitution progresses, this alteration causes the sulfur atom to form an increasingly strong intramolecular bond with the tin atom. Low barriers to ligand rotation for larger organotin(IV) compounds, as was determined for the thio<sub>n</sub> molecules, means difficulty in modeling XRC, in computationally determining an optimized structure, and for the solid-state NMR to generate a spectra that indicates the expected number of isotropic peaks. [8, 10, 12, 17, 20, 21, 25, 30, 31, 32, 33, 34, 39, 40]

The current research analysis of the application of COTs relative to X-ray crystallography for thio<sub>n</sub> molecules showed:

1. Intramolecularity:
  - a. Got increasingly stronger between the Sn-S atoms as each thio<sub>n</sub> ligand phenyl group was replaced with a chlorine atom, hence caused distance between Sn-S to get increasingly shorter
  - b. Hyperconjugation of this highly aromatic system pulled the ligands towards each other

2. Starting conformations affecting ending conformations: The effects on thio<sub>n</sub> COT output conformations and other properties were affected by variations in their input conformations:

Thio<sub>1</sub> generates output that had its stannyl-ligand rotated so that its structural components did not match with the Cl-Sn-S alignment results from XRC. Therefore, chlorine atom/ phenyl group alignment enabled thio<sub>1</sub> to generate a COM that matched XRC and that also had a lower energy of formation. Thio<sub>0, 2, 3</sub> required no alignment.

Current research confirms that reliable organotin COT models have predictive capabilities. The methods of applying reliable COTs to generate reliable COMs for the current research may assist future researchers of other organotin(IV) species to:

1. Predict actual molecular properties, before deciding on laboratory syntheses:
  - a. Less waste of time and materials from unnecessary syntheses
  - b. Less risk of researchers being exposed to dangerous molecules
  - c. Increased rate of comprehension evolution
2. Detect changes in bioactivity, structures, and other properties, from:
  - a. Individually substituting ligand phenyl groups with chlorine atoms
3. Enhance capabilities of future research
  - a. Engineer similar organotin molecules with specific properties for specific applications
  - b. Improve COTs, especially for modeling organotin(IV) molecules

A detailed study of COMs relative to experimental values has lead to a better understanding of the structure and properties of thio<sub>n</sub> and other organotin(IV) compounds.

## Chapter 6. Future Research

Organotin(IV) molecules have many interesting and useful properties that need further COT and COM research. The value of COT and COM research will increase as its usefulness towards developing new applications and understanding existing products increases. Improving the ability of researchers to predict accurately the properties of organotin(IV) molecules, enables an increasing number of research advances regarding the many applications being developed.

### 6.1 Solvent Effects

Examining thio<sub>n</sub> in the presence of THF solvent and applying the same COT: [15, 17, 20, 21, 30, 35, 42, 43]

- a. Thio<sub>n</sub> molecules *in-vacuo* were compared to thio<sub>n</sub> molecules in THF solvent. Both sets of molecules were optimized using the same COT and both were in the same pre-optimization conformations.
- b. Organotin compounds can be susceptible to solvent effects, even once the solvent has been fully removed. The thio<sub>n</sub> molecules showed a Sn-S intramolecular attraction that increased in strength as the ligand phenyl groups were substituted with chlorine groups. This is the same trend followed by the thio<sub>n</sub> molecules when in THF solvent. However, the thio<sub>n</sub> molecules in THF showed a marked increase in the strength of the Sn-S intramolecular bonding as compared to when they were modeled *in-vacuo*.

### 6.2 Bioactivity

As already discussed in detail, thio<sub>n</sub> can be a bioactive organotin(IV) molecule. Furthermore, theoretical computational modeling has determined a means to biologically

deactivate thio<sub>n</sub>. Expanding this control method to other bioactive molecules would be needed to more fully evaluate the method's application over organotin(IV) species.

### **6.3 Pretreatment**

Exploration into the causes and extent of influence caused by the various types of PT identified here may help researchers mitigate errors.

### **6.4 Thio<sub>1</sub>**

This research differentiated thio<sub>1</sub> as being the only Cl-bearing molecule in the thio<sub>n</sub> series for which Gaussian 03 did not align its Cl-Sn-S atoms to closely match the conformation indicated by XRC. This difference is likely the result of thio<sub>1</sub>'s conformations having low, poorly differentiated barriers of rotation between conformers. Further investigation is warranted.

### **6.5 Thio<sub>3</sub>**

Crystalline samples of thio<sub>3</sub> have not yet been synthesized. Therefore, neither single-crystal X-ray crystallography nor <sup>119</sup>Sn solid-state NMR was run. The COT model for thio<sub>3</sub> is presented herein as a predictive structure.



## References: Introduction, Conclusion, and Future Research

1. Buck, Bethany; Mascioni, Alessandro; Que, Lawrence, Jr.; Veglia, Gianluigi (2003) J. Am. Chem. Soc. 125:13316.
2. Buck-Koehntop, Bethany A.; Mascioni, Alessandro; Buffy, Jarrod J.; Veglia, Gianluigi (2005) Journal of Molecular Biology 354:3:652.
3. Pellerito, Claudia; Nagy, Laszlo; Pellerito, Lorenzo; Szorcsik, Attila (2006) Journal of Organometallic Chemistry 691:8:1733.
4. Atanasov, Atanas G.; Nashev, Lyubomir G.; Tam, Steven; Baker, Michael E.; Odermatt, Alex (2005) Environmental Health Perspective 113:11:1600.
5. Chasapis, Christos T.; Hadjikakou, Sotiris K.; Garoufis, Achilles; Hadjiliads, Nick; Bakas, Thomas; Kubicki, Maciej; Ming, Yang (2004) Bioinorganic Chemistry and Applications 2:1:43.
6. Rocha, Willian R.; De Almeida, Katia J.; De Almeida, Wagner B. (2000) Chemical Physics Letters 316:5:510.
7. Bulaj, G.; Kortemme, T.; Goldenberg, D. (1998) Biochemistry 37:25:8965.
8. Billingsley, M. L.; Yun, J.; Reese, B. E.; Davidson, C. E.; Buck-Koehntop, B. A.; Veglia, G. (2006) Journal of Cellular Biochemistry 98:2:243.
9. Davidson, Collin E.; Reese, Brian E.; Billingsley, Melvin L.; Yun, Jong K. (2004) Molecular Pharmacology 66:855.
10. Ruzicka, Ales (2001) Chemicke Listy 95:807.
11. Williams, T. Gavin; DeYonker, Nathan J.; Wilson, Angela K (2008) Journal of Chemical Physics 128:04:4101.

12. Lycka, Antonin; Micák, D.; Holecek, J.; Biesemans, M.; Martins, J. C.; Willem, R. (2000) *Organometallics* 19:703.
13. Harris, R.K. (1996) *Encyclopedia of Nuclear Magnetic Resonance*, D. M. Granty and R. K. Harris editors, v5, John Wiley & Sons, Chichester, UK.
14. Martins, José C.; Mercier, Frédéric A. G.; Vandervelden, Alexander; Biesemans, Monique; Wieruszeski, Jean-Michel; Humpfer, Eberhard; Willem, Rudolph; Lippens, Guy (2002) *Chemistry – A European Journal* 8:15:3431.
15. Engelhardt, Lutz M.; Leung, Wing-Por; Raston, Colin L.; White, Allan H. (1982) *Australian Journal of Chemistry* 35:11:2383.
16. Samskog, Olof; Lee, i Su-hwa; Arroyo, Carmen M.; Kispert, Lowell D.; Geoffrey, Michael (1984) *J. Phys. Chem.* 88:1804.
17. Gaussian 03, Revision C.02, M. J. Frisch, G. W. Trucks, H. B. Schlegel, G. E. Scuseria, M. A. Robb, J. R. Cheeseman, J. A. Montgomery, Jr., T. Vreven, K. N. Kudin, J. C. Burant, J. M. Millam, S. S. Iyengar, J. Tomasi, V. Barone, B. Mennucci, M. Cossi, G. Scalmani, N. Rega, G. A. Petersson, H. Nakatsuji, M. Hada, M. Ehara, K. Toyota, R. Fukuda, J. Hasegawa, M. Ishida, T. Nakajima, Y. Honda, O. Kitao, H. Nakai, M. Klene, X. Li, J. E. Knox, H. P. Hratchian, J. B. Cross, C. Adamo, J. Jaramillo, R. Gomperts, R. E. Stratmann, O. Yazyev, A. J. Austin, R. Cammi, C. Pomelli, J. W. Ochterski, P. Y. Ayala, K. Morokuma, G. A. Voth, P. Salvador, J. J. Dannenberg, V. G. Zakrzewski, S. Dapprich, A. D. Daniels, M. C. Strain, O. Farkas, D. K. Malick, A. D. Rabuck, K. Raghavachari, J. B. Foresman, J. V. Ortiz, Q. Cui, A. G. Baboul, S. Clifford, J. Cioslowski, B. B. Stefanov, G. Liu, A. Liashenko, P. Piskorz, I. Komaromi, R. L. Martin, D. J. Fox, T. Keith, M. A. Al-Laham, C. Y. Peng, A. Nanayakkara, M.

- Challacombe, P. M. W. Gill, B. Johnson, W. Chen, M. W. Wong, C. Gonzalez, and J. A. Pople, Gaussian, Inc., Wallingford CT (2004).
18. Hannachi, Yacine; Barthelat, Jean-Claude; Jolly, Luc-Henry; Silvi, Bernard; Bouteiller, Y. (2004) *International Journal of Quantum Chemistry* 42:3:509.
19. Wann, Derek A. (2005) *Gas-Phase Structures of Molecules Containing Heavy P-Block Elements*, PhD Dissertation, University of Edinburgh.
20. Chen, De-Li; Quan Tian, Wei; Feng, Ji-Kang; Sun, Chia-Chung (2007) *The Journal of Physical Chemistry A* 111:33:8277.
21. Crespo-Otero, Rachel; Montero, Luis Alberto (2005) *Journal of Chemical Physics* 123:13:4107.
22. Hladyszowski, Jerzy (2001) *Cell. Biol. Mol. Letters* 6:2A:398.
23. Perdew, John P.; Schmidt, Karla (2001) *Density Functional Theory and Its Applications to Materials*, V.E. Van Doren, C. Van Alsenoy, and P. Geerlings, editors, American Institute of Physics Conference Proceedings 577 pp 1-20.
24. Mann, J. B. (1968) *Atomic Structure Calculations II. Hartree-Fock Wave Functions and Radial Expectation Values: Hydrogen to Lawrencium*, Report LA-3691, Los Alamos Scientific Laboratory.
25. CRC Handbook of Chemistry and Physics, 74<sup>th</sup> edition, Special Student Edition (1993-94) David R. Lide, Editor-in-Chief, CRC Press, Inc.
26. Buntine, Mark A.; Kosovel, Frances J.; Tiekink, Edward R. T. (2003) *CrystEngComm* 5:58:331.
27. Cox, M. J.; Tiekink, Edward Richard Tom (1997) *Zeitschrift für Kristallographie - New Crystal Structures* 212:351.

28. Dakternieks, D.; Farhangi, Y.; Tiekink, Edward Richard Tom (1998) Zeitschrift für Kristallographie - New Crystal Structures 213:397.
29. Buntine, Mark A.; Hall, Veronica J.; Kosovel, Frances J.; Tiekink, Edward R. T. (1998) J. Phys. Chem. A 102:2472.
30. Gielen, Marcel (2003) Journal of the Brazilian Chemical Society 14:6.
31. McMurry, John (1988) Organic Chemistry, 2<sup>nd</sup> edition, Pacific Grove, Calif.: Brooks/Cole.
32. Pophristic, V.; Goodman, L. (2001) Nature 411:565.
33. Weinhold, Frank (2001) Nature 411:539.
34. Ingold, K.U.; Dilabio, G.A. (2006) Org. Lett. 8:592.
35. Munguia, Teresita; Lopez-Cardoso, Marcela; Cervantes-Lee, Francisco; Pannell, Keith H. (2007) Inorg. Chem. 46:4:1305.
36. Lebl, Thomas; Zoufalá, Petra; Brun, Clemens (2005) European Journal of Inorganic Chemistry 2536.
37. Mitchell, Tracy A.; Finocchio, Debbie; Kua, Jeremy (2007) J. Chem. Educ. 84:629.
38. Beckmann, Jens; Dakternieks, Dainis; Duthie, Andrew; Mitchell, Cassandra (2003) Dalton Transactions 3258.
39. Gillespie, R. J.; Silvi, B. (2002) Coord. Chem. Rev. 233:53.
40. IUPAC Compendium of Chemical Terminology, The Gold Book, 2<sup>nd</sup> Edition (1997) compiled by Alan D. McNaught and Andrew Wilkinson, Blackwell Science, Royal Society of Chemistry, Cambridge, UK.
41. Lebl, Tomas; Smicka, Ales; Brus, Jirí; Bruhn, Clemens (2003) European Journal of Inorganic Chemistry 1:143.
42. Li, Q.; Yang, P.; Wang, H.; Guo, M. (1996) Journal of Inorganic Biochemistry 64:3:181.

43. Di Stefano, R.; Scopelliti, M.; Pellerito, C.; Fiore, T.; Vitturi, R.; Colomba, M. S.; Gianguzza, P.; Stocco, G. C.; Consiglio, M.; Pellerito, L. (2002) *Journal of Inorganic Biochemistry* 89:3:279.
44. XWINNMR 2.6 is software provided by Bruker for managing NMR spectra.
45. Munguia, Teresita; Pavel, Ioana S.; Kapoor, Ramesh N.; Cervantes-Lee, Francisco; Párkányi, László; Pannell, Keith H., Lewis Acidity of Group 14 Elements Toward Intramolecular Sulfur in Ortho-aryl-thioanisoles *Can. J. Chem.* (2003) 81 11 1388 - 1397.
46. Munguia, Teresita; Cervantes-Lee, Francisco; Parkanyi, Laszlo; Pannell, Keith H., Organotin - Sulfur Intramolecular Interactions: Overview of Current and Past Compounds and the Biological Implications of Sn - S Interactions *ACS Symposium Series* (2006) 917 422 - 435.

## **Vita**

Michelle R. Stem Joseph, Ph.D., MBA

Materials Science and Engineering

Michelle R. Stem Joseph earned her Bachelor of Science degree in Chemistry from Florida Atlantic University in 1996, during which she was named a George F. Young Memorial Scholar. She received her MBA degree in 2003 from the University of Texas at Permian Basin, for which she won the Outstanding Student of the Year Award. In 2005, she joined the Materials Science and Engineering PhD program at UTEP, during which she was accepted into Sigma Xi, a scientific research honor society.

Dr. Stem Joseph has five publications in scientific research topics unrelated to her PhD dissertation. Directly related to her PhD dissertation topic, she has three manuscripts submitted and under review for publication, plus her dissertation. Dr. Stem Joseph has presented her research at regional and international conferences, such as: (1) the 24<sup>th</sup> Southwest Theoretical Chemistry Conference (2008) on molecular modeling, (2) the 21<sup>st</sup> Austin Symposium on Molecular Structure (2008) on thermodynamic effects on phonons, and (3) the 230<sup>th</sup> American Chemical Society National Conference (2005) on FTIR Synchrotrons.

Dr. Stem Joseph is pursuing a faculty academic career in Materials Science and Engineering at a university yet to be chosen.

Permanent address:

653 Abington Drive

El Paso TX 79912

This dissertation was typed by Michelle R. Stem Joseph